Western Washington University
Western CEDAR

WWU Graduate School Collection | WWU Graduate and Undergraduate Scholarship

Spring 1999

Structure and Metamorphism of the Talc Creek Area, Harrison Lake B.C.

Minda L. Troost
Western Washington University

Follow this and additional works at: https://cedar.wwu.edu/wwuet

Part of the Geology Commons

Recommended Citation

Troost, Minda L., "Structure and Metamorphism of the Talc Creek Area, Harrison Lake B.C." (1999). *WWU Graduate School Collection*. 847.
https://cedar.wwu.edu/wwuet/847

This Masters Thesis is brought to you for free and open access by the WWU Graduate and Undergraduate Scholarship at Western CEDAR. It has been accepted for inclusion in WWU Graduate School Collection by an authorized administrator of Western CEDAR. For more information, please contact westerncedar@wwu.edu.

WWU LIBRARIES

STRUCTURE AND METAMORPHISM OF THE TALC CREEK AREA, HARRISON LAKE B.C.

BY

MINDA L. TROOST

Accepted in Partial Completion

of the Requirements for the Degree

Master of Science

Moheb A. Ghali, Dean of the Graduate School

ADVISORY COMMITTEE

Chair, Dr. Edwin H. Brown

Dr. James L. Talbot

Dr. Scott R. Babcock

MASTER'S THESIS

In presenting this thesis in partial fulfillment of the requirements for a master's degree at Western Washington University, I agree that the Library shall make copies freely available for inspection. I further agree that copying of this thesis in whole or in part is allowable only for scholarly purposes. It is understood, however, that any copying or publication of this thesis for commercial purposes, or for financial gain, shall not be allowed without my written permission.

Signature ______________________

Date June 8, 1999

MASTER'S THESIS

In presenting this thesis in partial fulfillment of the requirements for a master's degree at Western Washington University, I grant to Western Washington University the non-exclusive royalty-free right to archive, reproduce, distribute, and display the thesis in any and all forms, including electronic format, via any digital library mechanisms maintained by WWU.

I represent and warrant this is my original work and does not infringe or violate any rights of others. I warrant that I have obtained written permissions from the owner of any third party copyrighted material included in these files.

I acknowledge that I retain ownership rights to the copyright of this work, including but not limited to the right to use all or part of this work in future works, such as articles or books.

Library users are granted permission for individual, research and non-commercial reproduction of this work for educational purposes only. Any further digital posting of this document requires specific permission from the author.

Any copying or publication of this thesis for commercial purposes, or for financial gain, is not allowed without my written permission.

Name: Minda Troost

Signature:

Date: 8/31/2018

STRUCTURE AND METAMORPHISM OF THE TALC CREEK AREA, HARRISON LAKE B.C.

A Thesis Presented to the Faculty of
Western Washington Universtiy

In Partial Fulfillment
of the Requirements for the Degree
Master of Science

by

Minda L. Troost
June 1999

ABSTRACT

The Slollicum and Cogburn terranes, metamorphosed country rock within the southern Coast Plutonic Complex, are juxtaposed along a thrust fault together with large slabs of ultramafic rock. The structure and metamorphism along and near this fault are the focus of this study.

Three periods of deformation (D_1-D_3) affected the study area. D_1 structures consist of penetrative foliation and lineations that are attributed to thrust stacking of the Slollicum and Cogburn terranes. Foliation, which parallels the fault contact, dips to the northeast at moderate to steep angles. Lineations have mainly down-dip orientations. D_2 structures record the intrusion of the Spuzzum pluton and consist of a foliation, defined mainly by biotite, that parallels the pluton contact. D_3 caused rotation and distention of post-tectonic porphyroblasts during localized reactivation of the D_1 foliation. D_3 is probably a result of orogen-normal contraction that caused large map scale folding that affected the region some time after thrusting ceased.

The metamorphic grade increases to the northeast across the study area from greenschist to amphibolite facies. Three metamorphic events (M_1-M_3) affect the rocks in the study area. M_1, associated with D_1, resulted primarily in greenschist facies metamorphism. M_2, a result of contact metamorphism from the Spuzzum intrusion, produced the index minerals biotite, hornblende and garnet. M_3, a high pressure event, is characterized by an overprint of large garnet and radiating hornblende, which grew

over the D_1 foliation. These M_3 porphyroblasts were then rotated or pulled apart suggesting D_3 began after the peak of high pressure metamorphism. M_3 also may have produced the randomly oriented hornblende that is observed on foliation surfaces of many Slollicum and Cogburn rocks. Terrane stacking must have taken place after 146 Ma, which is the U/Pb zircon age of the Slollicum rocks (Walker, in Bennett, 1989), and prior to the 96 Ma age (Brown and Walker, 1993) of the Spuzzum pluton.

ACKNOWLEDGMENTS

Much gratitude is owed to my thesis advisors, Ned Brown, Jim Talbot and Scott Babcock for their patience, guidance, and encouragement as I labored on this project.

Many thanks to those who assisted me in the field, Kierstin Swanson, Steven Sherotsky, Paul Pittman, and fellow investigators of different parts of the same region John Feltman and Tom Lapen. I would also like to thank George Mustoe for his repeated assistance with departmental machinery and instruments.

Funding for this study was provided by a National Science Foundation grant to Ned Brown.

Finally, I wish to thank my family and friends for their support and chiding to "move it along", I could not have done it without them.

TABLE OF CONTENTS

LIST OF FIGURES, TABLES AND PLATES

Figures

Tables

Plates

I. INTRODUCTION

Introduction

This study concerns the structure and metamorphism near a terrane boundary east of Harrison Lake, B.C. in the southern Coast Plutonic Complex (CPC). The Coast Plutonic Complex (fig. 1.1) is a plutonic/metamorphic complex that extends approximately 1800 km along the western North American Cordillera from Alaska to Washington state where it is called the North Cascades Crystalline Core (CC).(fig. 1.2)

Portions of the Coast Plutonic Complex/North Cascades Crystalline Core are observed in southern B.C. as slightly to highly metamorphosed packages of rock. Several of these packages lie east of Harrison Lake about midway up the lake, two of which are the subject of the present study.(fig. 1.3)

The study focuses on a terrane bounding fault that is possibly the main suture between the Alexander/Wrangellia terrane and the North American margin. This study attempts to characterize terrane suturing by detailed examination of fault structures and by investigating the role of plutonism, contraction and crustal thickening in the process of terrane accretion and orogeny.

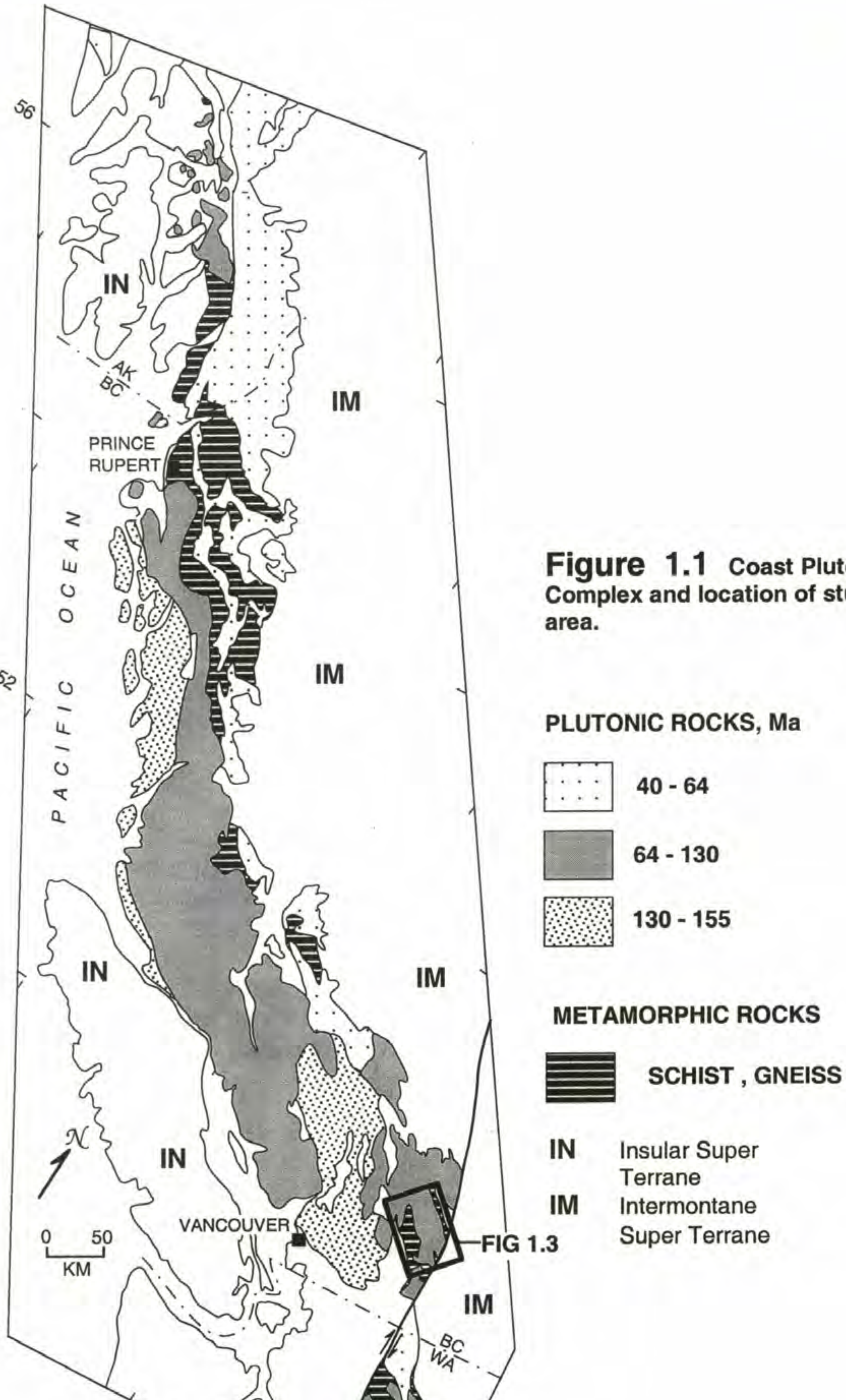

Figure 1.1 Coast Plutonic Complex and location of study area.

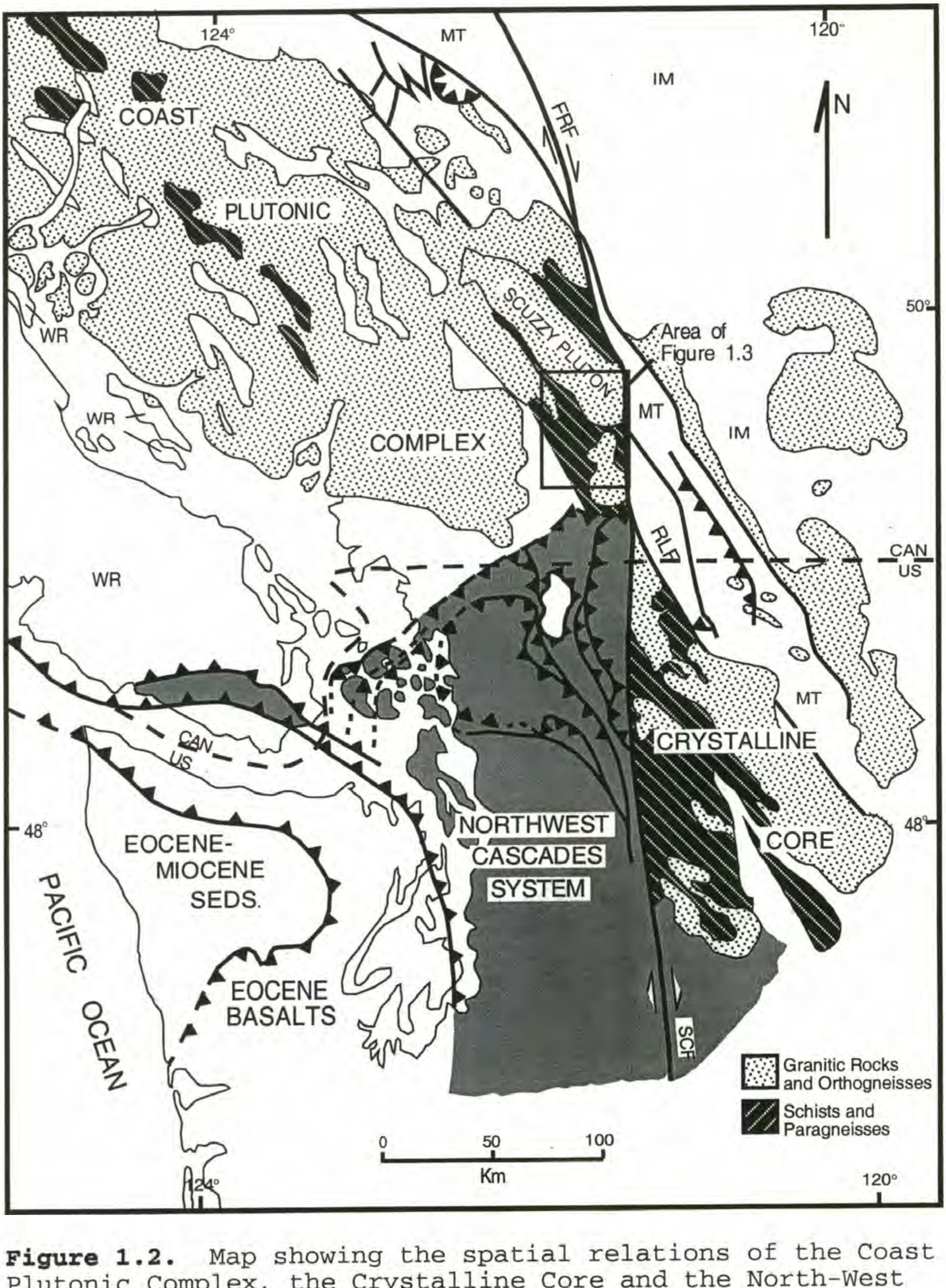

Figure 1.2. Map showing the spatial relations of the Coast Plutonic Complex, the Crystalline Core and the North-West Cascades System. (FRF) Frasure River Fault, (SCF) Straight Creek Fault , (RLF) Ross Lake Fault, (IM) Intermontane super terrane, (IN) Insular super terrane, (WR) Wrangellia terrane, (MT) Methow-Tyaughton terrane. Modified from Brown and Talbot (1989) and Brown and Walker (1993).

KEY

PLUTON AGES, MA

- AGE UNKNOWN
- 25
- 84-90
- 91-92
- 96-104
- 156
- 226

■ 91 U/PB ZIRCON AGE, MA

Anticline

Thrust contacts

Plutons

BK	Breakenridge Orthogneiss
BS	Big Silver pluton
CC	Clear Creek Orthogneiss
DP	Doctors Point pluton
FC	Fir Creek pluton
H	Hornet Creek pluton
HC	Hut Creek pluton
MM	Mount Mason pluton
SC	Settler Creek pluton
SP	Spuzzum pluton
TW	Tikwalis Creek pluton

Country rock

SE	Settler Schist
CG	Cogburn Group
SL	Slollicum Schist
um	Ultramafic rock
HLS	Harrison Lake Stratigraphic sequence

Structures

BCF	Butter Creek fault
BKF	Breakenridge fault
HLF	Harrison Lake fault

Figure 1.3 Key to map on following page which shows the regional geology of the Harrison Lake area.

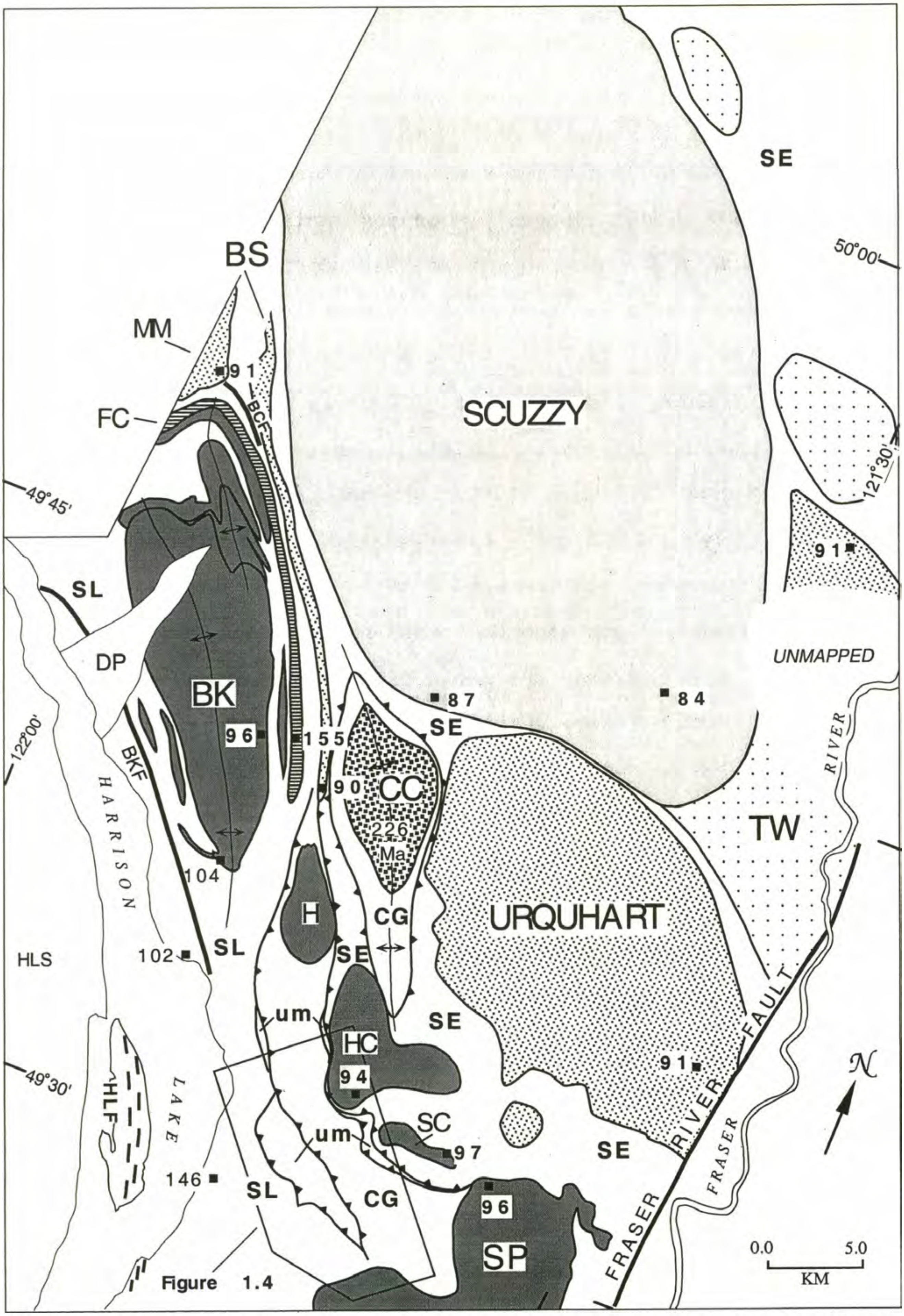

Figure 1.3. Regional geology of the Harrison Lake area. See previous page for key. Modified from Brown and McClelland (manuscript).

General Geology

The regional geology is characterized by three lithologically distinct terranes, (Monger, 1986); the Slollicum Schist, Cogburn Creek Group and Settler Schist (fig. 1.3, 1.4), and several plutons of mid-Cretaceous age.

The Slollicum rocks are mainly volcanic and sedimentary rocks metamorphosed regionally to greenschist facies (Lowes, 1972). U-Pb zircon ages of 146 Ma (Walker, in Bennett, 1989) and 102 Ma (Parish and Monger, 1992) (fig. 1.3) have been determined for the Slollicum rocks. The 102 Ma age is correlative to the age of Fire Lake-Gambier group rocks on the west side of Harrison Lake (Journeay and Friedman, 1993. They have correlated the Slollicum and Gambier rocks based on their similar lithologies. The 146 Ma age is correlative to the Jurassic age of volcanics in the Harrison Lake terrane on the west side of Harrison Lake. The Slollicum rocks are intruded by a Jurassic sill (157 Ma, Brown, pers. comm.) north of the study area indicating that part of the Slollicum rocks are older than 157 Ma. Lowes (1972) correlated the Slollicum Schist with the Devonian and Permian Chilliwack group south of the Fraser River (fig. 1.5). Jurassic ages for the Slollicum Schist from Bennett (1989) and Parish and Monger (1992) rule out this correlation.

The Cogburn group lies northeast of the Slollicum Schist and is comprised of phyllites, meta-basites and meta-chert with minor marble (Gabites, 1985; Monger, 1986, Bennett,

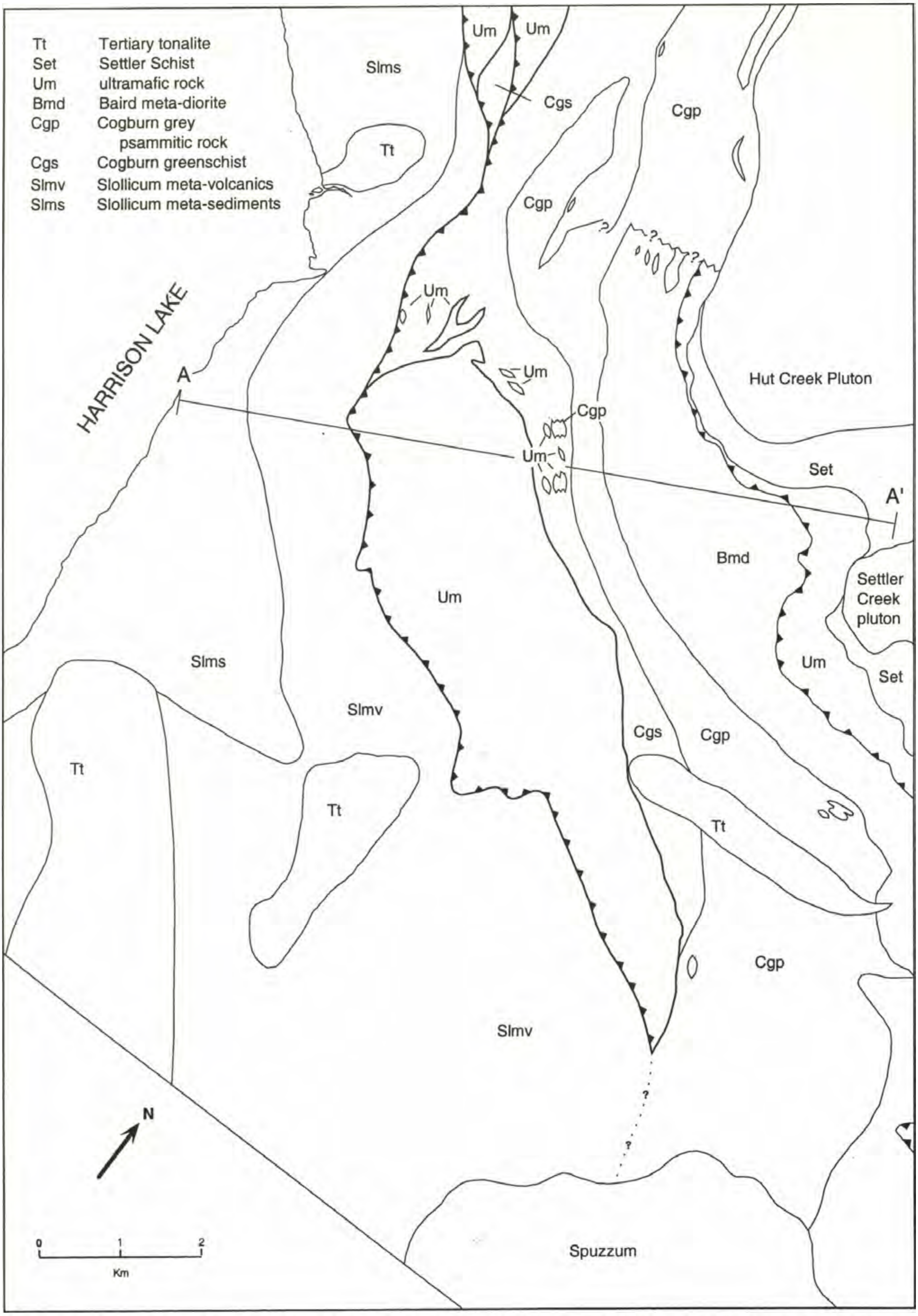

Figure 1.4 Map of study area and surrounding region showing rock units. Contacts based on Lowes (1972), Gabites (1985), and Bennett (1989) and this study. Section line A-A' corresponds to cross section in Figure 3.2.

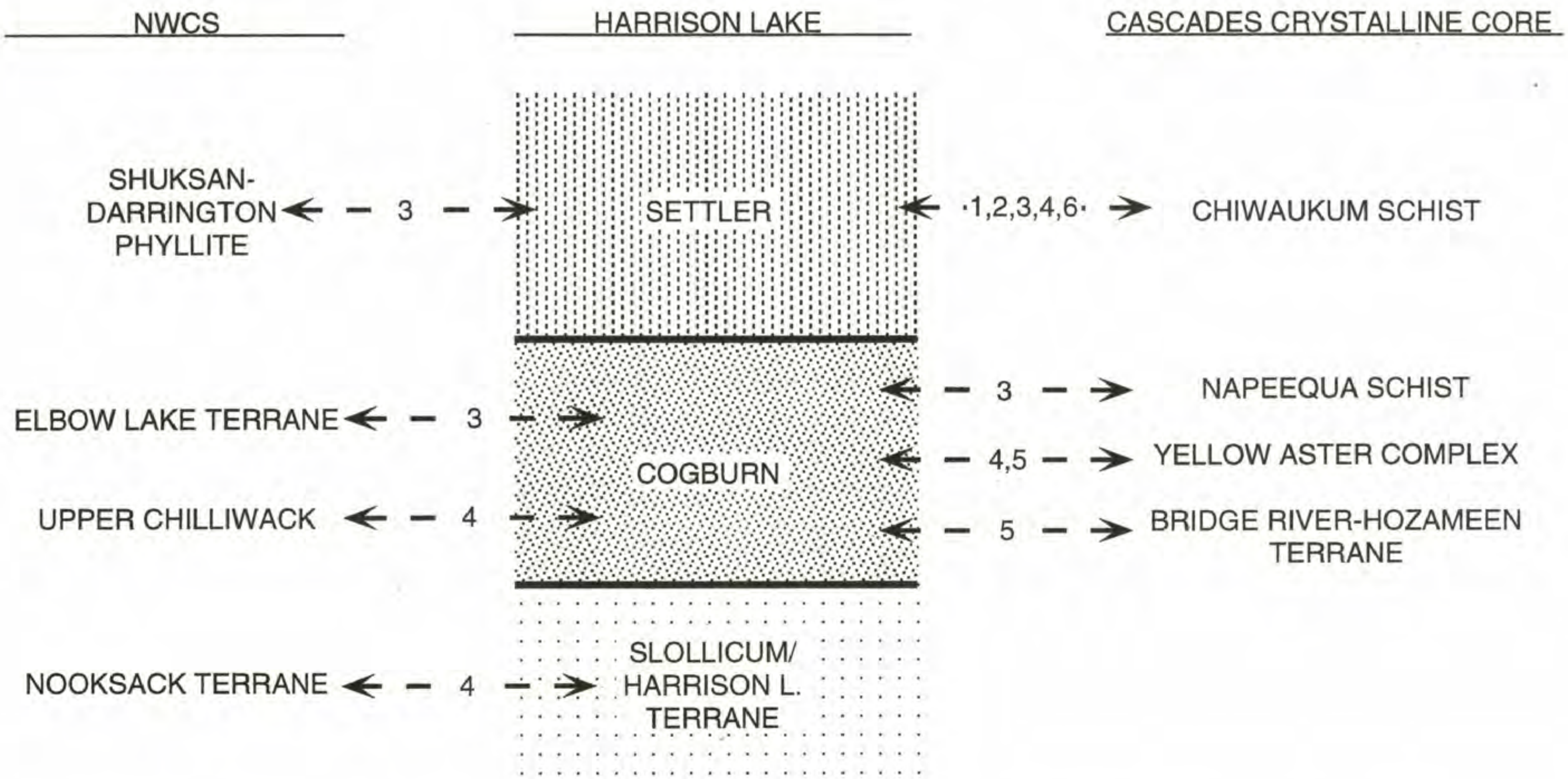

Figure 1.5. Chart showing correlation of units in the study area with units in the Cascades Crystalline Core and Northwest Cascades System. Numbers represent correlations proposed or advocated by various workers and correspond as follows: **1)** Misch, 1966; **2)** Duggan and Brown, 1994; **3)** Monger, 1990; **4)** Lowes, 1972; **5)** Gabites, 1985; **6)** Evans and Berti, 1986.

(1989). Metamorphism is in the amphibolite facies (Gabites, 1985; Monger, 1986). The Cogburn rocks are intruded by a Triassic pluton (226 Ma) along Hornet Creek, north of the study area (Brown, unpublished), constraining the younger age limit. Gabites (1985) suggests a correlation of the Cogburn group with the Bridge River-Hozameen rocks to the east and the Yellow Aster Complex in the North Cascades Crystalline Core (fig. 1.5). Monger (1990) suggests a correlation to the Elbow Lake terrane in north-western Washington (fig. 1.5).

The Settler schist is a pelitic unit lying east of the Cogburn terrane. Metamorphism is in the amphibolite facies up to the sillimanite zone (Pigage, 1973; Bartholemew, 1979; Gabites, 1985). The age of the Settler Schist is also unknown. Monger correlated the Settler with the Darrington phyllite of the Shuksan Suit in north-western Washington. (fig. 1.5) Lowes (1972) correlated the Settler Schist with the Chiwaukum Schist of the Nason terrane in the North Cascades Crystalline Core (fig. 1.5)

The Slollicum, Cogburn and Settler units are separated by layer-parallel faults (Monger, 1986). Large bodies of ultramafic rocks occur along these faults in some places. The faults appear to be terrane bounding thrusts; their lower age limit is constrained by the 96 Ma Spuzzum intrusion which cross-cuts the thrusts. The upper age limit is considered to be younger than the age of protolith formation of the Slollicum Schist (146 Ma, Walker, in Bennett, 1989). The Slollicum Schist-Cogburn group contact has been suggested to be a remnant of the main suture between the Alexander/Wrangellia terrane and North America (McGroder, 1991; Journeay and Friedman, 1993).

Metamorphic grade increases to the east and north. Metamorphic facies range from zeolite on west side of Harrison Lake through greenschist and amphibolite to kyanite and sillimanite.

Plutons important to the study area include the 96 Ma Breakenridge, the 91 Ma Urquhart (Brown and McClelland, manuscript), the 97 Ma Hut Creek, the 97 Ma Settler Creek and the 96 Ma Spuzzum (fig. 1.3).

Previous Work

The North American plate has been tectonically active since the Devonian, overriding subducting oceanic crust (Armstrong, 1988; Engebretson, 1985) resulting in crustal shortening and plutonic activity along its western margin (Coney, 1989). The Western Cordillera, including the Coast Plutonic Complex, formed as a result of this convergence during the Cretaceous and extends from northern Alaska to Mexico.

Many workers have studied the effects of orogeny in the Coast Plutonic Complex, but controversy remains over interpretation of metamorphic and structural elements and their relation to particular tectonic models. Three contrasting models for mid-Cretaceous orogeny in different parts of the Coast Plutonic Complex have been proposed: one invokes a collisional welt between the Insular super-terrane and North America with orogen-normal contraction (Monger et.al., 1982); another suggests an Andean type arc, also with orogen normal-contraction (Nelson, 1979; Armstrong, 1988; van der Heyden, 1992); and a third involves transpressional shear within an Andean type arc (Brown and Walker, 1993).

Collisional Welt Model

Monger et.al. (1982) suggest the collision of the Insular super-terrane with North America during the mid-Cretaceous, subsequent to closure of a large oceanic basin, the Bridge River-Hozameen basin. A variation of this model suggests a basin that was rather narrow and developed on a transform or at a time when oblique subduction dominated the margin (McGroder, 1991). In either case, collision and eastward subduction of the Insular super-terrane beneath the western edge of North America produced a margin-parallel metamorphic/plutonic welt involving pluton generation, terrane accretion, thrust stacking and Barrovian metamorphism (Monger et. al., 1982; Brandon and Cowan, 1985; Monger, 1986, 1990; McGroder, 1991; Journeay and Friedman, 1993).

Thrust stacking systems are observed throughout the western cordillera from southern southeast Alaska to Prince Rupert, B.C., to northwestern Washington. Rubin et.al. (1990) suggest all these systems are related, caused by the same collisional forces, and they group them into their mid-

Cretaceous thrust system. They include the collisional welt model as a possible tectonic model to explain the origin of the thrust system.

Rubin et.al. (1990) include thrusts in the Northwest Cascades Thrust System (NWCS) in Northwest Washington, but not the thrusts in the study area near Harrison Lake, in their mid-Cretaceous thrust system. However, several advocates of the collisional welt model associate the thrusts in the study area with those in the Northwest Cascades Thrust System (Lowes, 1972, Monger, 1990). The Northwest Cascades Thrust System (fig. 1.2) is a mid-Cretaceous terrane stacking thrust system in northwestern Washington and the San Juan Islands (Misch, 1966; Brown, 1987; Brandon et.al., 1988; Brandon, 1989). Brandon et.al. (1988) used fossil ages to bracket the thrusting between 100 Ma and 84 Ma. Lowes (1972) correlated the Slollicum-Cogburn contact in the study area with the Church Mountain thrust in the Northwest Cascades Thrust System, based on correlations of the Slollicum and Cogburn rocks with the lower and upper Chilliwack group (fig. 1.5). Lowes (1972) and Monger (1990) correlate the Cogburn-Settler thrust contact near the study area with the Shuksan thrust in the North West Cascades Thrust System. In this model, the Settler Schist is correlative with the Shuksan-Darrington phyllite and the Cogburn Group is correlative with the Elbow Lake terrane. (fig. 1.5) Hettinga (1989) and Bennett (1989) however, have both disputed Lowes' and Monger's correlations pointing out that the Jurassic U-Pb zircon age in the Slollicum Schist rules out correlation with the older Chilliwack and that lithologies are too dissimilar.

The Darrington phyllite contains high-pressure low-temperature minerals indicative of subduction zones. Monger (1990) suggested the Settler Schist is the metamorphosed equivalent of the Darrington phyllite. Duggan and Brown (1994) interpret Rb-Sr isotopic data for the two units to preclude a correlation, they prefer a correlation between the Settler Schist and the Chiwaukum Schist in the North Cascades Crystalline Core. Correlating the Darrington phyllite with the Settler Schist implies a former subduction zone in the study area directly prior to collision and terrane accretion during mid-Cretaceous. This would support the collisional welt model. However, at present, no evidence for an Early Cretaceous subduction zone within the Coast Plutonic Complex has been found (Rubin et.al, 1990).

Proponents for an orogen-normal collision as the main deformational event in the Northwest Cascades Thrust System infer that the Shuksan and the Church Mountain thrusts have undergone displacement to the southwest based on folds within the North West Cascades Thrust System (Misch, 1966), and the suggestion that the Nanaiamo Group is a foreland basin to SW directed thrusts that root east of the North Cascades Crystalline Core but west of the Methow-Tyaughton Basin (Brandon and Cowan, 1985).

Andean Arc Model

Nelson (1979), in opposition to the collisional welt model, proposed a different model in which orogenic development occurred across previously accreted and amalgamated terranes. Orogenic evolution involved metamorphism and plutonism in an Andean type arc. This model is advocated by Armstrong (1988), Walker and Brown (1991) and van der Heyden (1992). The deformation mechanism is thought to be oblique convergence with strain partitioning into contractional and shear components (Brown and Talbot, 1991; van der Heyden, 1992).

The Andean arc model implies pre-Cretaceous super-terrane assembly. Evidence includes overlap assemblages in the central and southern Coast Plutonic Complex, the Gambier group, and in the northern Coast Plutonic Complex, the Gravina-Nutzotin sequence. These assemblages indicate the Insular and Intermontane super-terranes were together before Early-Cretaceous in the southern Coast Plutonic Complex and before late Jurassic in the northern Coast Plutonic Complex (Woodsworth and Tipper, 1980; Brew and Ford, 1983). Extensional rift basins are proposed for the depositional settings of both assemblages (Brew and Ford, 1983; Monger, 1991).

Mahoney and Journeay (1993) describe the Jura-Cretaceous Cayoosh Assemblage as an overlap assemblage conformably lying atop the Bridge River Complex along or near the Insular/Intermontane super-terrane boundary. Evidence suggests basin closure (essentially terrane juxtaposition) and clastic sedimentation during mid to late-Jurassic with uplift and erosion in Early Cretaceous.

Other evidence for pre mid-Cretaceous terrane amalgamation includes an Early Cretaceous magmatic arc superimposed on both super-terranes along the Coast Belt (Armstrong, 1988) and the occurrence of wide spread Jurassic plutons inferred as evidence for a pre-Cretaceous link between the super-terranes (van der Heyden, 1989).

Continued plate convergence according to this model may have caused collapse of the above mentioned rift basins, resulting in the mid-Cretaceous deformation in the Coast Plutonic Complex (van der Heyden, 1992). This contrasts with the Monger et.al. (1982) hypothesis of closure of a regionally extensive oceanic basin involving subduction. This model also implies that the thrust faults in the Harrison Lake area would be much older than those of the Northwest Cascades Thrust System.

Transpressional Model

A model proposed by Brown (1987; 1989), Brown and Talbot (1989) and Maekawa and Brown (1991) involves northwest-southeast directed transpressional shearing in an Andean type arc as the main deformation mechanism in the Coast Plutonic Complex/North Cascades Crystalline Core. This model is in part based on abundant northwest trending orogen-parallel stretching lineations found in the North Cascades Crystalline Core and the southern Coast Plutonic Complex.

Advocates for this model propose that the terranes in the Northwest Cascades Thrust System were translated northward in the forearc following accretion and were structurally juxtaposed against the Coast Plutonic Complex/North Cascades Crystalline Core during middle to Late-Cretaceous (Maekawa and Brown, 1991). This is based partly on NW trending orogen parallel fabrics dominant in the Northwest Cascades Thrust System. Smith (1986;1988), Brown (1987) and Brown and Talbot (1989) interpret the fabrics in the North West Cascades Thrust System as stretching lineations that record NW-SE displacement. Brandon et.al. (1994) interpret NW trending fabrics in the Northwest Cascades Thrust System as a product of solution mass transfer cleavage and associate this fabric with NE-SW contraction.

Advocates for the transpressional model recognize evidence for orogen-normal dip-slip or possible contractional movement in the Northwest Cascades Thrust System but it is considered to be associated with left-stepping jogs in a dextral transcurrent fault system. Faults of the Northwest Cascades Thrust System were likely to the south of the Coast Plutonic Complex/North Cascades Crystalline Core.

Coast Belt Thrust System

Journey and Friedman (1993) describe a series of thrust faults in the Harrison Lake area they term the Coast Belt Thrust System (CBTS). They suggest a two-stage history of Late Cretaceous deformation and shortening subsequent to pre-Albian west-directed thrusting of terranes in their Central and Eastern belts of the Coast Belt Thrust System. The Settler Schist and Cogburn Creek Group are included in their Central belt and are inferred to have been juxtaposed prior to Albian time, prior to formation of the Coast Belt Thrust System.

The first stage of deformation in the Coast Belt Thrust System involves recumbent folding seen in the Breakenridge Complex and thin-skinned thrusting of the units such as the Slollicum Schist, and according to Journeay and Friedman (1993), the related Twin Island Schist. They suggest that the Twin Island Schist-Slollicum Schist assemblage formed as an arc assemblage on the inboard eastern margin of the Insular composite terrane. During the first stage of deformation, the assemblage was accreted to the toe of a westward prograding accretionary complex comprising of previously assembled terranes of the Central and Eastern Coast belts. The oldest age of this early stage deformation is bracketed by the 97Ma Breakenridge intrusion and the 96+6/-3 Ma Ascent Creek pluton north of the study area which are affected by the deformation.

The later stage event involved folding of thrusts and out of sequence reverse faulting. The older age for this event is constrained by the intrusion of the 96+6/-3 age of the Ascent Creek pluton and the younger age is bracketed by the 94+6/-5 Ma Mt. Mason pluton and the 91+/-3 Ma Castle Towers plutons that are folded or cut by the faults.

Metamorphism

The cause of the regional Barrovian metamorphism in the study area is still widely debated. Monger (1986) suggested the high-grade regional metamorphism took place during and as a result of the later stages of terrane stacking and juxtaposition of the Slollicum Schist, Cogburn Creek Group and the Settler Schist. Lowes (1972), Pigage (1976), Bartholemew (1979) and Monger (1986) among others, agree that metamorphism was accompanied by the intrusion of the northern Spuzzum pluton, now redefined as the Urquhart pluton by Brown and Walker (1993). More recent dating from Brown and Walker (1993) puts timing constraints on juxtaposition and metamorphism which will be discussed in a later section.

Other localities in the Coast Plutonic Complex contain Barrovian metamorphic sequences including Prince Rupert, B.C. (Crawford et.al., 1987), and the Cascade Mts. crystalline core (Duggan and Brown, 1994). Crawford et.al. (1987) attribute the metamorphism to structural inversion of country rock along thrust faults. Later isostatic uplift and erosion caused exposure of the inverted Barrovian metamorphic sequence. Journeay and Friedman (1993) attribute the Barrovian metamorphism in and near the study area to structural inversion of the country rock during their early stage of deformation between 97-96 Ma. They attribute the exposed metamorphic gradient not to isostatic uplift and erosion but to differential uplift of the metamorphosed country rock along high angle reverse faults during a late stage contractional deformation event between 96 and 91 Ma. Feltman (1997) presents evidence suggesting the Breakenridge plutonic complex is intrusive into the country rock, is in place and is not a stack of thrust sheets formed during the early stage of deformation as Journeay and Friedman (1993) suggest. This evidence precludes thrusting within the Breakenridge Plutonic Complex as a cause for Barrovian metamorphism. Lapen (1998) suggests the Terrarosa thrust, a southeast directed orogen-parallel thrust discovered by Lynch (1990), may be part of a family of now obscured thrusts that could have been the cause for loading of the Breakenridge Plutonic Complex. According to Journey and Friedman (1993), metamorphism had to have been after 96 Ma and before 92 Ma. The age of the Terrarosa thrust is bracketed between 102 Ma and the age of orogen normal shortening that caused D_2 deformation of Feltman (1997) and Lapen (1998).

Brown and Walker (1993) propose a process of magma loading or "magmatic overaccretion" as presented by Wells (1980) for the cause of crustal thickening and subsequent Barrovian metamorphism observed in the study area and Cascade

Mts. This model presents a possible mechanism for a loading event in a transpressional arc regime which might otherwise be hard to explain (Brown and Walker, 1993).

Purpose of this study

The Harrison Lake area provides opportunities for observation of a Barrovian metamorphic sequence, terrane bounding thrusts, a portion of the orogen-parallel Harrison Lake Shear Zone, and pre-syn- and post-tectonic plutons. The temporal and spatial relations of these components provide an excellent study area for the evaluation of tectonic processes, kinematics of thrusting, and metamorphism in the Coast Plutonic Complex orogenic belt.

Specific questions addressed in this study are: 1) the kinematics of the thrusting; 2) the relation of the high-grade Barrovian metamorphism to the thrusting and/or emplacement of the Scuzzy and Urquhart plutons; 3) the mutual relation of the high and low grade metamorphism; and 5) the relation of the low-grade event to thrusting.

Access to the study area is by logging roads east of Harrison Lake and up the valley of Talc Creek (fig. 1.3). Most of the area is wooded providing welcome shade but fewer outcrops in potentially crucial areas.

II. LITHOLOGIC DESCRIPTIONS

Slollicum Package

The Slollicum package crops out along the eastern shore of Harrison Lake (fig. 1.3, plate 1), and was divided into a metavolcanic and a metasediment unit by Lowes (1972). Both units contain volcanic and sediment components with limited exposure making a definite boundary difficult to determine. Detailed mapping in this study resulted in a modification of Lowes contact in the northwest portion of the study area near Harrison Lake (plate 1).

Two U-Pb isotope ages have been determined on zircon fractions from dacites from two different localities in the Slollicum unit. One dacite, South of the study area (Walker, in Bennett, 1989), gave an age of 146 Ma. The other locale, North of the study area, determined by Parish and Monger (1992) gave an age of 102 Ma (fig. 1.3).

Meta-Sedimentary component

Graphitic phyllite

The meta-sedimentary component occupies the western exposures of the Slollicum terrane in the study area. Outcrops are scarce in the study area but are found along logging road cuts and stream canyons. The predominant rock type is a blue-gray, pyrite-bearing, graphitic phyllite that weathers brown to greenish orange. The pyrite in some samples occurs as euhedral grains 2-5 mm in size but have since weathered out leaving only the hollow cubic imprints on the surface (fig. 2.1). The phyllite is fine-grained, typically well cleaved and exhibits pronounced kink banding at several localities. A relict clastic texture is distinguishable. The foliation commonly shows a down dip lineation defined by elongate grains and minerals (Bennett, 1989).

Mineral assemblages consist of plagioclase, quartz, biotite, muscovite, chlorite, pyrite, carbonate, and epidote. Thin sections show fine-grained quartz and feldspar aggregates generally in thin elongate bands or as flattened clasts parallel to foliation, separated by thin partings and graphite laminae that define the foliation. Quartz and feldspar are the main constituents (70-80%, visual estimation) and commonly exhibit a polygonal texture; larger relict clasts exhibit undulatory extinction. Biotite, muscovite and pyrite appear as accessory minerals in grains sub-parallel to foliation.

Psammitic rocks

Minor psammitic phyllites and schists are observed in the north-west portion of the field area (fig. 2.2). Mineral assemblages consist of plagioclase, quartz, muscovite, chlorite, hornblende, and garnet. Quartz and plagioclase are tabular or flattened in the plane of foliation, which is defined by the platy minerals muscovite and lesser chlorite. Garnets range from 3-5 mm in diameter, and hornblende prisms range from 1-3 cm in length. Hornblende prisms occur in radiating clusters, clearly cutting

Figure 2.2. Psammitic schist from site 181-155. Note large randomly oriented radiating hornblende prisms and large garnets across foliation and smaller randomly oriented hornblende on foliation surface.

across and growing over foliation. Marble, quartzite and meta-conglomerates, described in Bennett (1989), were not observed in the study area.

Meta-Volcanic Component

The meta-volcanic component is mostly comprised of amphibolitic schists and semi-schists resulting from the metamorphism of intermediate to basic volcanic flows and possibly terrigenous deposits of volcanic sediments. Well preserved plagioclase phenocrysts suggest porphyritic dacites and andesites for the protolith (fig. 2.3). This unit also contains minor felsic flows and is intruded by dikes and sills of varying composition.

Amphibolitic Greenschists

The meta-volcanic schists and semi-schists are light to dark green in color on fresh surfaces due to the presence of chlorite and green amphibole (fig. 2.3c). Weathered surfaces are gray to rusty brown. Grain size is mainly fine, although medium to coarse-grained greenschists are also observed throughout this unit. Beds as thin as 0.5 meters are observed while thicker layers up to 10 meters have contacts obscured by vegetation.

Variable protolith composition results in variable mineral content of the different flows within the metavolcanic unit. Mineral assemblages include quartz, plagioclase, chlorite, amphibole, epidote, sphene, and opaque minerals. Quartz and

Figure 2.3. **A.** Sample 181-32, a meta-dacite with well preserved but slightly deformed relic plagioclase phenocrysts. **B.** Cross polarized photomicrograph of sample 181-149. Arrow points to relict plagioclase (white porphyroclasts).

Figure 2.3.C. Hand sample of typical Slollicum meta-dacite from sample 181-74.

plagioclase are abundant in aggregates elongate parallel to foliation and make up 40%-70% (visual estimation) of the rock. Quartz commonly exhibits slight undulatory extinction. In many samples, coarser amphiboles are irregularly zoned with lighter cores and darker rims. A weak to moderate foliation on the rock consists mainly of chlorite with aphanitic, acicular amphibole. Epidote and clinozoisite occur commonly as small grains and aggregates. Opaque minerals and sphene are common as accessory minerals.

Fine grained greenschists composed mainly of acicular amphibole and chlorite occur sporadically within the matedacites. These rocks are extremely similar to greenschists of the Cogburn unit, a full description of these rocks is related in the chlorite-amphibole greenschist section in the Cogburn Package descriptions.

Meta-sediment layers 1-2 meters thick are intercalated throughout the volcanic component of the Slollicum in the study area. Most samples consist of what appears to be a fine grained metamorphosed feldspathic sandstone.

Felsic flows and mafic intrusives

Felsic flows are interspersed sporadically with the meta-dacites. Figure 2.4 is a cut hand sample of a felsic flow. They consist of plagioclase phenocrysts and quartz aggregates in a quartz/plagioclase/muscovite groundmass. The plagioclase phenocrysts vary from less than 1mm to 4mm in size, and commonly show Albite and/or Carlsbad twinning with sericite alteration.

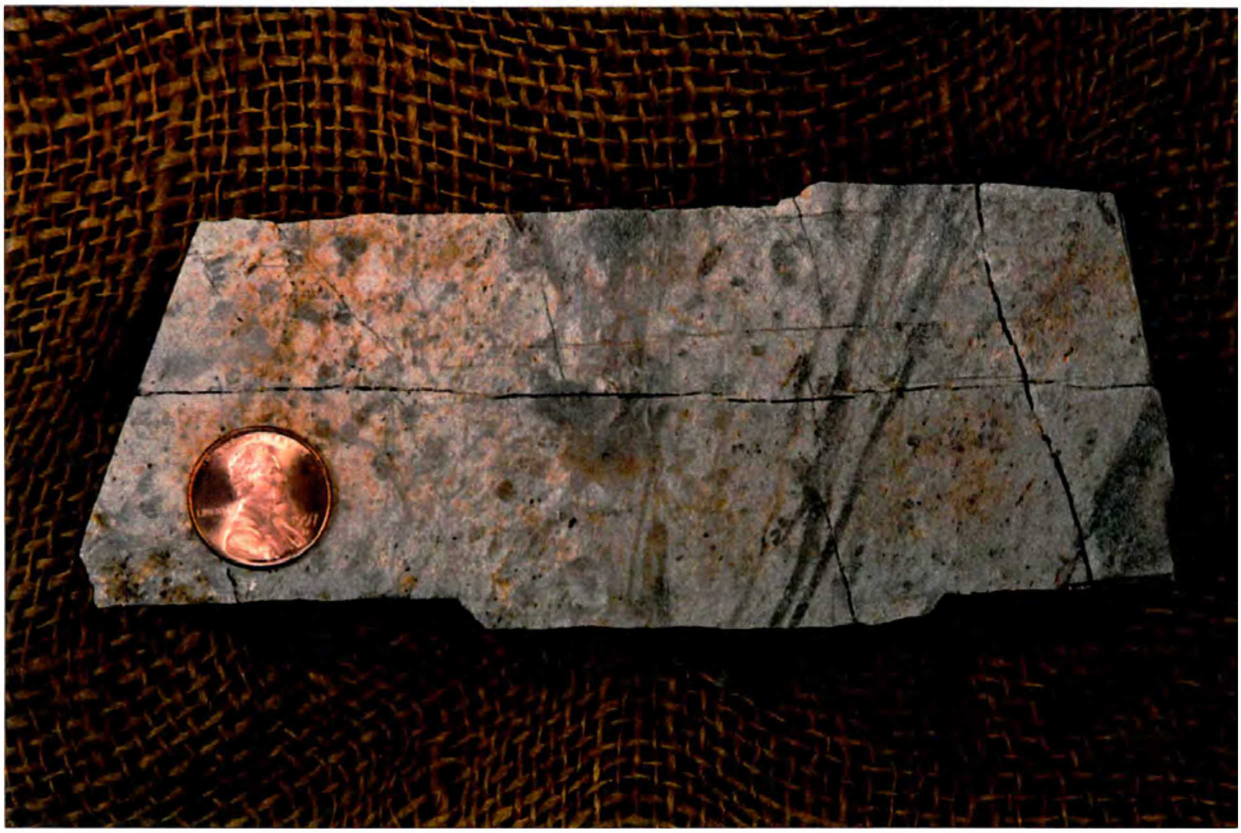

Figure 2.4. Cut hand sample of a rhyolitic flow from site 181-3.

Some phenocrysts exhibit undulatory extinction and grain size reduction is commonly observed. Muscovite, with a strong preferred orientation, and flattened quartz and plagioclase grains define a well developed foliation. Foliation wraps around the plagioclase phenocrysts. Grain size reduction occurs in pressure shadows around the plagioclase. These were probably rhyolitic flows.

The intrusive rocks are hornblende meta-gabbros that crop out near the thrust contact. These gabbros do not contain pyroxene. The meta-gabbros commonly intrude parallel to layering in the country rock and are approximately 1-5 meters, possibly more, thick. Fine (2-4mm) to medium (6-8mm) grained gabbros are observed and some exhibit a tectonite fabric which deforms the hornblende phenocrysts. Some hornblendes exhibit zoning with patchy cores, lighter mid-sections and darker rims.

Depositional Environment

The rock types of the Slollicum unit suggest a moderately deep to shallow marine shelf depositional environment. The meta-volcanic unit structurally lies atop the meta-sedimentary unit with intercalated beds of each unit within the other, and reflects a transition to increased arc volcanic activity.

Cogburn Package

The Cogburn Creek Group in the study area is located north-east of Talc Creek, and structurally lies above the Slollicum Schist and below the Settler Schist. The Cogburn Group crops out in a north-west trending belt (figs. 1.3, 1.4, and plate 1) and is composed primarily of phyllite, greenschist and meta-chert with minor marble (Gabites, 1985; Bennett, 1989). The Baird Meta-diorite lies along the north-east portion of the Cogburn outcrops. Gabites (1985) and Bennett (1989) include the Baird Meta-diorite as part of the Cogburn Creek Group. Gabites (1985) and Bennett (1989) also have described the Cogburn Group as a melange based upon the disrupted spatial association of the various rock types. The age of the Cogburn Group is unknown. However, the 225 Ma (Monger, 1989) Clear Creek Orthogneiss intrudes the cherts of the Cogburn package; thereby constraining the upper age limit (Brown, pers. comm.).

Gabites (1985), separated the Cogburn Group into several units: a chlorite-actinolite greenschist; a gray phyllite; and a meta-ribbon-chert. The greenschist and the gray phyllite are most abundant in the study area. Gabites (1985) described a massive chert unit, which was not observed; only bands or blocks of chert are found within the greenschist in the present study area.

Chlorite-Amphibole Greenschist

The greenschist component crops out adjacent to the ultramafic unit that separates the Cogburn and the Slollicum packages in the study area. The rocks in this unit are typically fine to medium grained, well foliated, and exhibit a variable bluish gray to dark green color on fresh surfaces (fig. 2.5) The weathered surface is rusty green to dark brown, in part due to iron oxide alteration. Layers from 2-6 meters thick were observed with local lamination and banding. Quartzo-feldspathic laminae and lenses up to 5 mm thick occur irregularly within the meter scale layers (fig. 2.6).

Mineral assemblages consist of quartz, plagioclase, actinolite or hornblende, chlorite, biotite, epidote, ilmenite and commonly tourmaline. Thin section analysis reveals 30-40% (visual estimation) of the rock consists of bladed or acicular amphibole. Bladed amphibole along with brown and green micas define the foliation which partially wraps small ilmenite porphyroblasts. Quartz and plagioclase occur in lenticular domains parallel to foliation. Epidote is not found in all samples but where it does occur, it is observed as small single grains, or less often as aggregates, scattered throughout the sample. Tourmaline is observed along or across foliation surfaces, and calcium carbonate is present in some of the greenschists. The protolith for these greenschists likely consisted of andesitic tuffs.

Figure 2.5. Typical Cogburn greenschist, greenish gray in color. Sample 181-183.

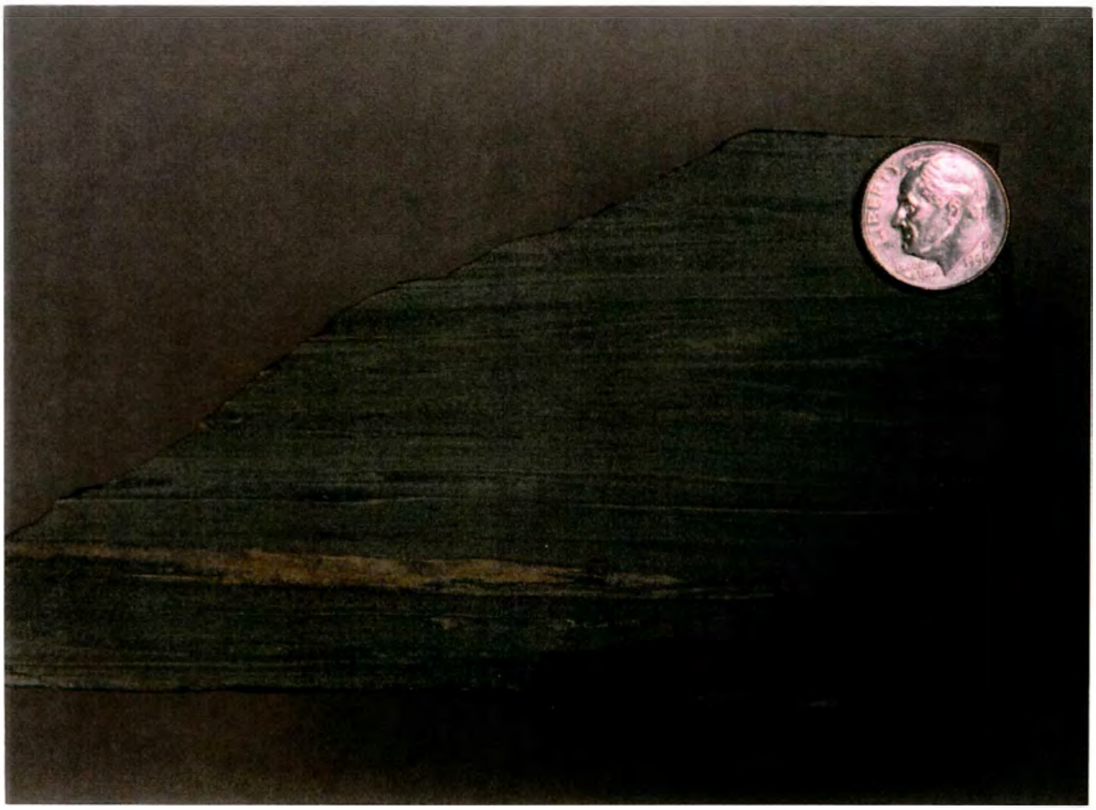

Figure 2.6. Sample 181-15b from the Cogburn greenschists showing lamination.

Figure 2.7. Hand sample of a biotite schist from site 181-60a. Note randomly oriented hornblende on foliation surface.

Plagioclase-Biotite Schists

Plagioclase-biotite schists (fig. 2.7) were observed scattered within the Cogburn greenschists. These schists commonly contains coarse, mainly tabular hornblende crystals partially wrapped by and partially cutting across a foliation defined by biotite. Garnet is commonly present and was also observed to cut across foliation as well as being wrapped by it in some samples. Minor calcium carbonate is present in some samples.

Chert

Meta-chert is found as isolated blocks and lenses, about 12 meters across, within the greenschists in the study area; contacts between the chert and greenschists are not well exposed. The chert is gray and light brown on fresh surfaces and dirty gray to dark brown on weathered surfaces. The chert is coarsely crystalline with a sugary texture and consists of recrystallized quartz which commonly exhibits a polygonal texture and undulatory extinction. Fine grained biotite, brown to green in color, exists in a sub-parallel orientation. Opaque inclusions are also observed within the chert.

Gray psammitic rock-phyllite

This unit crops out to the north-east of the chlorite-actinolite greenschist (fig. 1.3, plate 1). The rock is light to dark gray to black in color and weathers a dark gray to rusty brownish black. Color differences reflect a variation in the amount of graphite. The rocks are mostly fine-grained, but some contain coarse porphyroblasts of biotite and garnet.

The degree of foliation development varies from strong to weak. Samples collected closer to the ultramafic unit exhibit a more pronounced foliation, which generally trends parallel to the ultramafic contact. Many samples show kink banding.

Mineral assemblages consist of quartz, plagioclase, and ilmenite along with a variable graphite component; locally, samples contain biotite, muscovite, chlorite, garnet, carbonate, and zoisite. Quartz and plagioclase make up the bulk of the rock. The quartz commonly exhibits a polygonal texture and undulatory extinction. Garnets are embayed or poikiloblastic. Carbonate is found surrounding some ilmenites. Zoisite varies in abundance, existing mostly as isolated grains peppered throughout the section.

Foliation is defined by the platy minerals graphite, biotite and muscovite; while quartz and plagioclase grains are flattened or recrystallized into lenses or tabular forms. Foliation partially wraps garnet porphyroblasts which may be slightly dissolved on sides within the plane of foliation.

The presence of quartz, graphite and muscovite suggest this unit may represent metamorphosed silts with substantial organic and carbonate content.

Depositional Environment

The association of the gray phyllite and greenschist with chert and calcareous rocks suggests variable depositional environments for the different units of the Cogburn Creek Group. These rock types commonly occur together as a melange suggesting tectonic juxtaposition and telescoping within an accretionary prism of previously formed units.

Ultramafic Package

Outcrops of ultramafic rocks are scattered throughout the eastern Harrison Lake area. In the study area, a large map-scale sized slab of ultramafic rock was emplaced along the contact between the Slollicum and Cogburn units (fig. 1.3, 1.4, plate 1). It crops out in an elongate pattern oriented NW-SE parallel to the fault line and makes up the north-east face of the hill south-west of and adjacent to Talc Creek. This ultramafic unit covers a surface of approximately 7 sq. km.

Much of the ultramafic rock is unaltered or weakly serpentinized. The ultramafic rock is mainly hard, fine-grained, and dark green in color with a dark purple tint on fresh surfaces. It weathers a dark rusty-brownish-orange color. The serpentine (fig. 2.8) is mainly in the form of antigorite and commonly displays the typical smooth texture and greasy feel. However, the fibrous form of serpentine, chrysotile, is also present.

Figure 2.8. Hand sample 181-10c, an ultramafic rock showing a fresh green surface of antigorite and the orange weathering color.

Minerals recognized in thin section are serpentine, olivine, talc, carbonate (likely magnesite), and chromite or magnetite; no pyroxene was found. Analysis suggests the rock was a dunite prior to metamorphism. Olivine commonly shows alteration to serpentine that is slightly oriented in some samples, random in others or in a typical cross hatched pattern. Olivine also displays granoblastic texture and strain lamellae in less altered samples. Where present, talc and tremolite occur in a random pattern overprinting serpentine. The opaque mineral, in several samples, formed discontinuous layers or bands that were tightly folded.

X-ray diffraction analysis on 12 samples of the ultramafic rocks showed the serpentine most closely corresponds with the antigorite and chrysotile varieties. The olivine has a forsterite composition. The amphibole pattern is subject to interpretation but tremolite has been determined as the amphibole present in some samples. The carbonate was undetermined in x-rays due to inadequate resolution of weak signatures for the carbonate.

Thin section samples show trace amounts of serpentinization to upwards of 30% alteration to serpentine (visual estimation). However, no pattern of intensity of serpentinization was distinguishable between the core and margins of the unit.

Blocks and sheets of ultramafic rock of same composition, 12-20 meters across, also crop out near the main unit and thrust fault within the Cogburn greenschists in the study area.

Spuzzum Pluton

The Spuzzum pluton intrudes the Slollicum and Cogburn units in the eastern-most portion of the study area. Surface exposure of the Spuzzum pluton is approximately 250 km^2. Outcrops are abundant, mostly as cliff faces due to the resistance to erosion of the pluton. Boundaries between the Spuzzum pluton and the country rock mapped by Lowes (1972), and Monger (1986) have been modified in this study after detailed mapping (plate 1). Brown and Walker (1993) determined a 96 Ma U/Pb zircon age for the Spuzzum pluton at the northern end. Richards and McTaggart (1976) provided several K/Ar ages in the southern areas of the Spuzzum pluton; those are 81.79 Ma, 83 Ma, and 89 Ma nearer to the margins, and a 103 Ma age in the interior of the intrusion.

The Spuzzum pluton is a zoned pluton with an inner dioritic complex and an outer tonalite (Richards and McTaggart, 1976). The Spuzzum rocks in the study area are part of the tonalite body (fig. 2.9a). Visual estimations give values of 60-75% feldspars, entirely plagioclase; 15-30% mafic minerals including hornblende and biotite; 5-10% quartz; and up to 5% other minerals including muscovite, in the form of sericite, chlorite, and epidote as secondary or accessory minerals. Sodium-cobaltinitrate and Alizarin staining of three samples (170b, 173b, and 178) from near the margin of the pluton showed no K-feldspar was detected in any of the samples.

The hornblende grains in most samples are zoned with brown cores and green rims interpreted as metamorphic alteration.

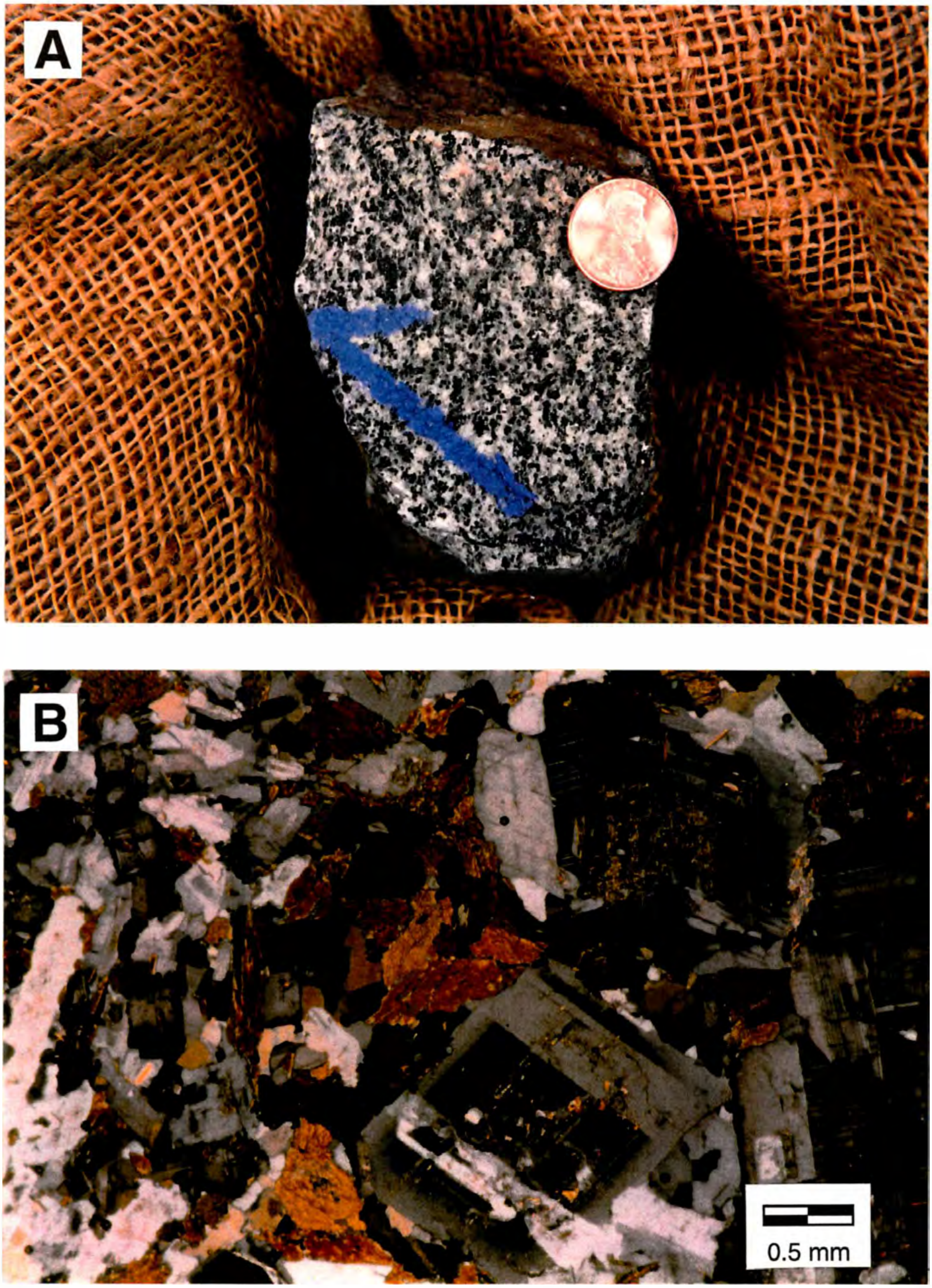

Figure 2.9. Spuzzum tonalite. **A.** Hand sample from site 181-173b. **B.** Photomicrograph in cross-polarized light from site 181-170a. The left side of photo is a finer grained tonalite while to the right is the more typical coarser grained tonalite.

Hornblende phenocrysts are commonly twinned and poikilitic with inclusions mainly of plagioclase but also minor, early-formed hornblende. Plagioclase grains are commonly concentrically zoned, display Carlsbad and Albite twinning, and show varying degrees of sericite alteration (fig. 2.9.b). Veins and larger zones of finer plagioclase laths and interstitial quartz with larger relict plagioclase phenocrysts crop out near the margins of the pluton. These zones contain interstitial chlorite and epidote as accessory minerals.

A weak magmatic foliation with a strike of approximately N20-35°E and a dip of 65-75°E, is observed locally in the tonalite in the study area. It is defined by lenticular zones of hornblende and parallels the pluton contact with the country rock.

Outcrops that expose the contact of country rock and pluton show injection zones and migmatization in some localities and sharp contacts in others.

Younger Intrusives

There are several late stage, post mid-Cretaceous intrusive stocks in the Harrison Lake area; two of which crop out in the study area. The first is an east-west elongate body that intrudes the Cogburn package and is located south-west of Old Settler Mountain (fig. 1.4, plate 1). Personal observation of this body is limited to one sample locality, but Gabites (1985) describes it as a light-gray fine-grained biotite-hornblende tonalite with quartz, plagioclase, biotite and hornblende. Much of the quartz and plagioclase has been recrystallized into smaller anhedral grains. Relict igneous textures preserved in the remaining larger plagioclase grains include zoning and twinning. The stock is unfoliated.

The second tonalitic stock observed in this area is located just north of the mouth of Talc Creek. The tonalite contains abundant plagioclase, commonly displaying Carlsbad and Albite twinning; some grains are compositionally zoned. Minor quartz grains show undulatory extinction and myrmekitic texture. Biotite makes up 1-2% of the rock and interstitial chlorite is a minor constituent. Although relict igneous textures are preserved, many quartz and plagioclase grains are highly recrystallized into smaller sub-grains. Two samples contain garnet: one in a vein that cuts a weak foliation, yet foliation slightly wraps around some of the garnets. In the other sample the garnets appear to have formed in a static environment.

Intrusive dikes and sills are common in the study area and cut across older units including the Slollicum and Cogburn packages and, according to Gabites (1985), the Spuzzum pluton as well. The dikes and sills observed in this study consist of: hyperbyssal dacites and tonalites with 3-15% mafic minerals consisting mainly of biotite; fine grained diorites with 25-40% hornblende and biotite; hornblende diabases and gabbros with over 50% mafics of hornblende and biotite. Some samples are unmetamorphosed or deformed, others are sheared or altered to varying degrees.

III STRUCTURE

Introduction

The rocks in the study area record at least three phases of deformation, designated D_1-D_3. The dominant regional deformational event (D_1) is associated with a terrane bounding thrust and is characterized by a strong foliation (S_1), lineations, and folds. D_1 fabrics are crosscut locally by a later fabric (D_2) associated with intrusion of the Spuzzum pluton. A third episode (D_3) resulted in localized zones of heterogeneous strain and reactivation of the dominant foliation. D_3 was a minor event of unknown origin that rotated and pulled apart minerals.

Dominant D_1 Structures and Fabrics

Terrane Bounding Thrust

The largest and most important D_1 structure is a terrane-bounding fault marked in the study area by a large slab of ultramafic rock emplaced between the juxtaposed terranes: Slollicum to the west, Cogburn to the east (fig. 1.3, 1.4, plate 1). The trace of the ultramafic unit and fault boundary across the topography along the southwest part of the contact suggests the geometry of the ultramafic unit could be a shallow dipping slab. Plate 1 illustrates how the ultramafic unit extends up a valley to the South-West and the contact is traced around knolls of the Slollicum unit. However, detailed field mapping revealed congruent foliations in both footwall and hanging wall rocks. Contacts of ultramafic and country rock (fig. 3.1) seen in the field area suggest that the ultramafic unit contact is sub-parallel to foliation, which dips moderately to the north-east. Gabites (1985) proposed the intrusion of several Spuzzum plutons as the cause for the irregular outcrop patterns of other ultra-mafic slabs. If that is the case, it may be applied to this ultramafic unit on the SW side where a younger pluton intrudes the country rock (plate 1).

An alternative that could explain the irregular outcrop pattern is large scale folding of the fault after thrusting as interpreted by Reamsbottom (1974) and Feltman (1997). Large anticlines are shown in figure 1.3. A cross section of the study area, incorporating this interpretation, (fig. 3.2) shows the terrane boundary as a folded thrust fault dipping moderately to the north-east. The folds depicted in the cross section could help explain outcrop patterns of ultra-mafic rocks and greenschists along strike of the fold. Differing orientations of the same, albeit untraceable, rock unit at different outcrop localities supports the idea that large scale folding of country rock accompanied or followed faulting.

Figure 3.1. Contact between the Cogburn greenschist (on the left) and the ultramafic unit (on the right). View is to the SE approximately parallel to trace of the contact. Note the steepness of the contact.

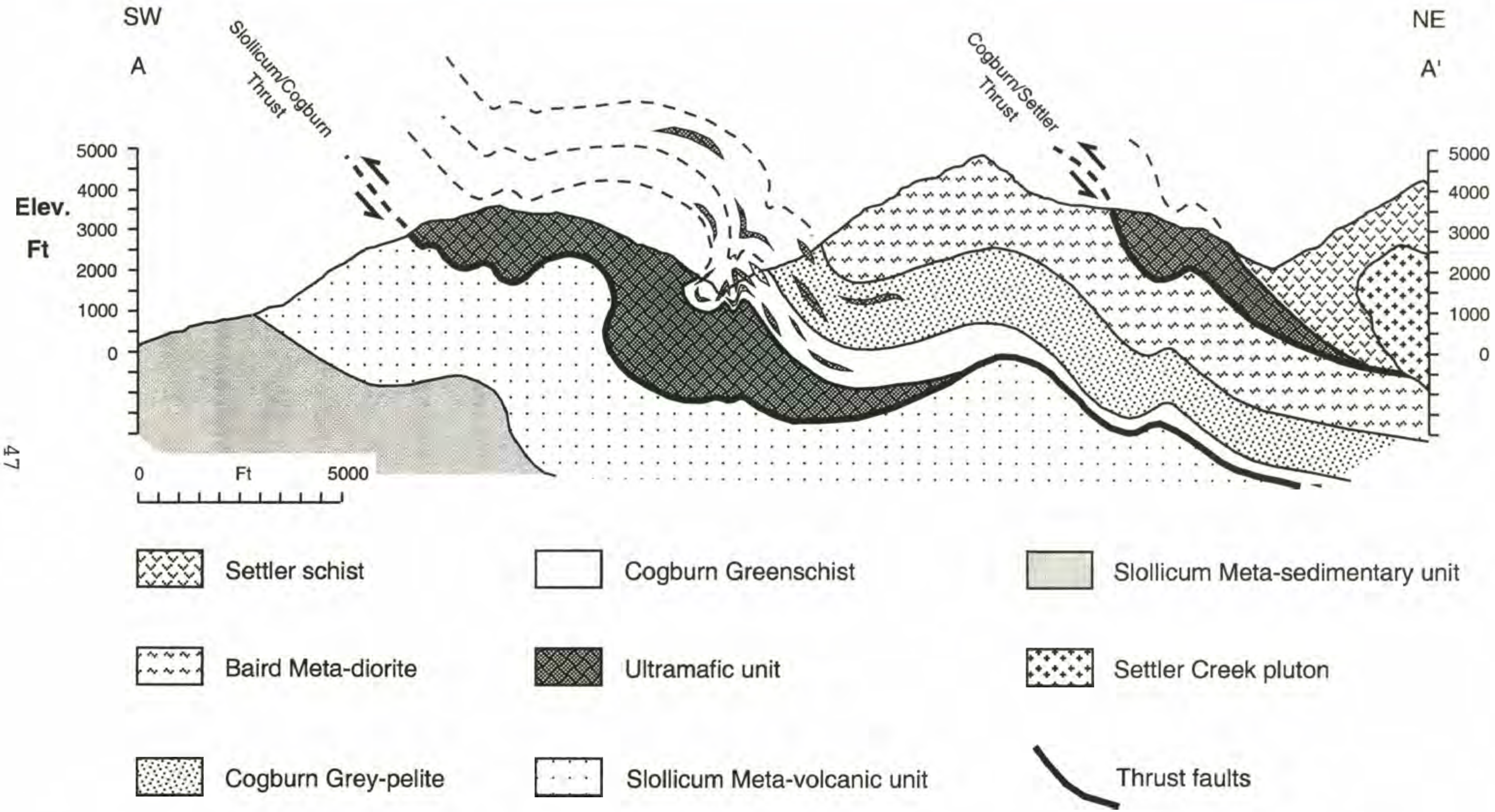

Figure 3.2 A cross section of the map area along A-A' in plate 1 and shown in figure 1.4. Diagram depicts folding of the rock units and the Slollicum/Cogburn thrust fault. No vertical exaggeration.

Ductile shear zones are abundant over approximately a 1 km wide area on either side of the fault, mainly near the north west boundary of the ultramafic unit. Slollicum rocks locally display thin-section scale shear zones 1-2 mm thick (fig. 3.3a) marked by metamorphic minerals, mainly chlorite and actinolite. Greenschists of the Cogburn unit display spaced outcrop-scale shear zones near fault contacts (fig. 3.3b). Shears are marked by zones of very closely spaced foliations and highly fissile textures. Zones range from 10 cm to 3 meters wide, commonly anastamosing, and exceed 6 meters in length with terminations obscured by ground cover.

Blocks between shear zones are commonly long with tapered ends, where ends are exposed and not covered by vegetation. Internal foliation within the greenschist blocks is well developed and is commonly parallel to the shear zones. The degree of intensity of internal fabric depends on lithology.

Some blocks of meta-gabbro are virtually unfoliated adjacent to bounding shear zones. Other blocks of meta-gabbro display internal fabric, for example S-C fabric (fig. 3.3c), and small scale anastamosing shears with increasingly pervasive foliation near the shear zones.

Imbrication of blocks is not discernible from outcrop observations. Kinematic indicators are also not observable at outcrop-scale in the Cogburn greenschists. However, coarse meta-gabbros near the fault that are partially

Figure 3.3. Fabrics displayed near the fault zone. **A.** sample 181-74 in the Slollicum meta-volcanic unit displays small thin section scale shear zone.

Figure 3.3.B.1. Outcrop scale shear zones in greenschist of the metavolcanic unit, shear zones are anastamosing and commonly range from 1/2 meter up to 3 meters wide. Fabric in shear is penetrative and fissile.

Figure 3.3.B.2) Sketched overlay of B.1, darker shaded areas represent shear zones.

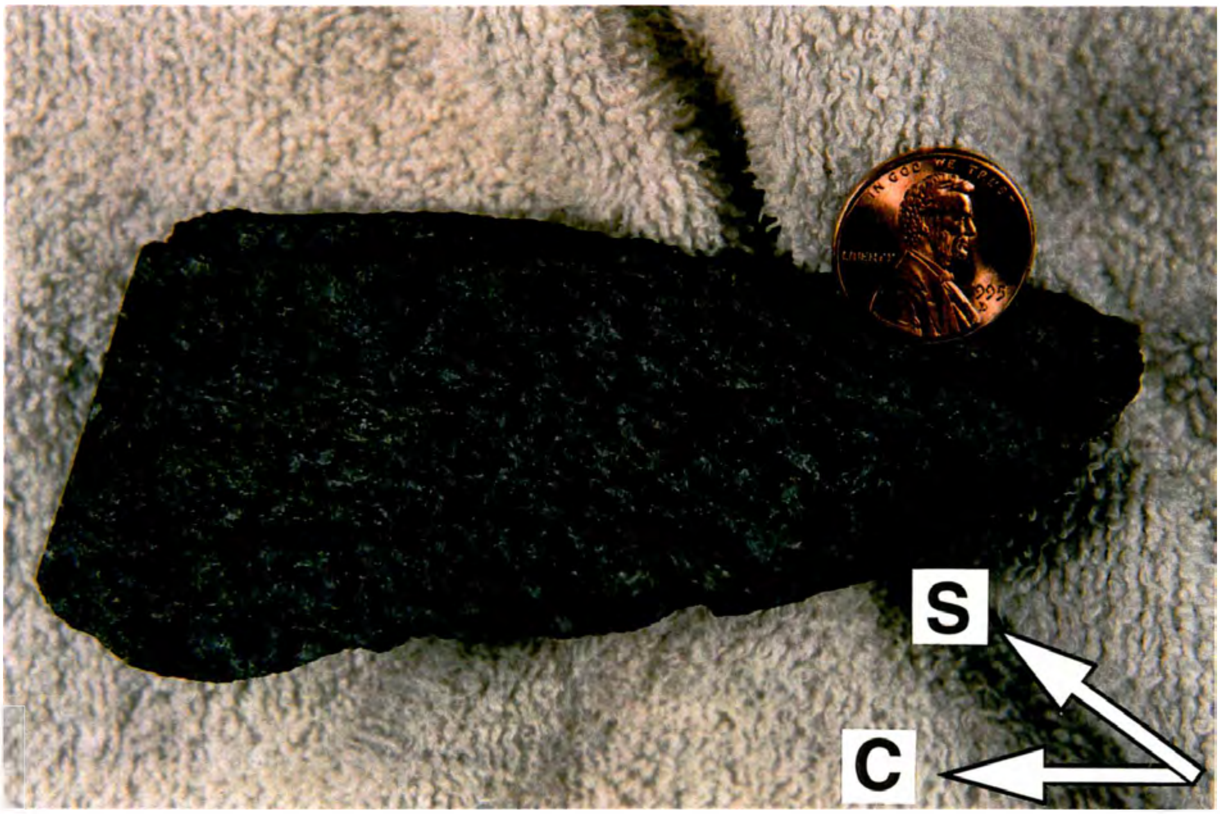

Figure 3.3.C. Sample 181-203 is a gabbro which displays excellent S-C fabric.

foliated or contain S-C fabric give top to the SW movement. Kinematics are discussed in detail below.

Isolated blocks of chert or ultra-mafic rock are observed within the greenschists of the Cogburn unit. Internal fabric was found to be fairly consistent and parallel to the margins of the blocks and to the foliation in surrounding greenschist. Greenschist fabric surrounding these blocks is the same as that observed in the shear zones; extremely penetrative and highly fissile.

Slickensides in serpentine (fig 3.4a) are characteristic near fault contacts. Small scale slickenfibers (fig. 3.4b) are also observed in some greenschists near the fault.

Figure 3.5 shows an example of the ultra-mafic/Cogburn greenschist contact marked by a 2-3 meter wide shear/fault zone. Foliation in the greenschist block to the left at this particular contact is a foliation oriented approximately perpendicular to the contact with the ultra-mafic rock. A second foliation parallel to the contact was developed as shearing took place. This second foliation in the greenschist within the contact zone consists of a combination of small scale shears defined by reoriented minerals and penetrative fractures filled with secondary minerals giving the greenschist a very fissile texture. The shears are discontinuous and run into the fractures, suggesting conditions overlapping the brittle-ductile boundary during deformation. Slickensides are present on the fracture

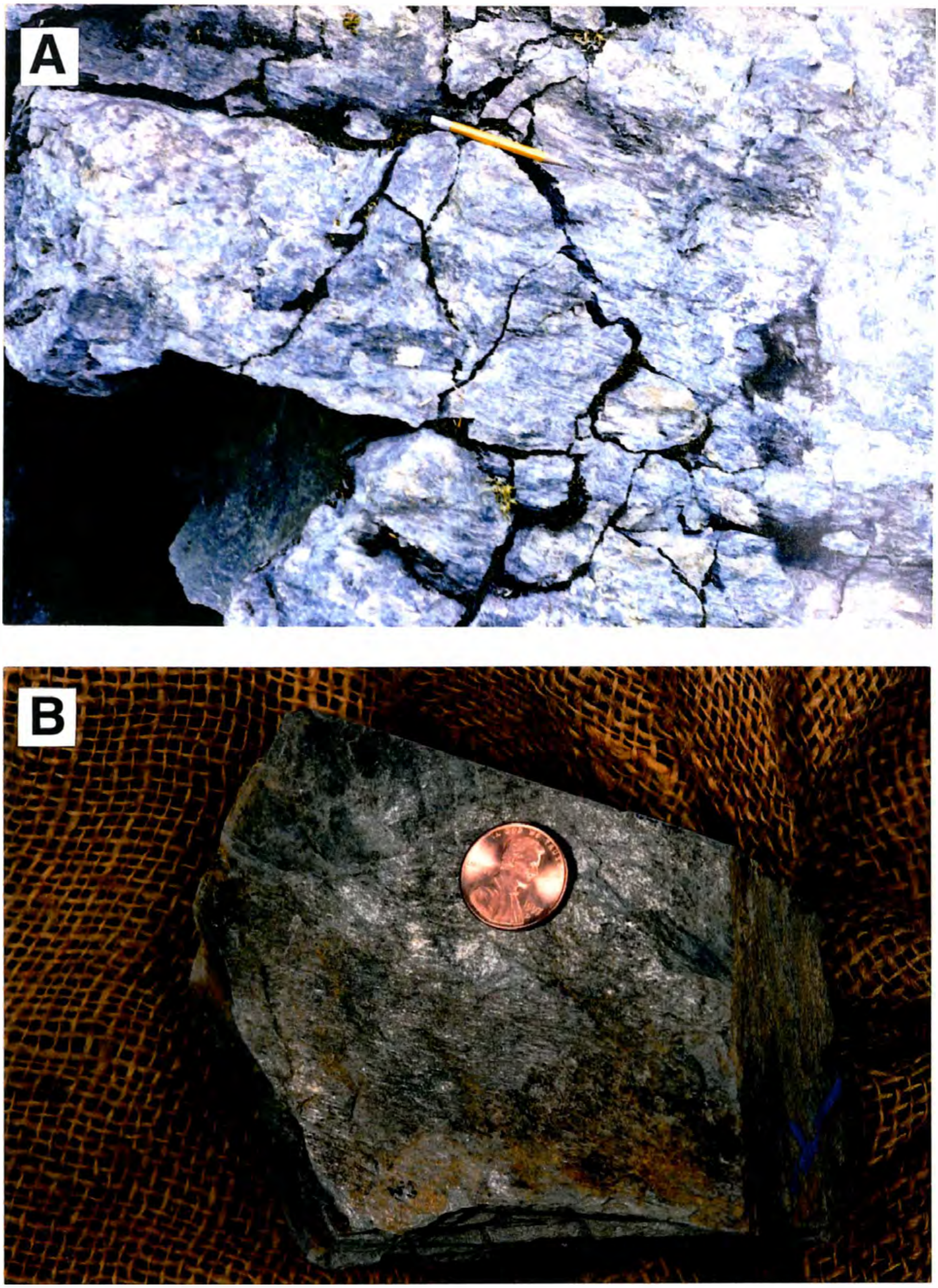

Figure 3.4.A. Slickensides in serpentine in field, pencil is oriented parallel to fabric; **B.** Sample 181-50a displays slickenfibers on foliation of greenschist of the Slollicum unit; fibers are approximately parallel to pencil in 3.4.A.

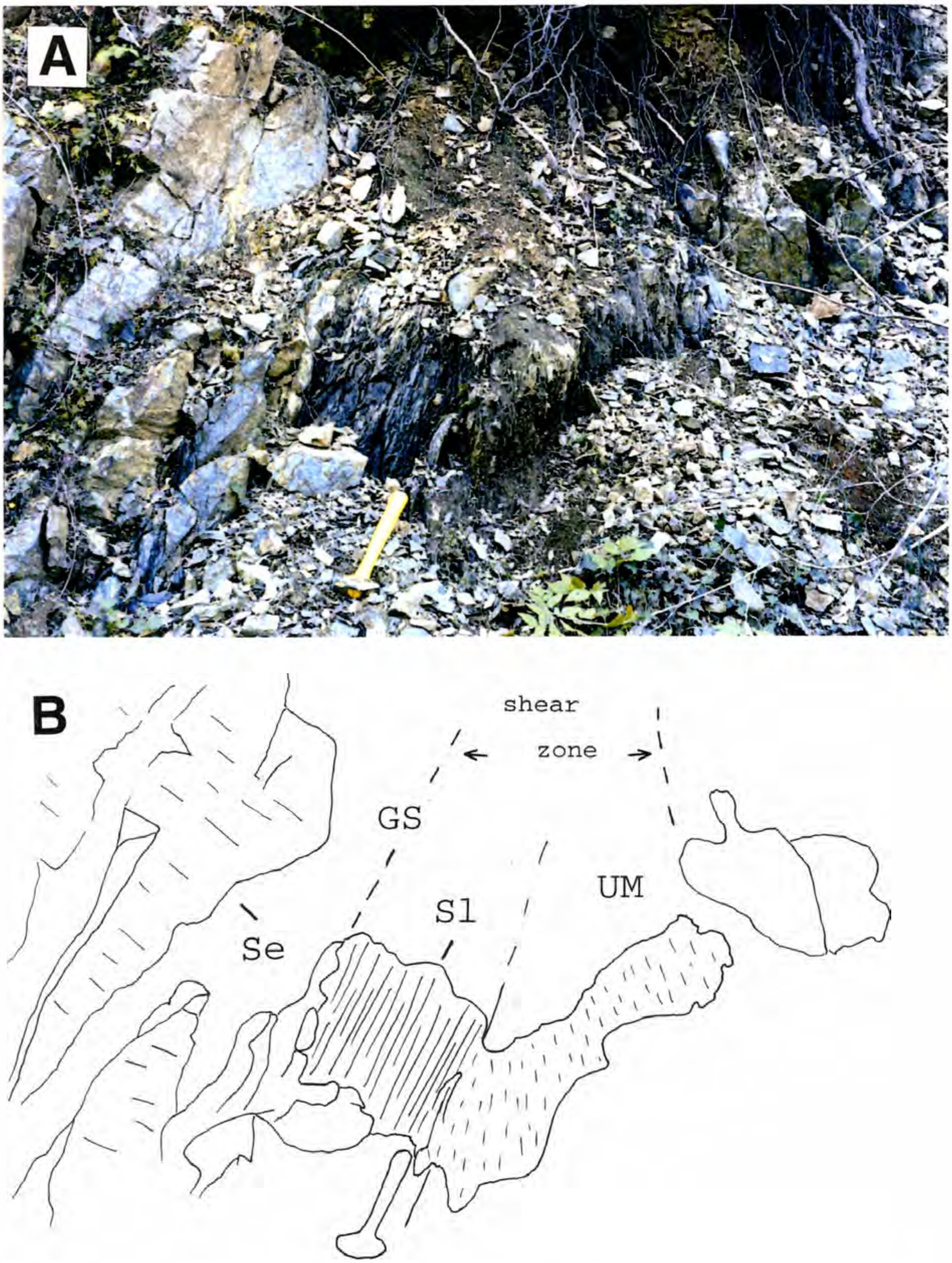

Figure 3.5. Detail of the contact of the Cogburn unit and ultramafic rock. **A.** Cogburn greenschist to the left, ultramafic unit to the right (hammer for scale is in line with the contact). **B.** Sketched overlay of 3.5.A illustrating where shear zones are. GS=greenschist, UM=ultramafic, Se=early foliation, Sl=later foliation related to shear zone.

Figure 3.5.C. Close up of 3.5.A. Greenschist fabric (left side of hammer) is much more penetrative than fabric in adjacent ultramafic rock.

surfaces. The fabrics at this locality are typical of those along the fault with the exception of the orientation of the early foliation in adjacent blocks which is commonly parallel to sub-parallel to the fault.

Outcrop scale, open to closed to isoclinal folds and kink bands in the Cogburn unit (fig. 3.6 a,b,c) are common near the main fault. Some beds in the Cogburn unit near the fault show imbrication with layers of ultramafic rock. This interlayering may be a result of isoclinal folding or fault slicing, but poor outcrops make it difficult to distinguish between these alternatives. However, some sites clearly show isolated lozenge-shaped blocks of ultra-mafic rock or chert completely surrounded by foliated Cogburn greenschist. A combination of fault slicing or shearing and folding of separate ultramafic blocks with country rock is the most likely scenario.

D_1 Foliation

Metamorphic foliation (S_1) is the predominant deformational fabric throughout the study area (fig. 3.7). Bedding (S_0) is generally parallel to foliation in both the Slollicum and Cogburn packages.

S_1 in the meta-volcanic unit of the Slollicum schist is a weak to moderate foliation, defined mainly by chlorite and acicular amphibole. Thin sections show foliation wrapping

Figure 3.6 Folds in the Cogburn unit **A.** Open fold at outcrop scale.

Figure 3.6 B. Small outcrop scale open to close folds; **C.** Kink banding.

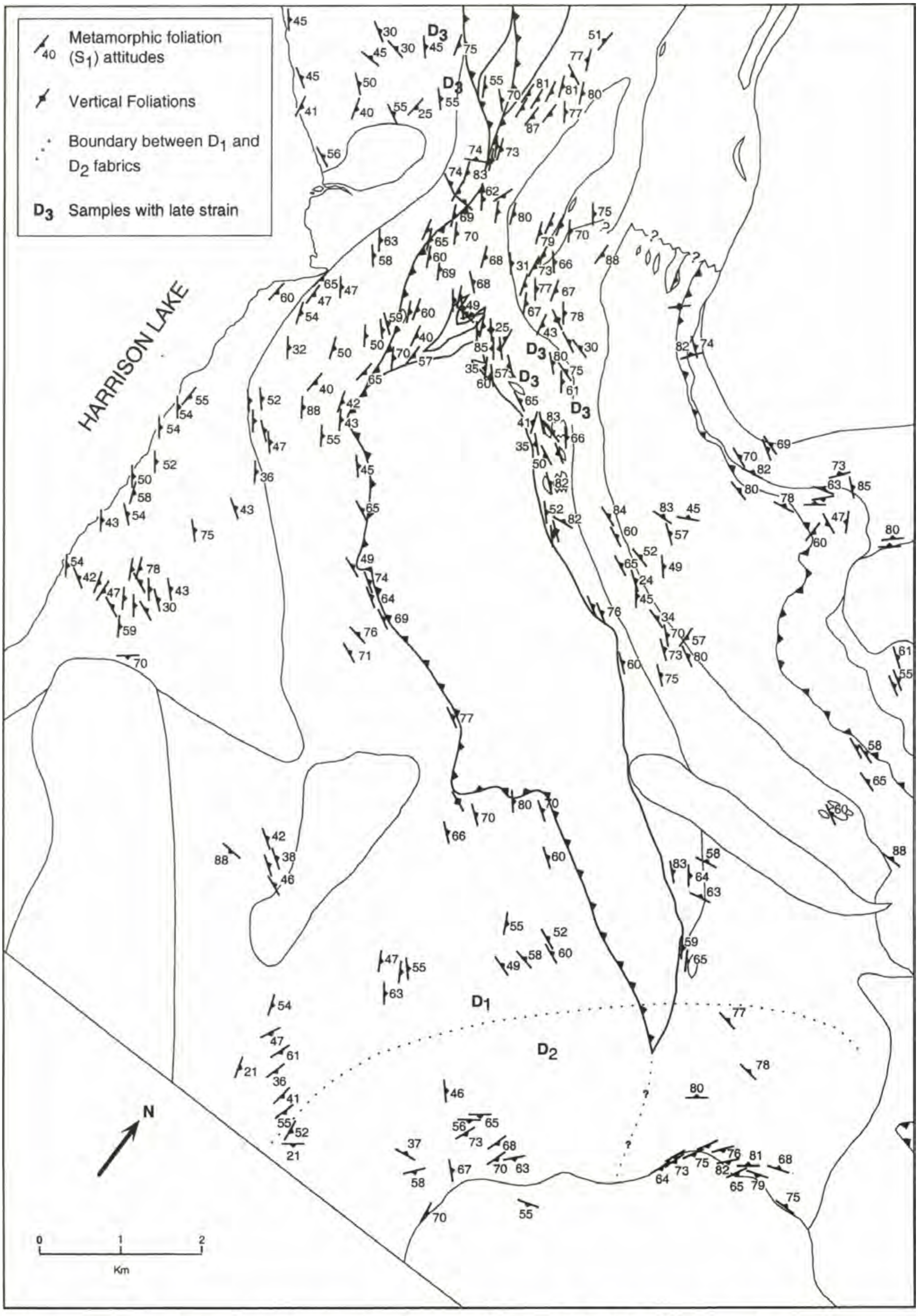

Figure 3.7. Distribution and orientations of foliations. Data from current study, Bennett (1989), Gabites (1985) and Brown (pers.comm).

relict igneous amphibole and feldspar phenocrysts, giving the rocks a braided appearance (fig. 2.3.b, 3.8).

Foliation in the more felsic flows varies from weak to moderate. Muscovite and chlorite define the foliation in these rocks.

S_1 Foliation in the fine grained greenschists of the Cogburn Ck. Group is well developed and is defined by acicular green amphibole, chlorite, and quartz and feldspar laminae. Asymmetric zonal crenulation foliations were observed in two different tectonites near the terrane-bounding fault contact (fig. 3.9).

Coarser-grained plagioclase biotite schists are less foliated than greenschists and contain large, partially wrapped amphibole and garnet. Biotite is the dominant mineral defining foliation in these rocks, with felsic laminae and minor acicular amphibole.

The gray phyllite displays a strong foliation defined by graphite laminae and flattened quartz grains (Bennett, 1989). Locally, biotite is a major constituent defining the foliation. Chert beds contain a weak foliation defined by discontinuous but aligned biotite.

Foliation in the ultra-mafic unit (fig. 3.10), defined by serpentine, is uncommon but is sub-parallel to the Cogburn-ultra-mafic contact as mapped (plate 1). Weak, discontinuous chromite or magnetite laminae, observed in thin sections of few ultramafic samples found near the fault zone are further evidence of foliation in the ultramafic unit.

Figure 3.8. Foliation, defined by amphibole and chlorite, wraps quartz and feldspar porphyroclasts giving the rocks a braided appearance. This section is from sample 181-149, dark material is stretched sphene aggregates.

Figure 3.9. Hand sample of specimen 181-6a showing chevron folds and a crenulation cleavage along hinges that is parallel to the long axis of photo.

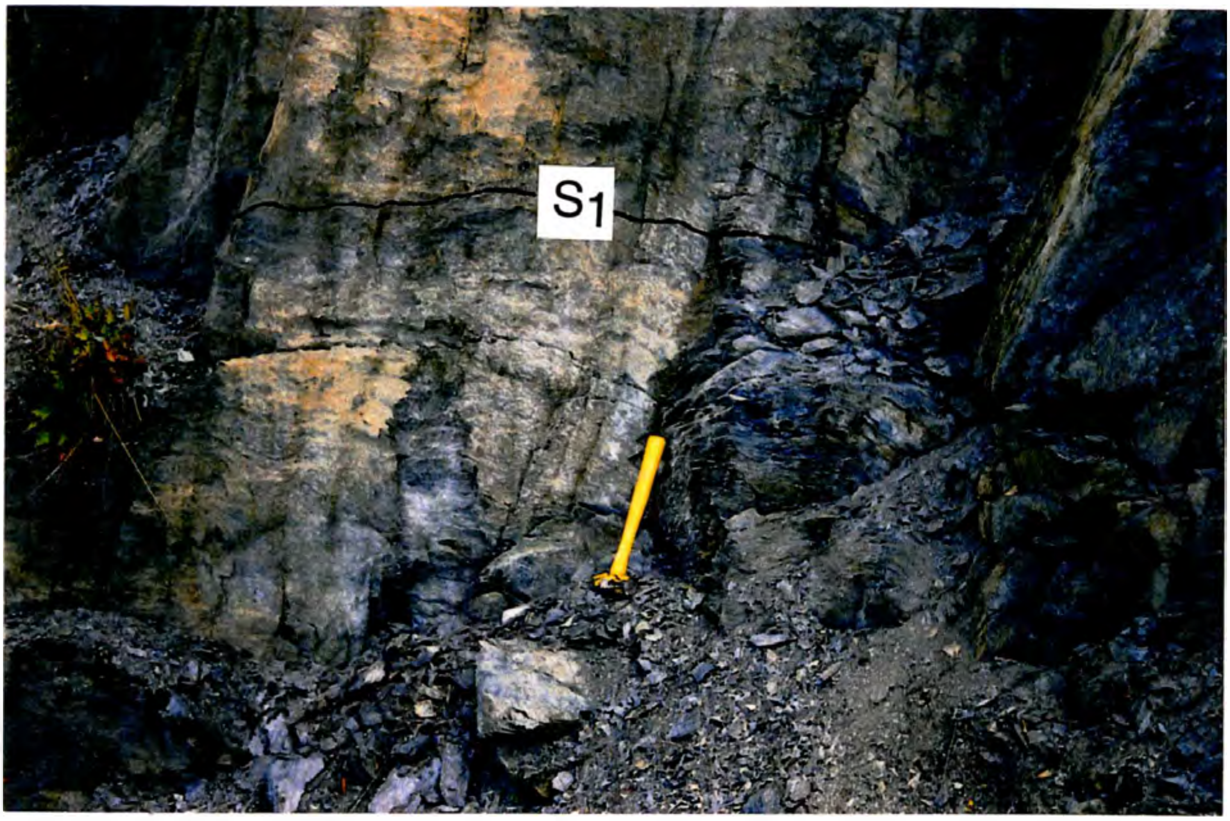

Figure 3.10. Ultramafic unit near the fault exhibits foliation parallel to length of long axis of photo. Foliation is also subparallel to fault contact (not pictured) and highly crenulated. Hinge line of crenulations are approximately parallel to length of hammer in photograph.

D_1 Lineation L_1

L_1 lineation consists of: 1) stretched plutonic grains (fig. 3.11.a); 2) lithologic streaking on foliation surfaces (fig.3.11.b); or 3) a mineral alignment, typically amphibole and less often biotite.

Lineations in the meta-volcanic component of the Slollicum schist are common and trend mostly north to northeast and plunge down-dip in the plane of foliation (fig. 3.12). Lineation directions in the rocks of the Cogburn unit are more varied. Lineations are observed trending to the NE, SW, N, and E suggesting disruption of the rock by folding or possibly faulting after formation of L_1.

D_1 Folds

Outcrop and microscopic scale folds are common within the Cogburn rocks near the Slollicum-Cogburn fault contact. Several styles of folds are observed. One style shows the foliation is axial planar to open F_1 folds and the fold axis parallel to the intersection lineations of S_1 onto S_0 (fig. 3.13).

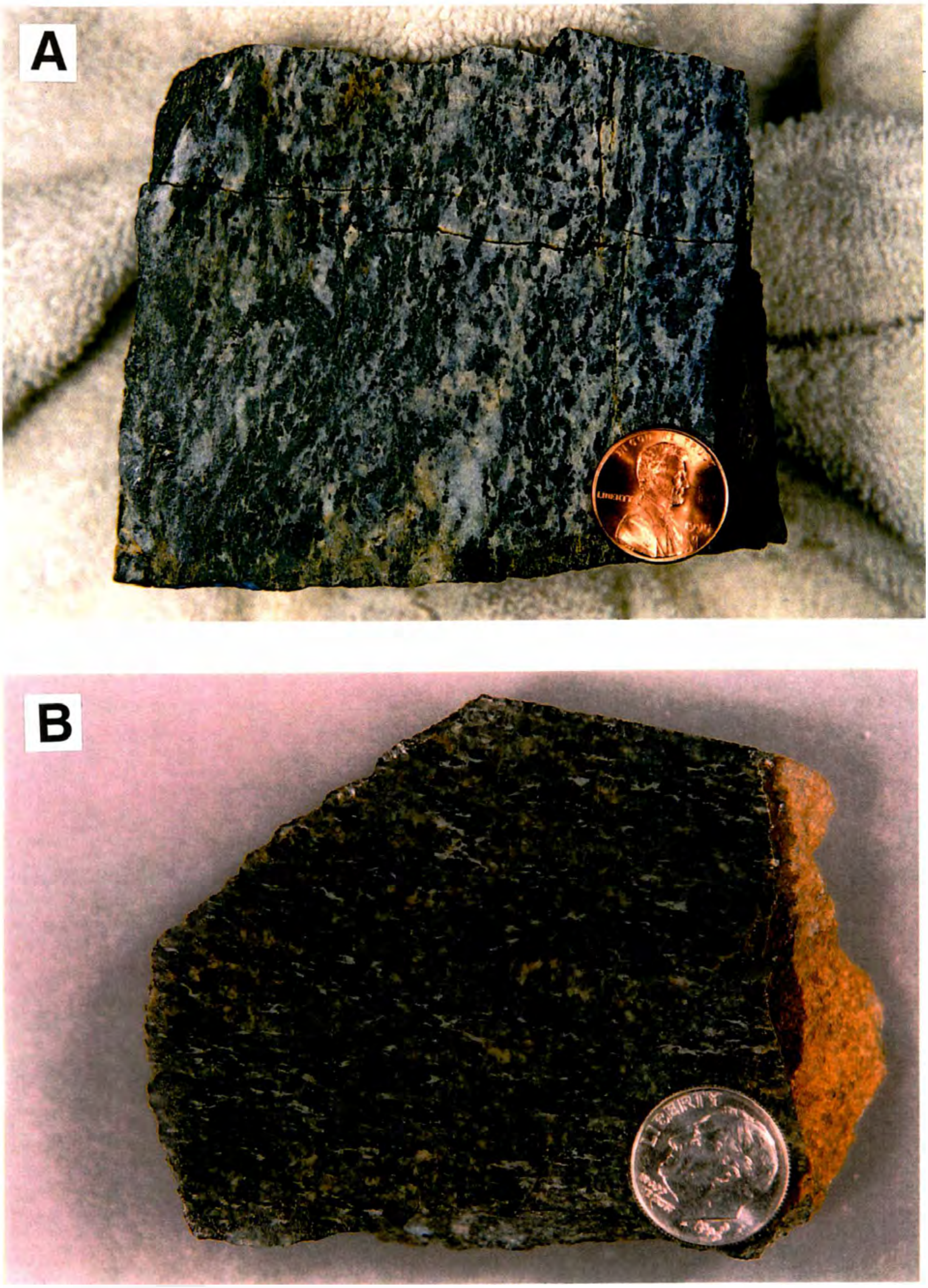

Figure 3.11. Examples of lineations on cut foliation surfaces. **A.** Stretched plutonic grains in a meta-gabbro, sample 181-201a. **B.** white streaks made by plagioclase in Slollicum meta-volcanic rock, sample 181-74.

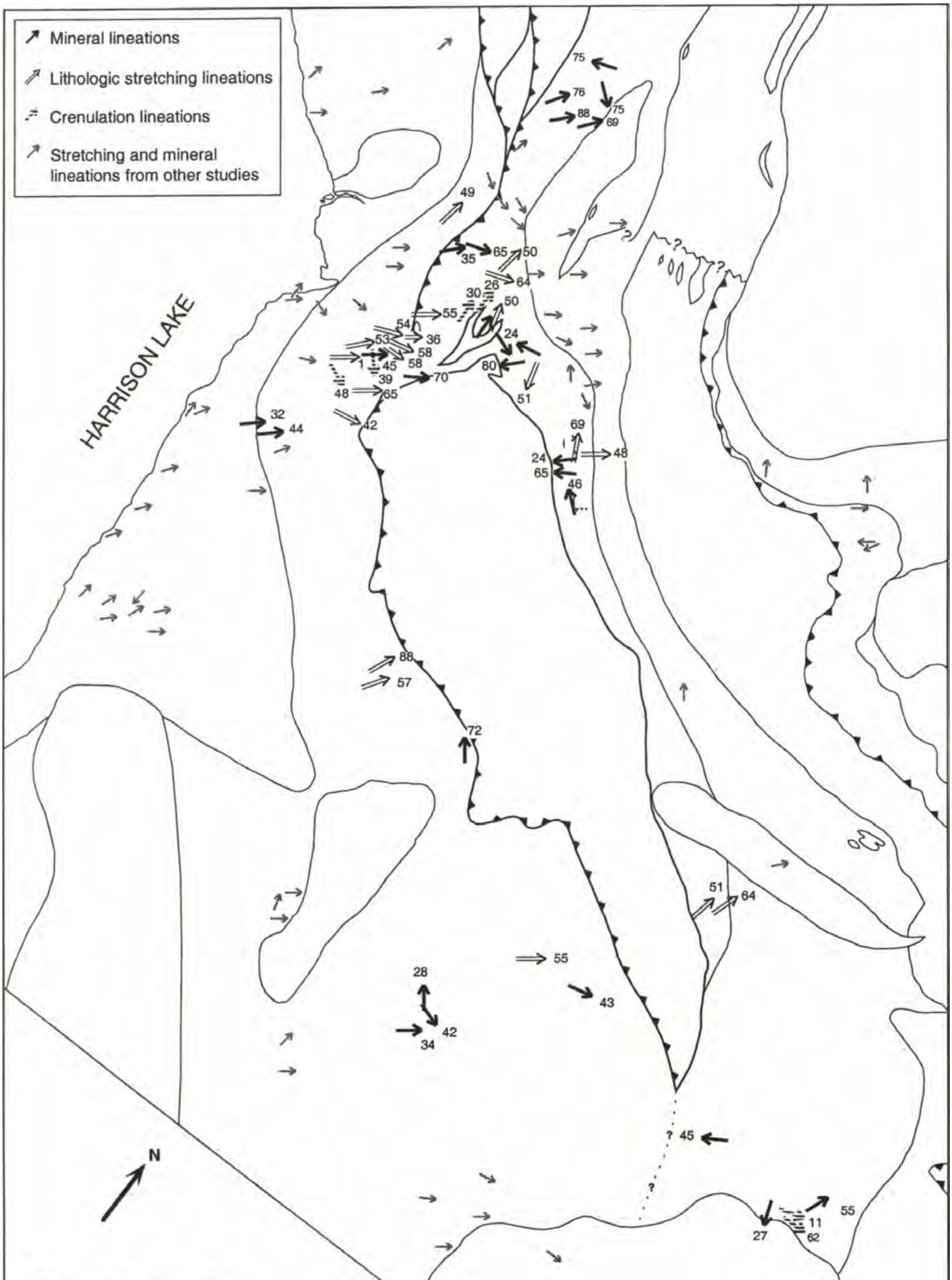

Figure 3.12. Distribution and orientations of lineations. See figure 1.4 for rock units.

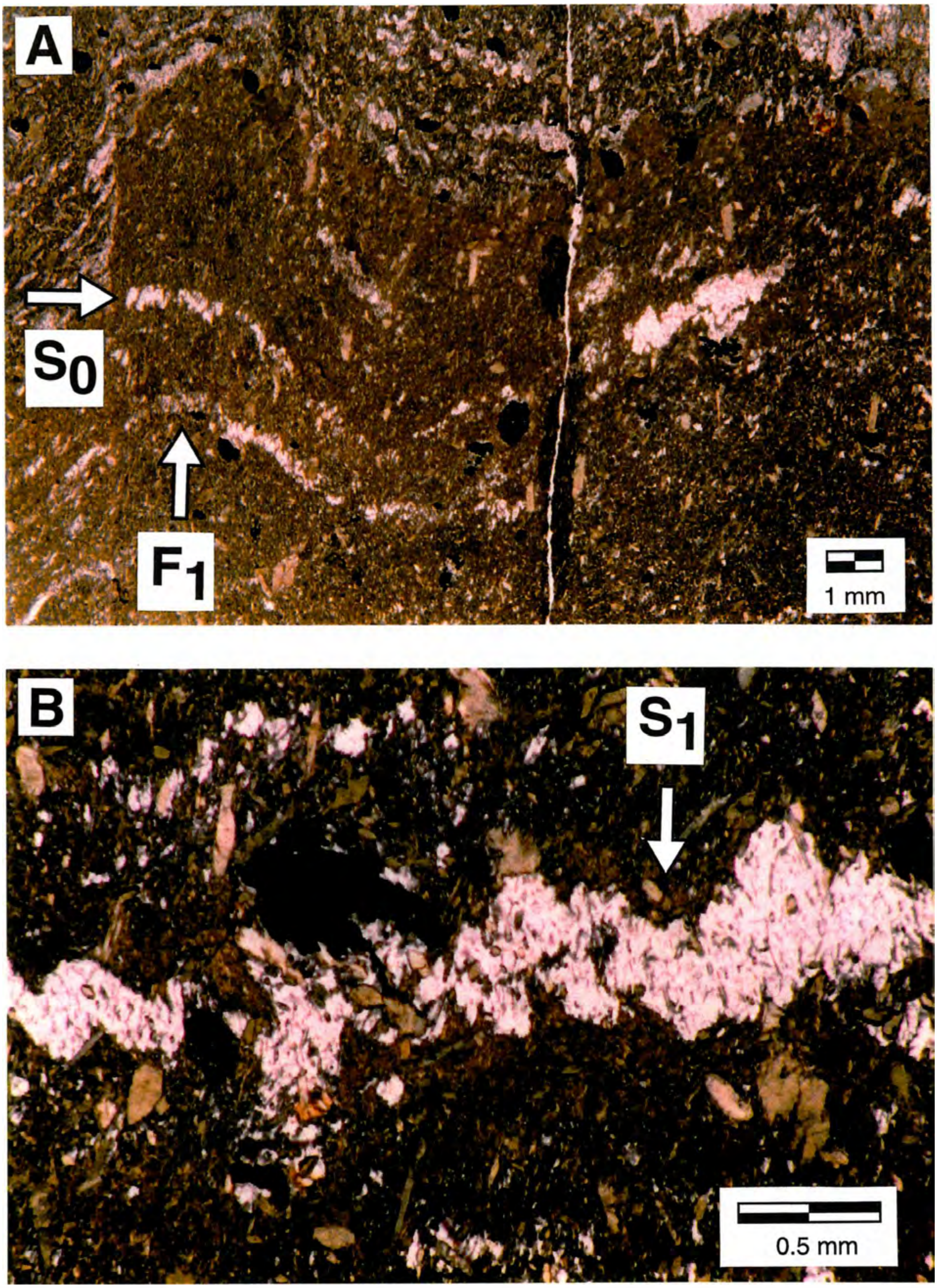

Figure 3.13. Thin section of fold in sample 181-187 showing relation of S_0, S_1 and F_1. **A.** Thin felsic laminae S_0 in an upright open fold which was later offset along S_1 cleavage plane. **B.** Close up of laminae displaying parasitic folding and S_1 cutting across laminae.

A second style of folds is nearly isoclinal with west verging axial planes, and inclined axes plunging to the north (fig. 3.14a). These folds are F_2 and occur in greenschists where the S_1 foliation is defined by thick quartz layers separated by thin epidote-rich layers with lesser aphanitic amphibole. The quartz layers are more competent than the greenschist layers resulting in disharmonic and parasitic folding of the greenschist layers (fig. 3.14b). Amphibole prisms are randomly oriented within the epidote-rich layers and across axial plane surfaces in some hinges suggesting they are syn to post folding. Locally, the folds are accompanied or later affected by metamorphism as evidenced by amphibole and quartz that are recrystallized with a partial axial planar preferred orientation (fig. 3.15). It is possible that this second style of folds may be related to the D_3 event and its' origin which is discussed below.

Small scale asymmetric chevron folds are observed in localities (figure 3.16) and are responsible for the zonal crenulation foliations illustrated in figure 3.9. The weak chromite or magnetite laminae in the ultramafic unit near the fault boundary are folded at thin section scale (fig. 3.17). These also may be a result of the D_3 event.

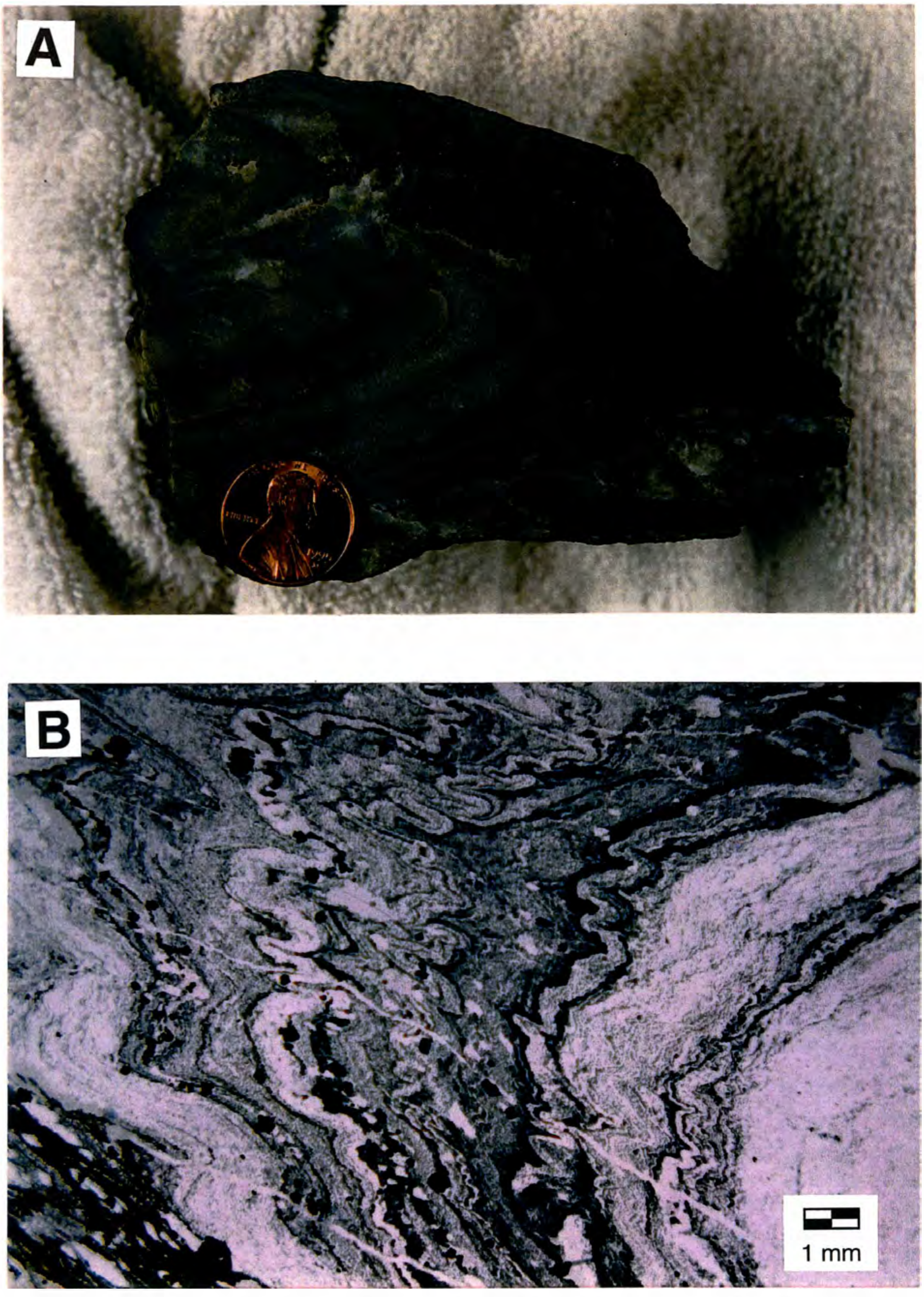

Figure 3.14. Folding in sample 181-57. **A.** Hand sample showing folded foliation. **B.** Thin section of same sample showing disharmonic folding of less competant thinner greenschist layers.

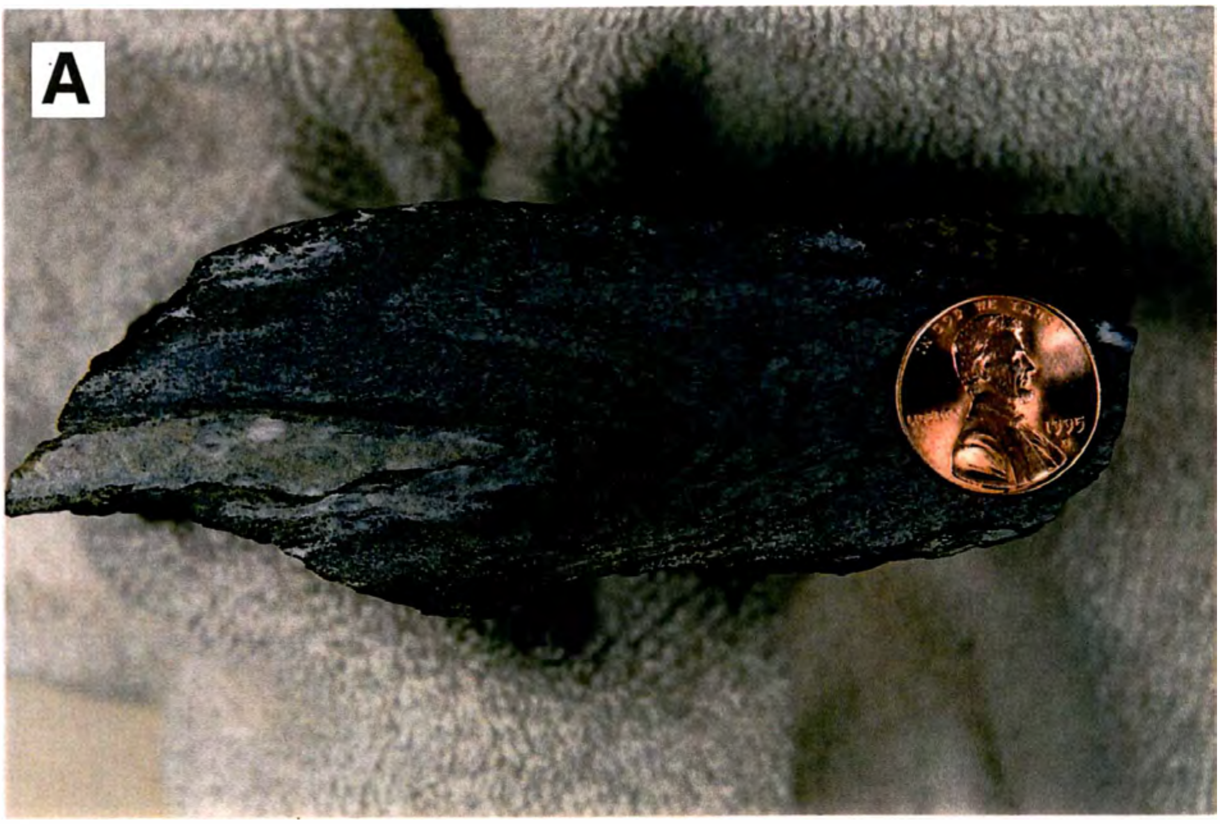

Figure 3.15. Folding in sample 181-182. **A.** S_1 foliation is folded. **B.** Thin section of same sample showing axial planar recrystallization of amphibole indicating continued metamorphism during folding.

Figure 3.16. Chevron folds and asymmetric zonal crenulations in thin section of sample 181-6a.

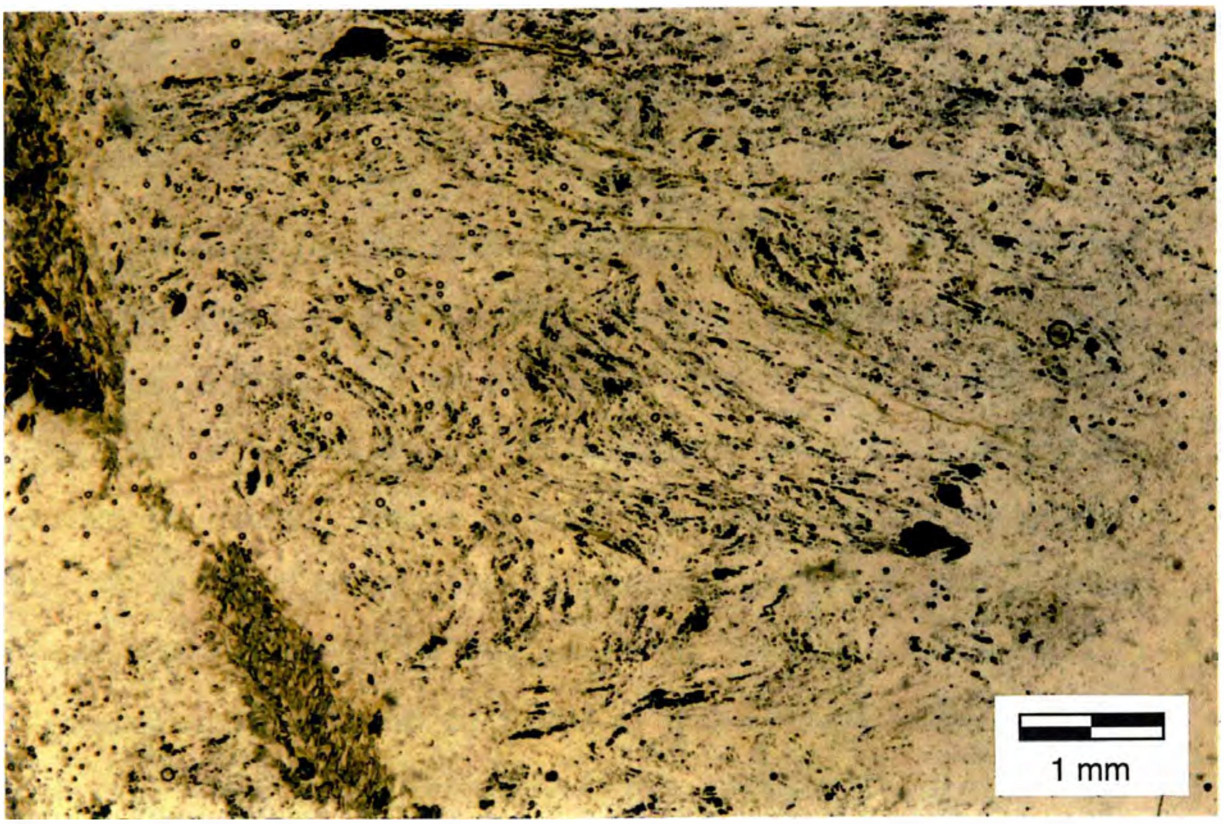

Figure 3.17. Folded disconnected magnetite layers in the ultra-mafic unit possibly formed from the reaction of olivine and water to serpentine and magnetite.

D_1 Kinematic Indicators

Kinematic indicators observed in the meta-volcanic unit of the Slollicum schist consist of asymmetric pressure shadows and tails on porphyroclasts. A typical example is shown in figure 3.18, which is a rhyolite flow within the meta-volcanic unit. The thin section of this sample shows large plagioclase phenocrysts with asymmetric pressure shadows consisting mainly of muscovite and lesser recrystallized quartz and plagioclase. Rocks near the terrane-bounding fault commonly show tails of chlorite and acicular amphibole wrapping around relict feldspar and amphibole phenocrysts in the greenschists and partially foliated gabbros. Pressure shadows around epidote grains in the Cogburn greenschists and stretched quartz aggregates are common yet only a few are asymmetric.

The majority of these indicators (8 of 13) show upper plate movement to the SW (fig. 3.19) in agreement with previous findings (i.e. Bennett, 1989). Two samples show upper plate to the SW but with normal movement instead of thrust movement. Three others show upper plate movement to the NE in NE dipping beds displaying normal fault geometry. These samples might be explained by large-scale, multilayer, flexural-slip folding of bedding and foliation in which flexural shear was taken up within certain layers instead of between layers. These also could be explained by an opposite

Figure 3.18. Sample 181-3 showing well developed pressure shadows around an igneous feldspar porphyroclast seen here in plane light.

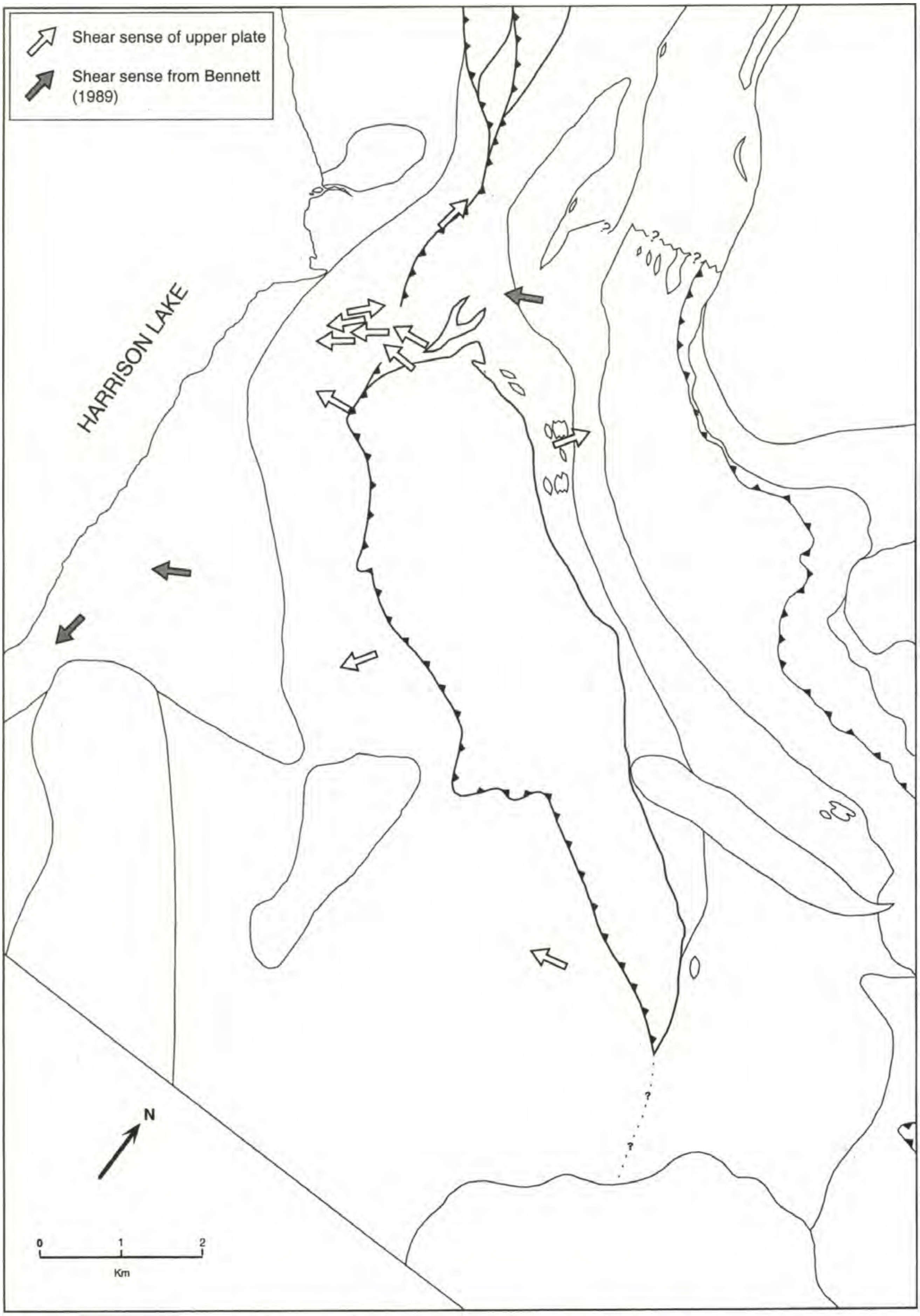

Figure 3.19. Shear sense of upper plate. See figure 1.4 for rock units.

sense of rotation for the simple shear component as described in Ghosh and Ramberg (1976) and referenced by Maekawa and Brown (1991) among others.

D_1 Summary

The D_1 event is characterized in the study area by stacking of the Slollicum and Cogburn terranes. Fabrics resulting directly from thrusting include foliations, lineations, and folding. The related foliation is the dominant regional fabric in the study area which formed mainly as a result of pressure solution. Associated kinematics indicate top to the southwest movement.

D_2 Deformational Fabrics

The second deformation fabrics (D_2) are restricted to a narrow zone around the Spuzzum pluton. The dominant D_2 fabric is a steeply dipping foliation that is subparallel to the contact of the Spuzzum pluton (fig. 3.7). The degree of foliation development varies from weak to moderately strong. Biotite is the main constituent that forms foliation with minor recrystallized acicular hornblende and lesser amounts of insoluble material occurring in laminae.

One sample near the perimeter of the aureole preserves a poorly developed crenulation cleavage suggesting foliation formed partly due to physical rotation of previously formed grains or material that defined D_1 foliation. Flattened grains in the plane of foliation suggest pressure solution also played a role in foliation development.

Lineations are rare and have shallow to moderately steep plunges with variable trends (fig. 3.12). Two lineations consist of biotite aligned on the foliation surfaces; one of long bladed chlorite crystals in the plane of foliation; and several are crenulation lineations.

Shear sense indicators are very rare. One sample displays an ambiguous S-C fabric. Shear sense from one sample shows top to the NW movement in a NW dipping foliation, which may be consistent with upward drag on an expanding pluton.

D_2 deformation is a direct result of intrusion of the Spuzzum pluton. D_2 post-dates the regional D_1 event as evidenced by the cross cutting nature of D_2 foliation. The time constraints of the D_1 and D_2 deformations are discussed later.

Late stage D_3 strain

A third event is characterized by rare local occurrences of large post-D_1 garnet and amphibole porphyroblasts which show heterogeneous late stage deformation (D_3) including rotated and pulled apart grains. These large porphyroblasts are considered post D_1 because they are randomly oriented across S_1 (fig. 2.2) and often incorporate the S_1 foliation from the D_1 event (fig. 3.20). S_1 is reactivated during the D_3 event causing rotation and separation of grains in many samples.

Large biotite porphyroclasts within the Cogburn grey phyllite observed in this study contain somewhat ambiguous dusty trails of inclusions of insoluble material. These trails could represent vestiges of an early pre-S_1 fabric described by Gabites (1985), Bennett (1989) and commonly observed by Talbot (pers. comm.), in which biotite, garnet, and hornblende grew over and incorporated an early fabric into the porphyroblasts.

An alternative is that the trails in the biotite porphyroblasts observed in the Cogburn gray phyllite in this study are vestiges of the S_1 foliation. Like the garnet and hornblende porphyroblasts mentioned above and described below, these biotites are post-regional tectonism and are rotated and pulled apart by reactivation of the S_1 foliation during the later D_3 event. The trails observed in porphyroblasts in this study appear to curve into parallelism with the dominant fabric (fig 3.21). They are also truncated along the plane of foliation and are partially recrystallized in pressure shadows (fig. 3.22) suggesting deformation occurred after majority of porphyroblast growth.

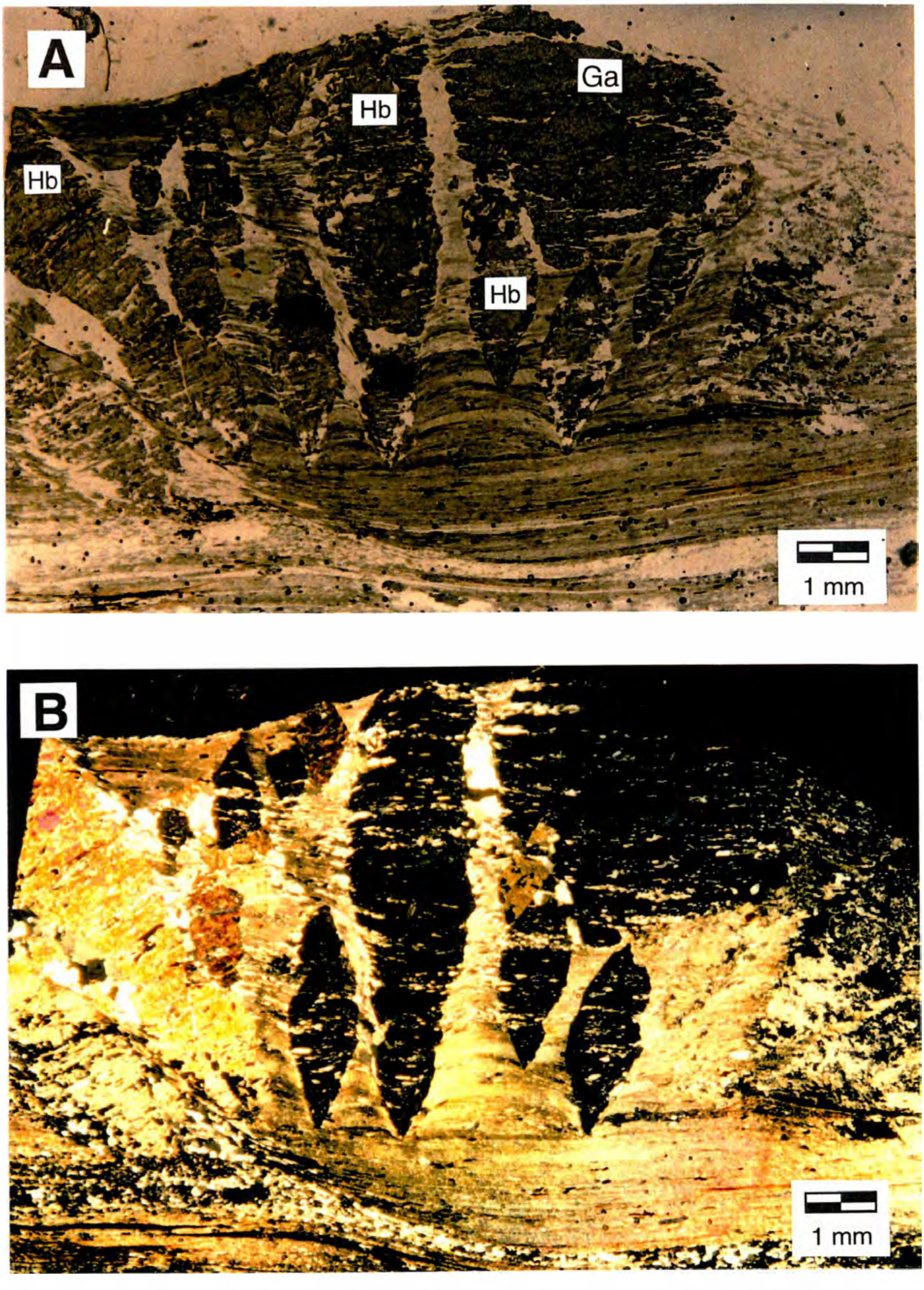

Figure 3.20. Helecitic hornblende and garnet overprinting S_1. Sample 181-155. **A.** plane light **B.** polarized light. Ga=garnet, Hb=hornblende.

Figure 3.21. Schematic diagram of dusty trails of inclusions in biotite porphyroblasts sketched from sample 181-94c.

Figure 3.22. Distended biotite porphyroblasts related to D_3. Sample 181-94c.

D_3 began during later stages of porphyroblast development. Figure 3.23 (a and b) shows two different samples of the same psammitic schist in the Slollicum unit, both show differing degrees of porphyroblast rotation. One sample of the Slollicum schist (NB66) shows slip along foliation planes off-setting a porphyroblast in one direction yet it appears other porphyroblasts are slightly rotated in the opposite direction.

Figure 3.23.b, a schematic diagram of a garnet porphyroblast from sample 181-155, shows rotation most likely a result of simple shear in which the porphyroblasts are competent but were rotated during later stages of growth as evidenced by overgrowth of crenulations in S_1 at the margins. The presence of new inclusion-free growth on parts of the garnet suggests continued heating after D_3 deformation ceased at this particular locality.

Sample 181-37 (fig. 3.23.c) contains large hornblende porphyroblasts that appear rotated in different directions, it is possible they have grown over a fold or are partially syntectonic with D_3 foliation reactivation. Sample 181-42c (fig. 3.23.d) shows moderate to large porphyroblasts of garnet and amphibole pulled apart by the same foliation they grew across and, in the case of the hornblende, encompassed.

The presence of post-D_1 porphyroblasts indicates this late stage strain is a deformational event, other than D_1, which resulted in local manifestations of strain in less

Figure 3.23. Pictures and illustrations depicting late stage D3 strain in which large porphyroblasts overgrew foliation and were then rotated and pulled apart within the same foliation they overgrew.

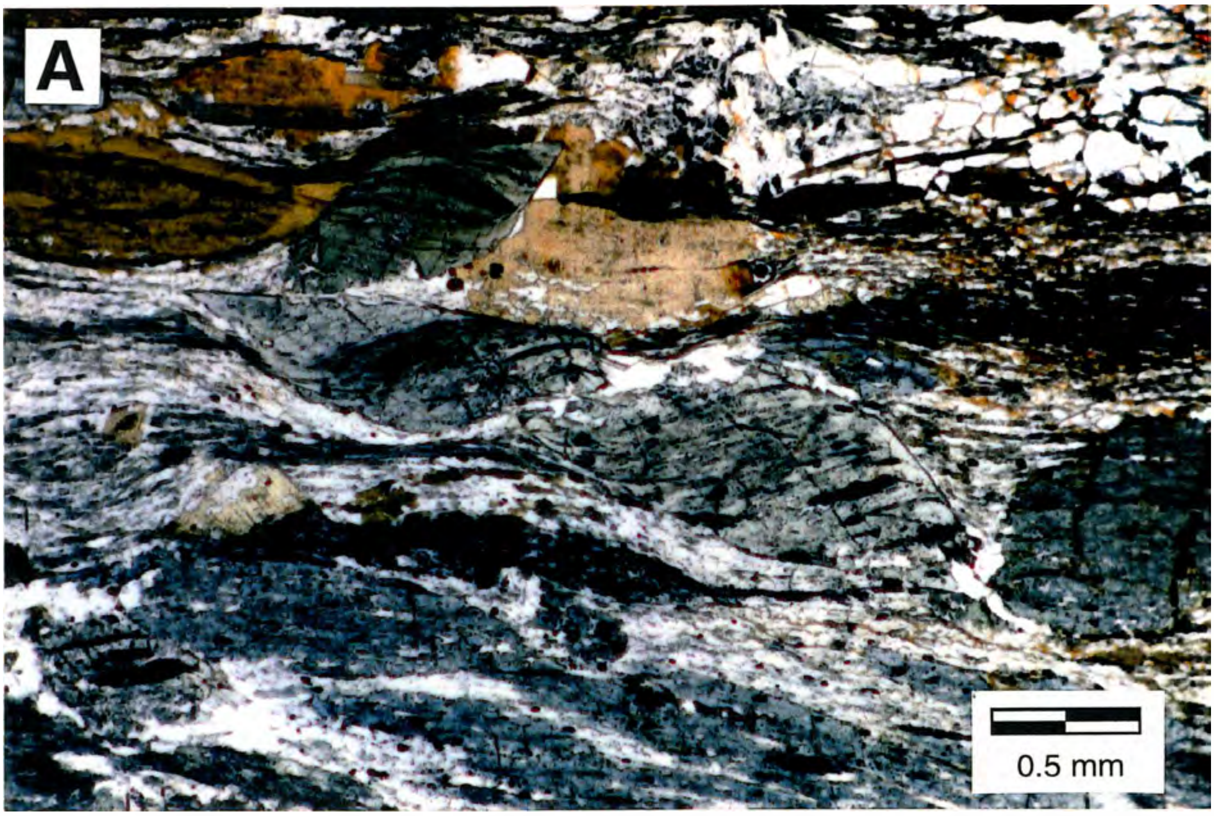

A. Sample NB66 showing offset hornblende with slight top to left rotation. Other grains show top to right rotation in other parts of sample.

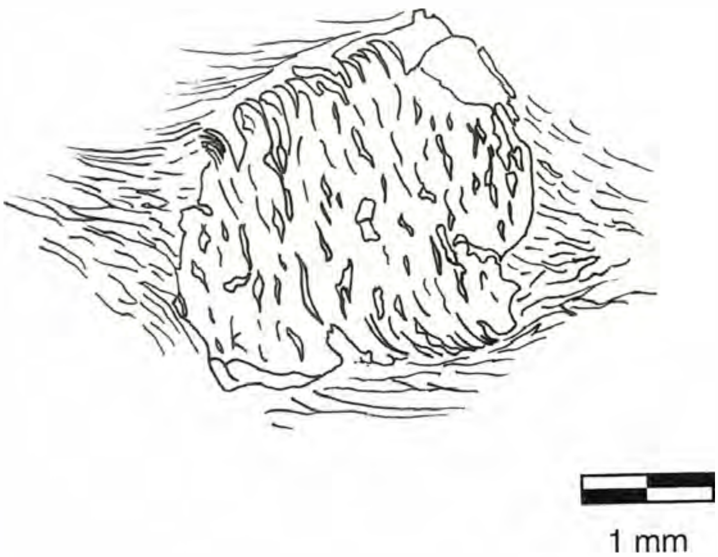

B. Diagram of large garnet in sample 181-155 which has overgrown the foliation and is later rotated within that same foliation.

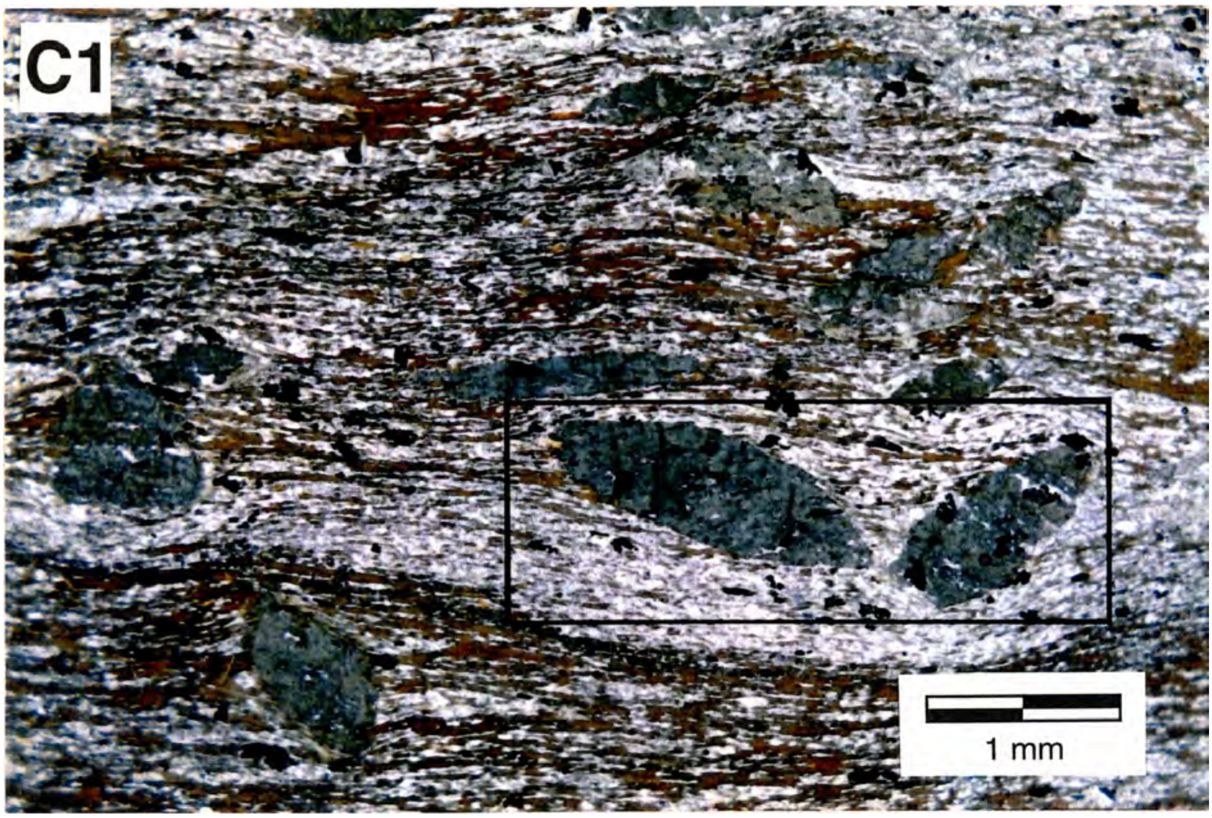

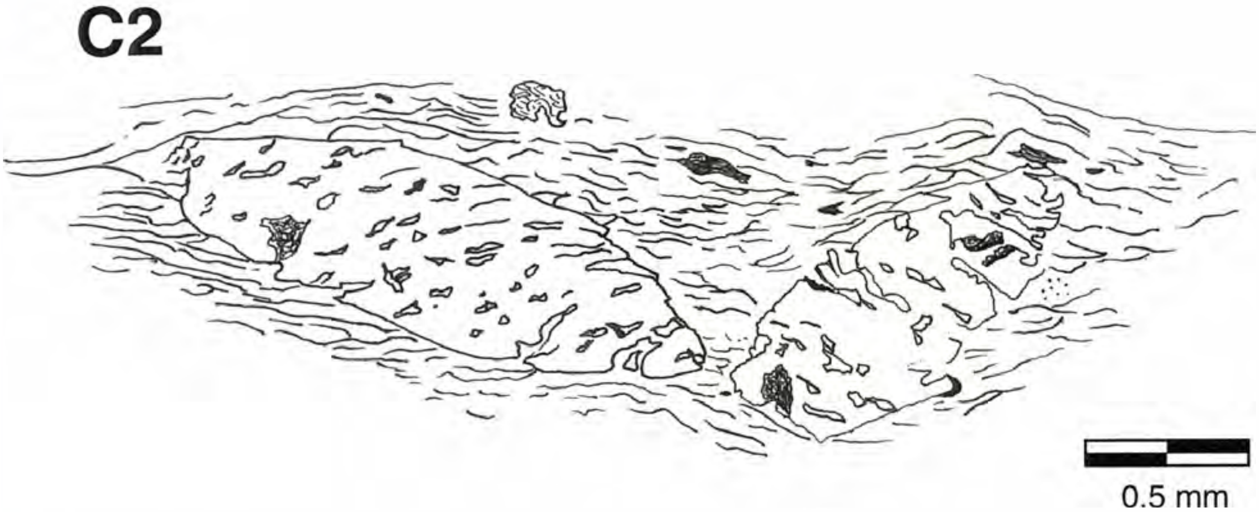

3.23.C. 1) Large hornblendes overprint foliation. Sample 181-37. **2)** Sketch of detail in box in lower right of photo.

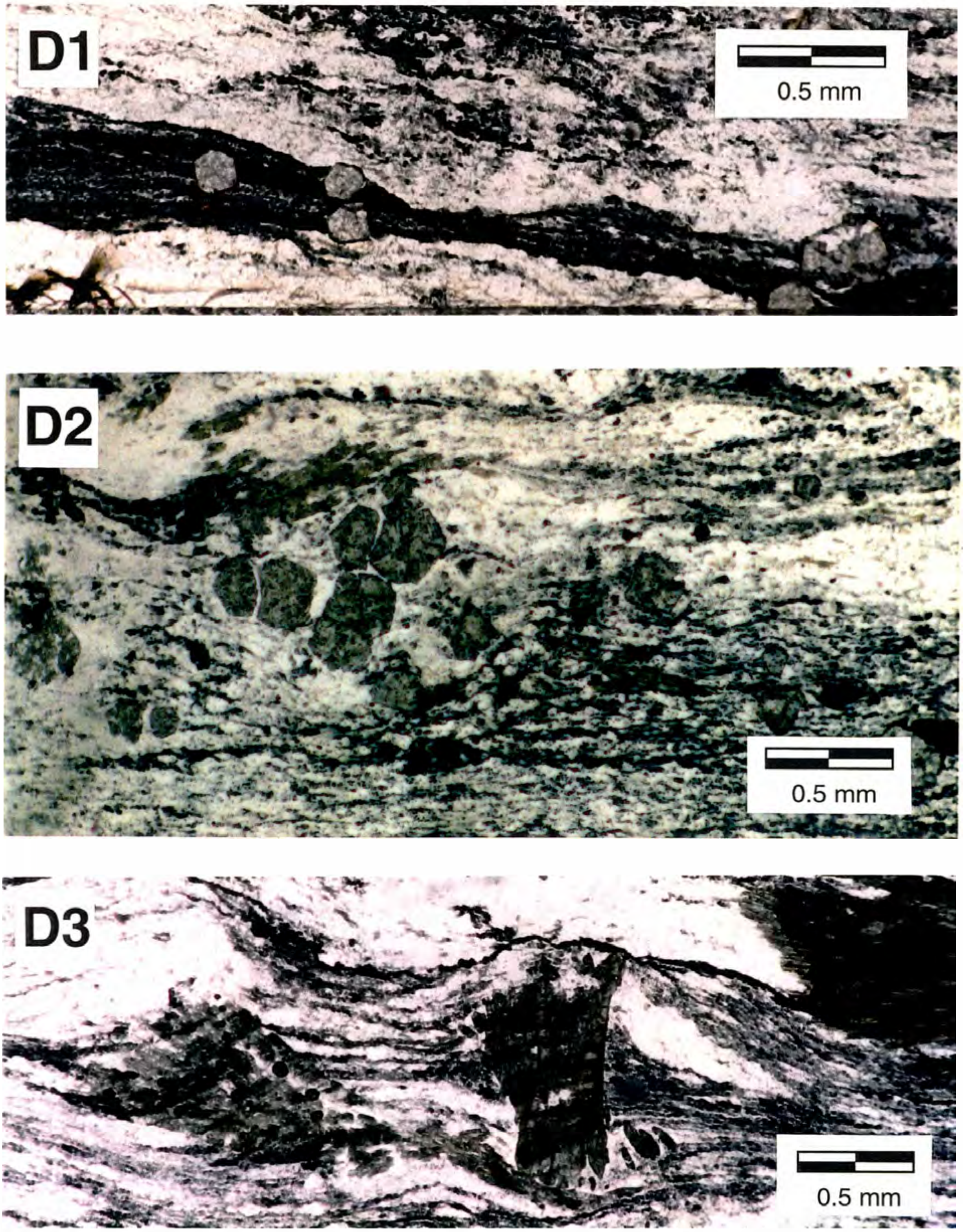

3.23.D. Garnet and hornblende overprint foliation and are pulled apart within the same foliation: **1)** garnet overgrowing foliation; **2)** pulled apart garnets; **3)** hornblende that grew across foliation and was pulled apart within the same foliation. Photos from sample 181-42c.

competent lithologies. Crenulation lineations (L_2) are observed. Shear sense was not determined.

The relation of the late D_3 event to D_2 deformation is uncertain; the large porphyroblasts and strain could possibly be a result of burial and contact metamorphism from intrusion of the Hornet Creek pluton dated at 98.3+/-2 (Brown and McClellend, in review) or D_3 could be a far reaching affect of Spuzzum intrusion and D_2 deformation.

Alternatively D_3 could be a result of orogen normal contraction and map scale upright folding discussed in Feltman (1997) and Lapen (1998) assigned as their D_2 event. If so, then the second style of folding described in D_1 Folds could be a result of this deformation and not D_1. Whatever the origin, this third episode of deformation utilized previous planes of weakness causing no change in original fabric orientations as foliation was at least partially or locally reactivated.

Strain Analysis

In contrast to adjacent areas with metaconglomerates that show evidence of strain (X:Z ratios commonly exceed 10:1; Feltman, 1997; Bennett, 1989; Gabites, 1985), suitable rocks for measurements of strain are virtually absent in the field. However, several thin sections reveal pulled apart grains that record more than 100% elongation (visual estimation; fig. 3.22). Biotite porphyroblasts in the gray phyllite are distended along the dominant foliation.

Other microscopic strain attributed to D_1 includes subgrains and recrystallization in quartz, minor flexing of twin planes in plagioclase, undulose extinction and deformation bands. Together these features suggest solid state flow in a high strain zone.

Extension cracks and en echelon gash fractures were observed in places (fig. 3.24) suggesting limited strain as rocks were uplifted to near the brittle-ductile boundary some time after D_1 ductile deformation.

Summary

Regional fabric began forming with the onset of terrane stacking and thrust imbrication of the Slollicum and Cogburn terranes (D_1). Early foliation (S_1) formed by pressure solution and recrystallization. Bent twin planes in plagioclase, strain lamellae or deformation bands in olivine from the ultramafic unit (fig.3.25) indicate crystal plasticity, requiring minimum temperatures associated with depths below 10-15 km.

Deformation continued as the rocks rose to near the brittle-ductile boundary as evidenced by extension cracks and en-echelon gash fractures. Foliation in the strain aureole of the Spuzzum pluton (D_2) formed as a result of intrusion, and cross-cuts regional thrust fabrics representing ductile

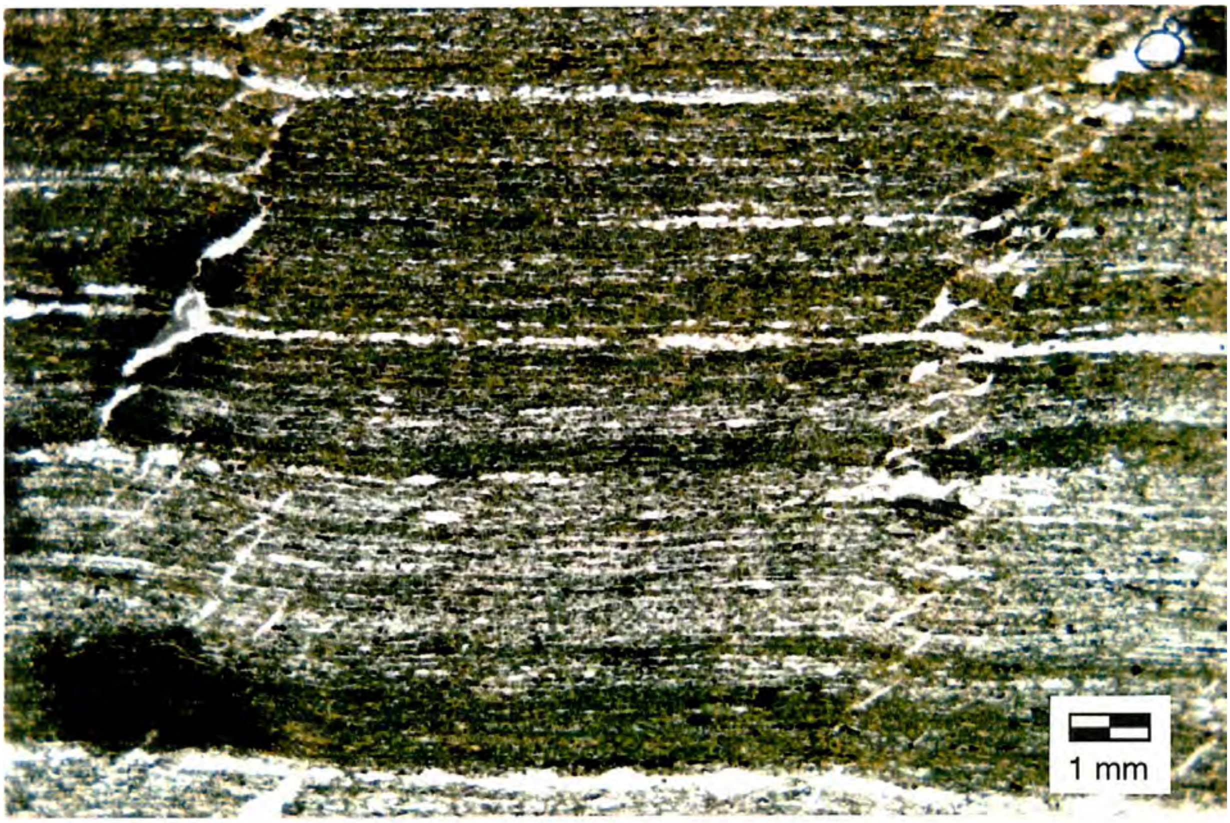

Figure 3.24. En echelon gash fractures in sample 181-127.

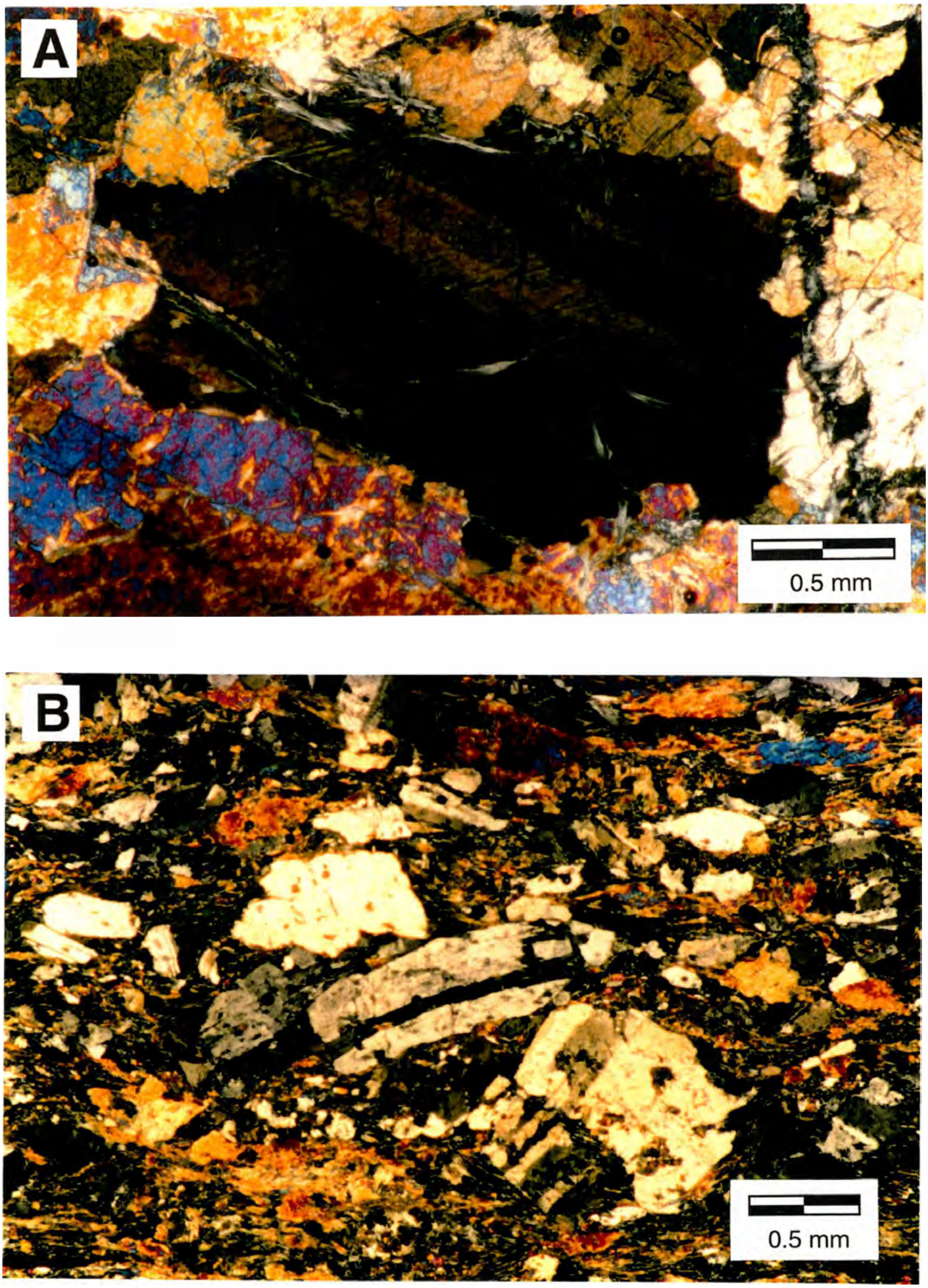

Figure 3.25. Evidence for crystal plastic deformation. **A.** Undulatory extinction among deformation bands in olivine in sample 181-106 from the ultra-mafic unit. **B.** Bent twin planes in plagioclase in a Slollicum metavolcanic rock sample 181-149.

flow of wall rock around the intrusion.

Locally late stage ductile strain (D_3) is recorded as pulled apart, offset and rotated post-tectonic high-grade minerals. This late stage deformation reactivated foliation utilizing the planes of weakness (S_1) formed during D_1 but did not alter S_1 orientation. Most likely the deformation is a result of orogen-normal contraction which produced major map-scale folds after the Slollicum-Cogburn amalgamation.

IV METAMORPHISM

Introduction

Three metamorphic phases (M_1-M_3) are recorded in the rocks in the study area. M_1, and M_2 are associated with D_1 and D_2 deformations respectively. M_3 is a high grade mainly static event with peak grade occurring prior to late stage D_3 deformation.

A greenschist to amphibolite facies metamorphic gradient from south-west to north-east is recorded in the rocks in the study area. Metamorphic index minerals, biotite, garnet, and hornblende, which define regional isograds were mapped by field observations and thin section study.

Metamorphic Phases and Textural Relations

M_1 Event

M_1 is a greenschist grade metamorphic event associated with regional thrust stacking. Bennett (1989) suggests a pressure of approximately 3.0 kb for this greenschist metamorphism. The resulting metamorphic index minerals include chlorite, biotite, actinolite, and possibly hornblende, with quartz and feldspar recrystallized into distinct laminae parallel to foliation. The new and recrystallized minerals lie in the S_1 foliation and are considered to be syntectonic with D_1.

In thin section, mainly chlorite, acicular amphibole, and quartz and feldspar laminae define the foliation related to D_1. Acicular amphibole is both aligned and randomly oriented on the plane of foliation.

The amphibole present in the rocks that makes up the foliation is actinolite and hornblende. It occurs as aligned and randomly oriented prisms. The relation of the occurrence of hornblende to the different events, however, is somewhat ambiguous and is discussed below.

M_2 Event

M_2 metamorphism at 96 Ma is restricted to the aureole of the Spuzzum pluton and is coeval with the D_2 fabrics in the aureole. Chlorite, biotite, and garnet grew in the aureole as a result of contact metamorphism. Biotite is recrystallized into layers defining a foliation that is sub-parallel to the intrusive contact (fig. 3.7). Lineation is rare and defined by chlorite clusters and crenulations.

Many garnets in the Spuzzum aureole within the Cogburn gray pelite display growth zones in which the outer rim commonly incorporates inclusions in a ring pattern around the core (fig 4.1.) suggesting two phases of development. There is no major difference in composition from rim to core, suggesting similar metamorphic conditions for both phases.

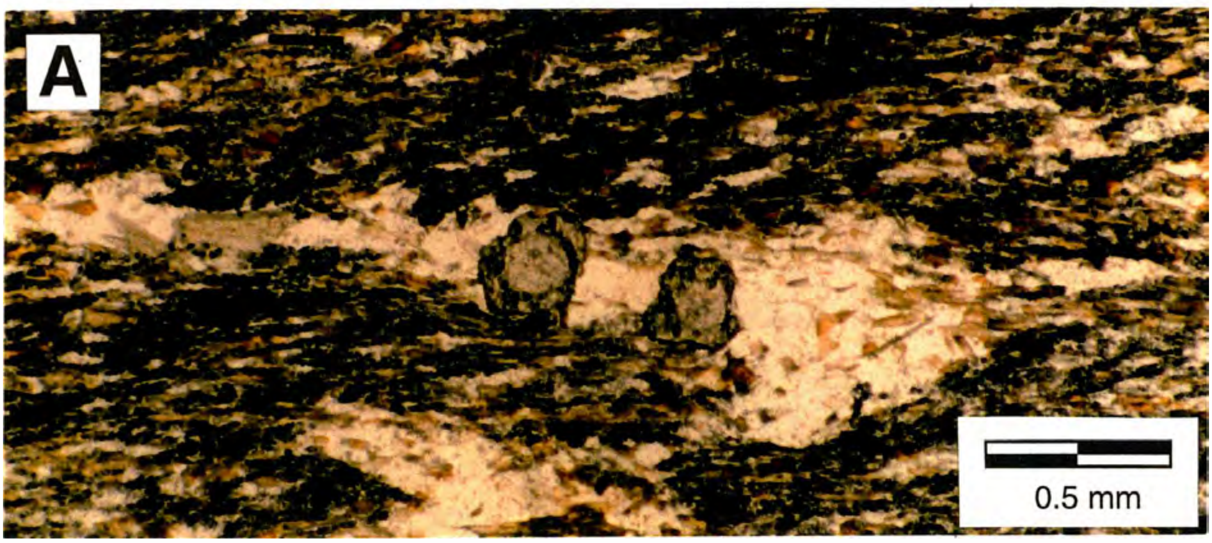

Figure 4.1. Different patterns of growth zoning of garnets in the Spuzzum aureole. **A.** Inclusion poor cores and mottled rims from sample 181-176. **B.** Tracings of garnets from sample 181-171 with singular, often discontinuous, rings of insoluble material at a fairly uniform distance from the edge of the garnet. Also, the width of the rims is fairly uniform from garnet to garnet.

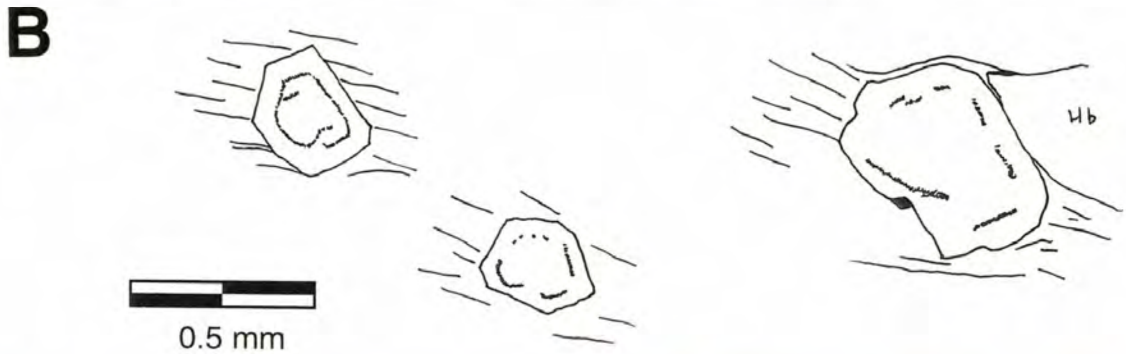

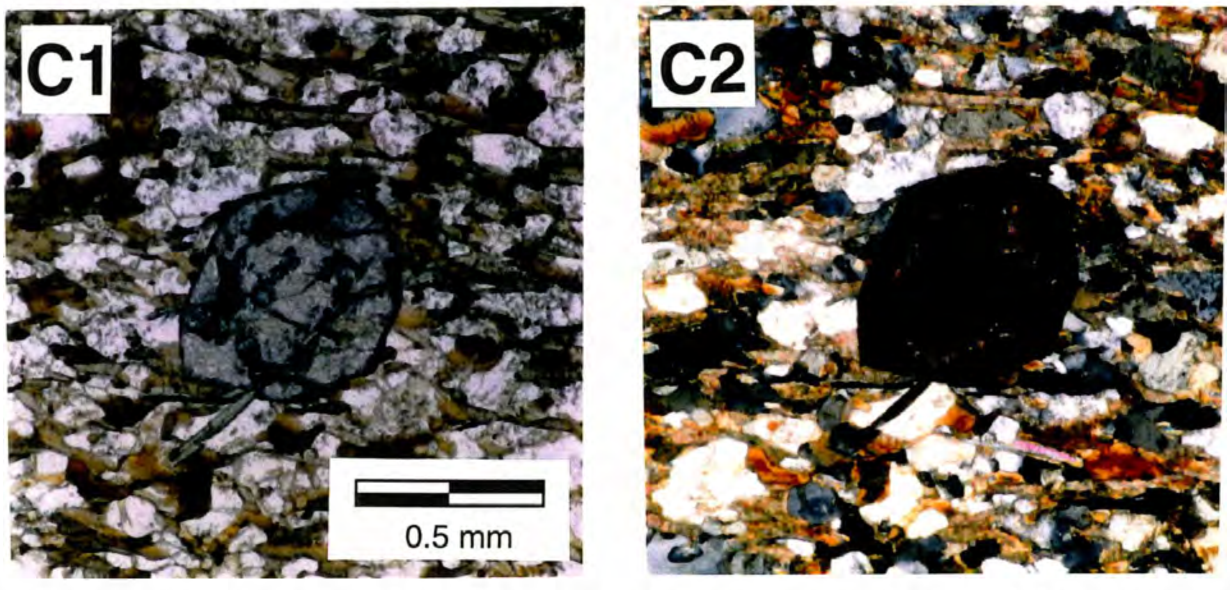

C. Garnet in sample 181-173a containing inclusions of biotite in a ringed pattern around core. **1)** plain light. **2)** polarized light.

M_3 Event

This third metamorphic event, observed mainly in the northwest part of the study area, is marked by the presence of large porphyroblasts of biotite, garnet, and randomly oriented, radiating hornblende which overgrew and incorporated the dominant D_1 foliation as illustrated in figures 3.20, 3.21, and 3.22. Some of these porphyroblasts were then rotated or pulled apart by that same foliation (fig. 3.22.d). Overgrowth of crenulations by the rims of several garnets (fig. 3.22.b), suggests M_3 metamorphism outlasted D_3 deformation in some places (sample 181-155). In other areas (e.g. samples 181-42c and 181-94c (plate 1)) deformation outlasted metamorphism as foliation appears to wrap garnets (fig. 4.2) and biotite (fig. 3.23), garnet, and hornblende porphyroblasts are pulled apart (fig.3.22.d).

Relation of hornblende growth to M_1 and M_3

The relation of hornblende to the separate metamorphic events is yet unknown. Many Cogburn meta-tuffs display a hornblende lineation. The mineral lineations (fig. 4.3) are down dip, consistent with D_1 deformation. Other samples of these rocks also display randomly oriented hornblende prisms growing on and, less often, across the foliation surfaces of greenschists mainly in the Cogburn unit (fig. 4.4). These hornblende crystals are clearly post-tectonic suggesting hornblende grew after D_1.

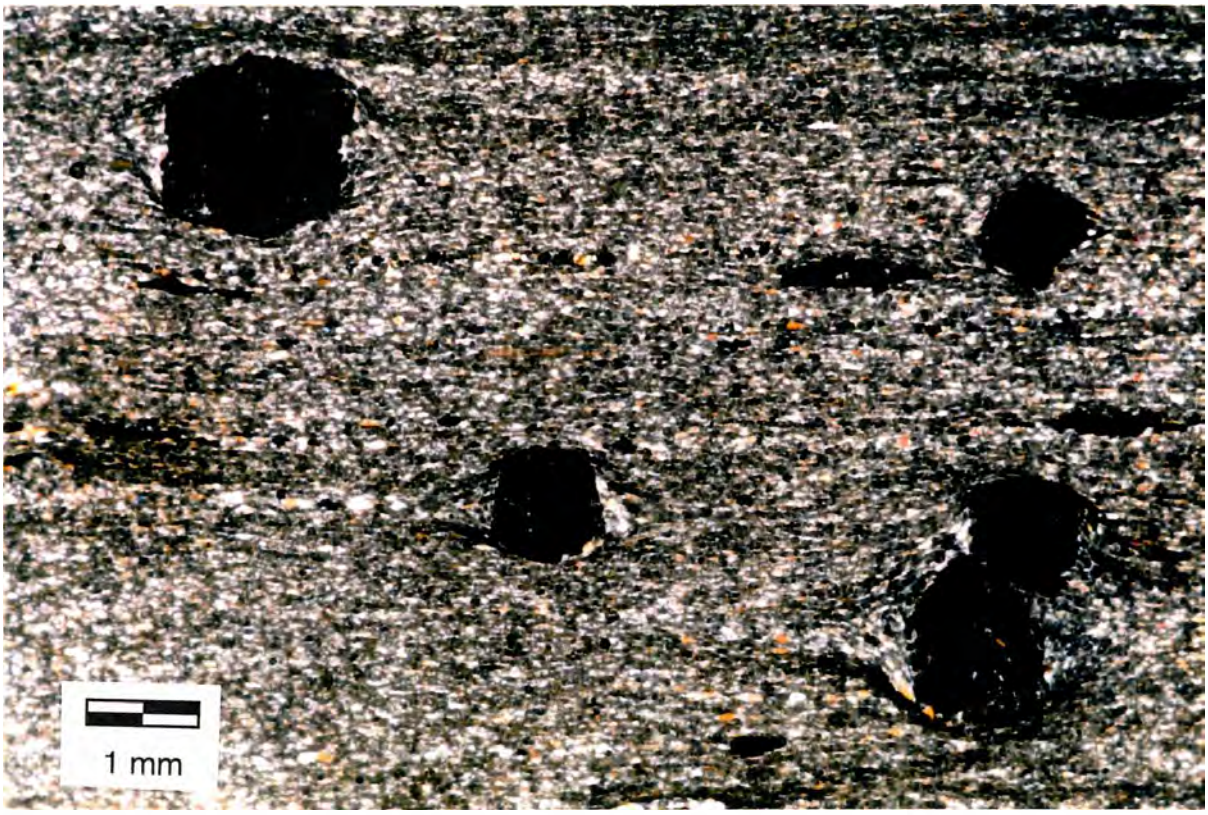

Figure 4.2. Garnet wrapped by foliation but also cuts across foliation. Sample 181-93c.

Figure 4.3. Aligned M_3 hornblende on surface of foliation. Sample 181-54a.

Figure 4.4. Randomly oriented hornblende on foliation surface. Sample 181-91B.

The amphiboles record two stages of growth. Both aligned and randomly oriented hornblende porphyroblasts in many samples are zoned with light washed out cores (actinolite) and dark rims (hornblende). Figure 4.5 shows a back scatter color image of a zoned amphibole. The actinolite to hornblende transition and the continuous growth texture suggest grade rose during amphibole growth, as figure 4.6 illustrates.

Several interpretations are possible to explain the zoning and orientations of the amphiboles. The first may be that M_1 metamorphism outlasted D_1 thrusting producing aligned actinolite during thrusting and randomly oriented actinolite after thrusting. Metamorphic conditions may have risen to the greenschist-amphibolite transition resulting in the growth of hornblende, thus producing the zoned aligned and random amphiboles upon the foliation surfaces.

A second explanation is that the hornblende grew as a result of the M_3 event, part of which was static and part of which was syntectonic. A third possibility is that the hornblende is entirely a result of M_3 and grew in a static environment. This would produce the randomly oriented amphibole and would allow for mimetic growth to explain the presence of the aligned amphibole.

Randomly oriented tremolite in ultra-mafic rock (fig. 4.7) restricted to the length of the northeast margin of the unit, shown in figure 4.10, is also a result of metamorphism that post-dates regional deformation metamorphism. The occurrence of tremolite is probably a result of the same metamorphic event that produced the post-tectonic randomly oriented hornblende.

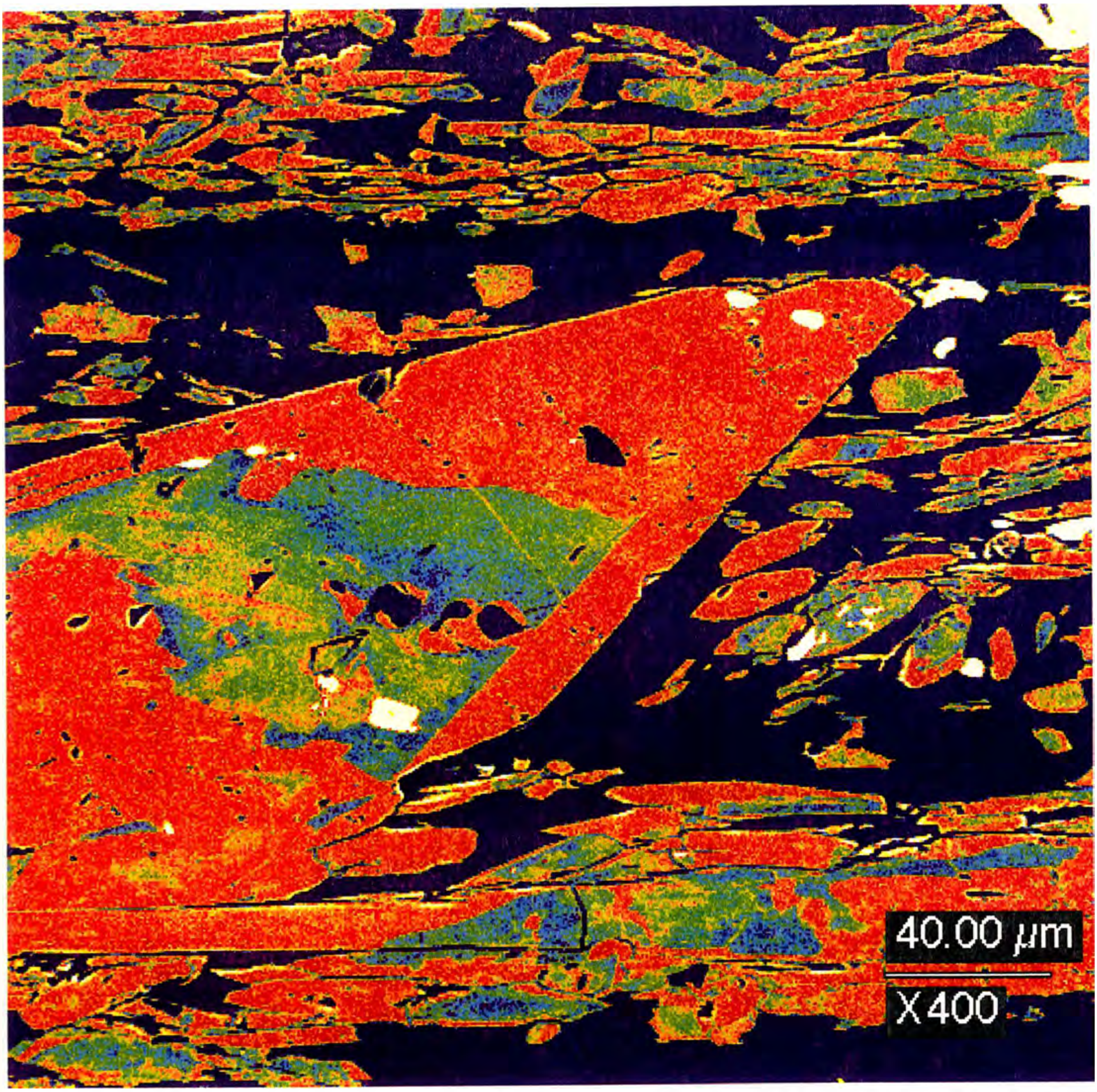

Figure 4.5. Back scatter color image of a zoned amphibole from sample 181-6a. Green color represents high Si content (Si> 7.25) indicative of actinolite. Red/orange color represents lesser Si content (Si< 7.25) indicative of hornblende. The image was taken using the JOEL electron microprobe at the University of Washington.

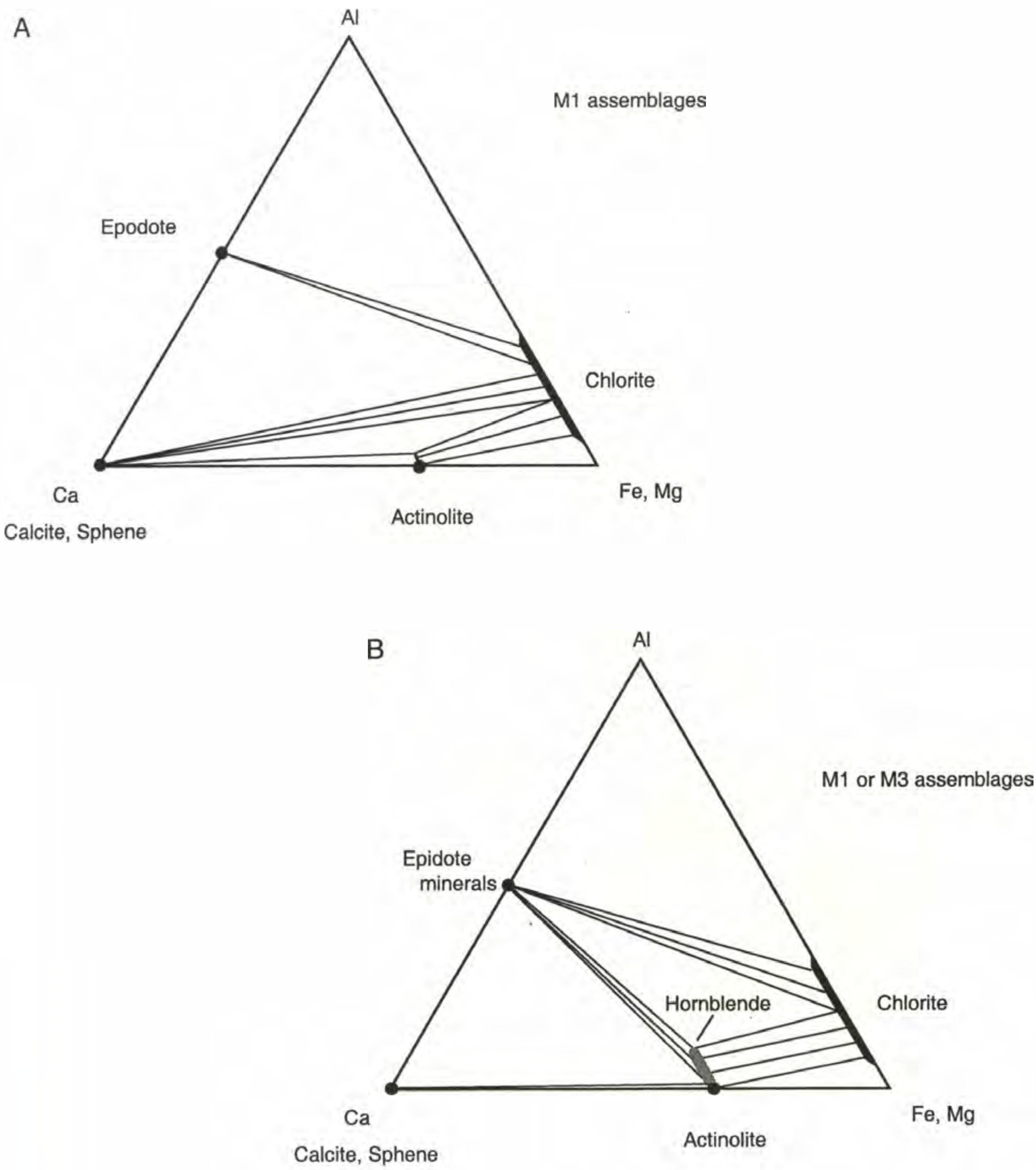

Figure 4.6 ACF diagrams showing typical mineral assemblages found within the greenschists in the study area. **A.** represents a lesser greenschist grade assemblage found in Slollicum meta-volcanic rocks indicative of M1 metamorphism. **B.** represents assemblages common in some Slollicum and most Cogburn greenschists indicative of high-greenschist or epidote-amphibolite grade metamorphism. This diagram represents assemblages that may have grown during M1 or M3 metamorphism. As temperatures rose, actinolite was replaced by hornblende. The zoned amphiboles represent an increase in metamorphic grade as the growth of actinolite gives way to hornblende. Modified from Blatt and Tracy, 1996.

Figure 4.7. Random tremolite in ultramafic rock, photomicrograph taken from sample 181-8a.

The textural relationship of M_3 porphyroblasts to D_1 foliation is somewhat problematic. The porphyroblasts may be a result of continued heating after waning but not full cessation of D_1 deformation. If so, then D_1 would be the cause for rotated and pulled apart grains, essentially eliminating the need for a separate D_3 event. However the large size of the porphyroblasts suggests a long static growth, and therefore that a significant amount of time elapsed between D_1 and D_3.

Relative Timing of M_1-M_3

The textural relationship of high-grade minerals requires that loading took place after the terrane stacking and deformation of D_1 and produced amphibolite grade metamorphism. The timing of contact metamorphism (M_2) in relation to the post-tectonic hornblende and garnet (M_3) is uncertain. Figure 4.8 summarizes the interpreted timing of the three different deformation events and the three different metamorphic events.

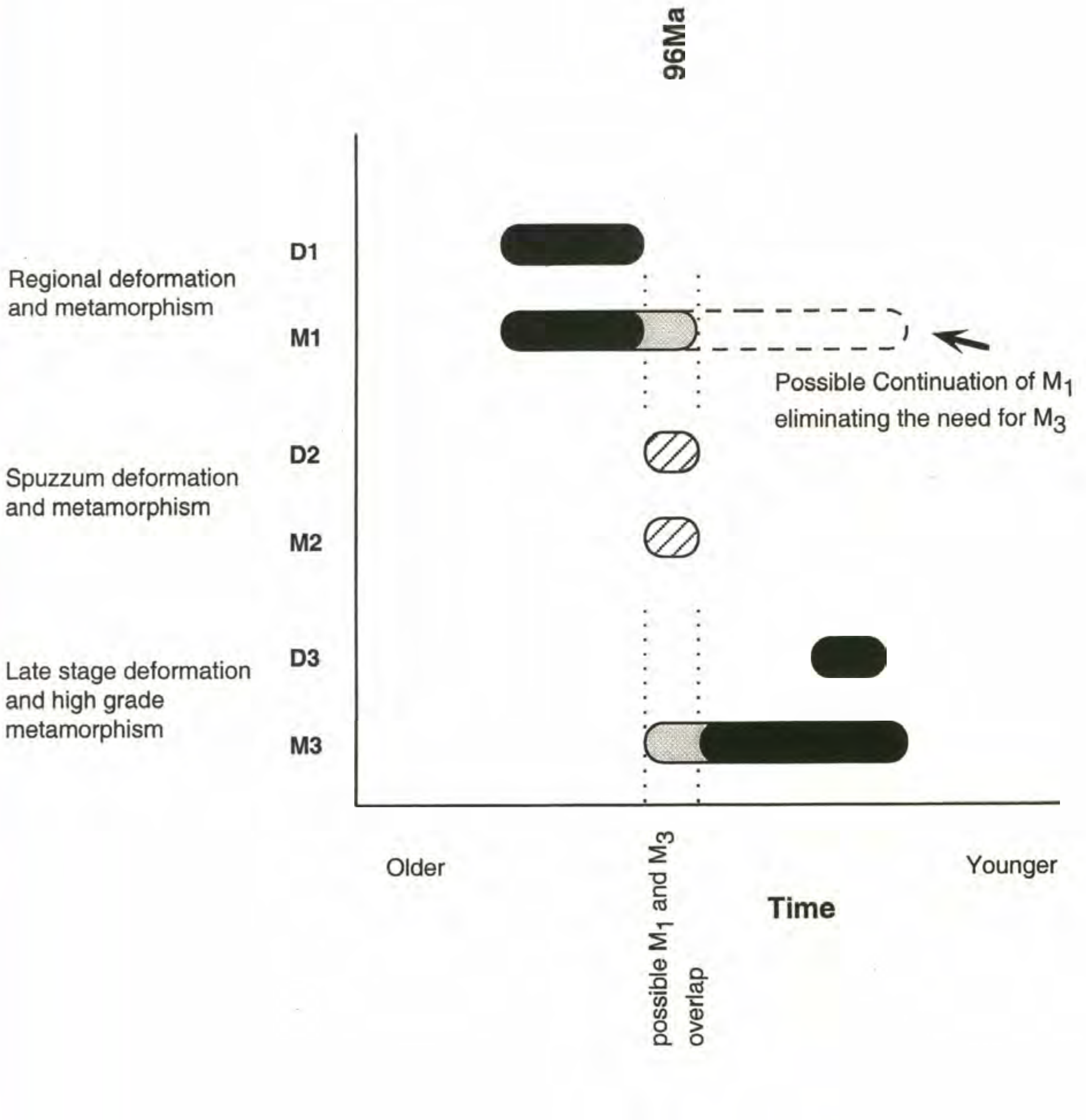

Figure 4.8. Chart showing relative timing of deformational and metamorphic phases temporal relationship chart. Lengths of boxes do not represent actual lengths of periods of ongoing metamorphism or deformation. Boxes are meant to illustrate relative timing of event.

Metamorphic Zones and Isograds

Introduction

The finding that three different episodes of metamorphism are recorded within the rocks in the study area makes it difficult to evaluate the effects of a single episode of pro-grade metamorphism. Isograds were delineated from the first appearances of metamorphic index minerals including biotite, garnet and hornblende. Although the isograds are representative of different episodes of metamorphism, they are used together to define the regional thermal gradient.

Biotite isograd

Biotite is widespread throughout much of the Harrison Lake area. Bennett (1989) places the biotite isograd within the meta-sedimentary unit of the Slollicum schist SW of my study area (fig. 4.9). The isograd is shown as a north-west trending line extending from the shoreline of Harrison Lake to the south-east toward the Spuzzum pluton. The syn-tectonic character of the biotite is evidence that this isograd is representative of the regional deformational event (D_1).

Biotite throughout the study area exhibits mainly syn-kinematic textures and crystallization is considered to be a result of regional greenschist metamorphism associated with thrusting. Biotite crystallization and re-crystallization from the M_2 event is recognized in the aureole of the Spuzzum pluton where it defines a foliation sub-parallel to the pluton contact.

The large biotite porphyroblasts in figure 3.23 are suggested to represent the M_3 event; however, insufficient data and the fact that some M_3 biotite is partially coeval with a deformation that reactivated regional foliation, makes it virtually impossible to define a separate biotite isograd for the M_3 event.

Garnet Isograd

The first appearance of garnet constraining the isograd (fig. 4.9) is within an igneous body in the Slollicum schist meta-sedimentary unit in the north-west portion of the study area (samples 181-150,152; plate 2). Garnet in sample no. 181-125 in another igneous dike within the Cogburn package constrains the isograd to the south-east of samples 181-150,152. From here the isograd is lost through the ultra-mafic unit. The isograd along this portion may be a result of the M_1 event, the M_3 event or both.

Toward the South-East the isograd turns sharply to parallel the Spuzzum pluton as shown in figure 4.9. Here the isograd is a result of the Spuzzum intrusion and the M2 event.

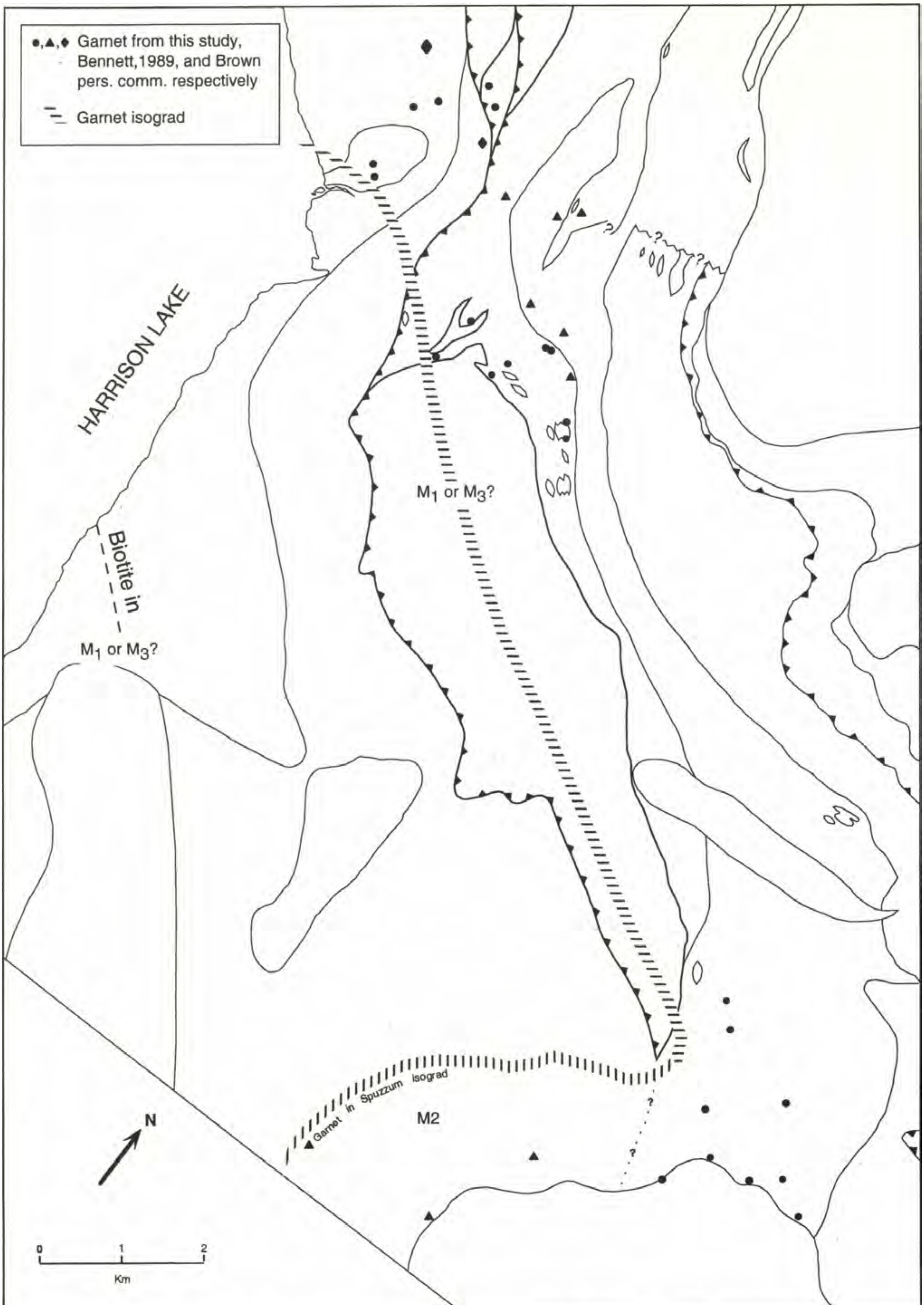

Figure 4.9. Garnet and biotite isograds for M_1-M_3 metamorphic events. See figure 1.4 for rock units.

Hornblende Isograd

Electron microprobe analysis of silica content in amphiboles was carried out on eight samples in order to determine actinolite (Si>7.25%) vs. hornblende (Si<7.25%). These data in conjunction with information from Bennett (1989) are used in the placement of the hornblende isograd (fig.4.10). In all eight microprobe samples from this study, rims on the amphibole grains produced hornblende signatures. One microprobe sample form Bennett (1989) gave an actinolite signature and many more amphiboles from thin section analysis were determined to be actinolite. Further data are needed to reliably constrain the hornblende isograd.

The isograd can be arguably placed along the southwest border of the ultra-mafic unit (fig. 4.10) where three of the amphiboles along the contact gave hornblende signatures determined from microprobe analysis. Insufficient data prevents extension of the isograd to the northwest. To the southeast, the occurrence of hornblende is controlled by the Spuzzum pluton and the isograd is deflected around it.

As discussed earlier, the relation of the hornblende to the M_1 and M_3 metamorphic events is undetermined, therefore, the isograd along the southwest border of the ultramafic unit is not assigned to one single event. The isograd here could potentially be a superimposed isograd representative of both M_1 and M_3 events.

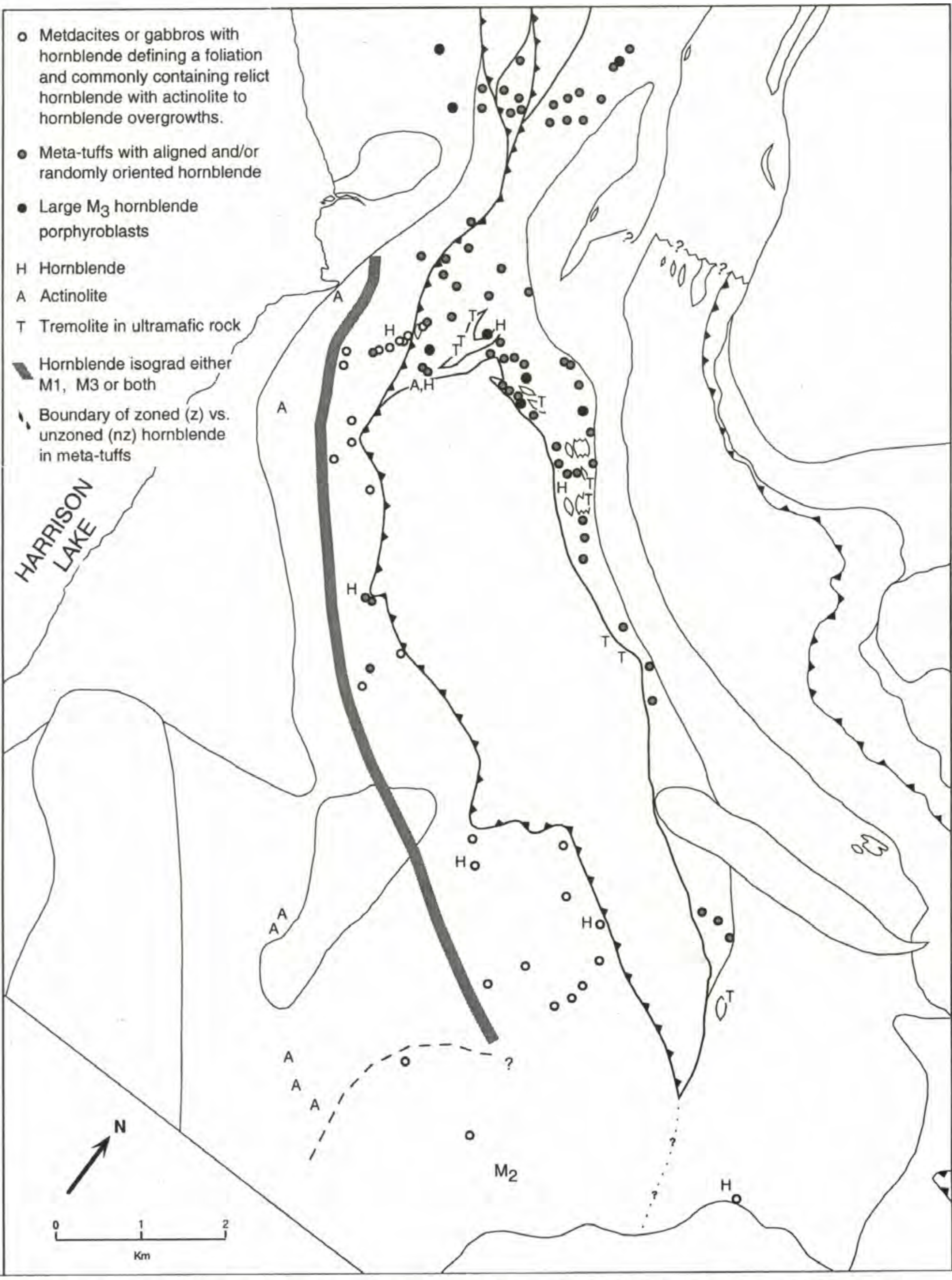

Figure 4.10. Distribution of metamorphic amphibole showing different orientations, fabrics, and compositions. Microprobe analysis was used to determine Si content (Leake, 1978). Data: this study and Bennett (1989). Identification of hornblende vs. actinolite based partly on microprobe analysis (Si<7.5 = hornblende, Si>7.5 = actinolite) and partly on optical properties.

Albite-Oligoclase Transition

Co-existing albite and oligoclase (peristerite pairs) are found in many progressive metamorphic belts (i.e. Maruyama et.al, 1982). Turner (1981) suggested from other workers observations that "co-existence of albite and oligoclase is a general phenomenon that immediately precedes the full development of the amphibolite facies". Peristerite pairs are an indication of a transitional zone between greenschist and amphibolite facies metamorphism in which the albite to oligoclase/andesine transition occurs discontinuously with no plagioclase composition of approximately An_{5-20} (Maruyama et. al., 1982). This abrupt change in composition is considered to be a miscibility gap (Crawford, 1966; Maruyama et. al., 1982) and is known as the peristerite gap.

Microprobe analyses on 8 samples (this study) combined with pre-existing data are used to map the albite-oligoclase transition in the study area. A distinct gap in plagioclase composition from $An_{(1-4)}$ to $An_{(13-19)}$ was found in samples from this study and is mapped in figure 4.11.

The albite-oligoclase isograd/transition zone generally follows the south-west border of the ultramafic unit as the hornblende isograd does. It is uncertain whether the isograd along this tract is related to the M_1 or the M_3 events or both. It is deflected around the Spuzzum pluton in the south-east. In the NW portion of the map area, the isograd curves to the NW away from the terrane bounding fault, just as the garnet isograd does.

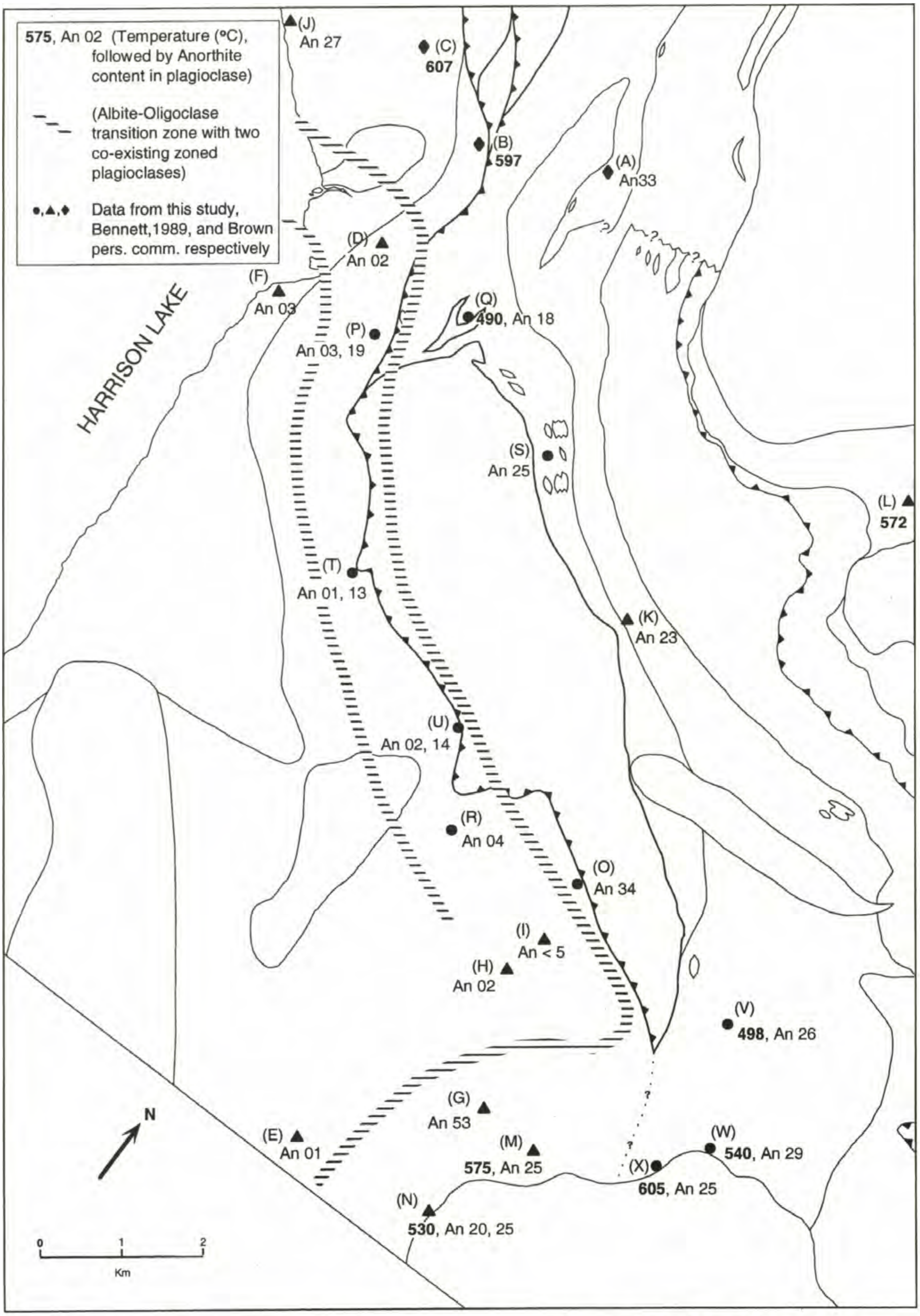

Figure 4.11. Temperatures, Anorthite content, and Albite-Oligoclase transiton zone. Letter sites are keyed out to table 4.1. See figure 1.4 for rock units. Data for this study's thermobarometry analysis is in Appendix B.

The isograd near the southeast end of the ultramafic unit abruptly turns and parallels the Spuzzum pluton contact. Here the Spuzzum related oligoclase defines the regional isograd. The superimposition of the isograds results in a composite regional oligoclase isograd.

Variation in the anorthite component of plagioclase with increasing temperatures is dependent on bulk rock composition and is buffered by the assemblage plagioclase(0-50)+epidote+Ca-amphibole+chlorite+quartz (Maruyama et. al., 1982) as is seen in this study. Figure 4.12 shows a compositional phase diagram for rocks in the study area and a T-X_{An} graph to illustrate these relations.

The temperature and pressure of the transition zone in the study area can only be generally estimated due to lack of data available. Maruyama et. al. (1982) indicate that transition temperatures are pressure dependent, estimating an increase of 20°C/kb. By knowing pressures for the study area and comparing them to a separate belt of similar bulk rock composition and known pressure regime, it may be possible to estimate a temperature for the transition zone in the study area.

Metabasic rocks from the Kasagamura aureole and Yap Island (2-3 kb) described in Maruyama et. al. (1982) may be most similar to study area rocks. Suitable rocks for thermobarometry within or near the transition zone were not obtained. However, pressures for the current study area were previously estimated by Brown and Walker (1993) to be 3-5 Kb. Using figure 7 in Maruyama et. al.

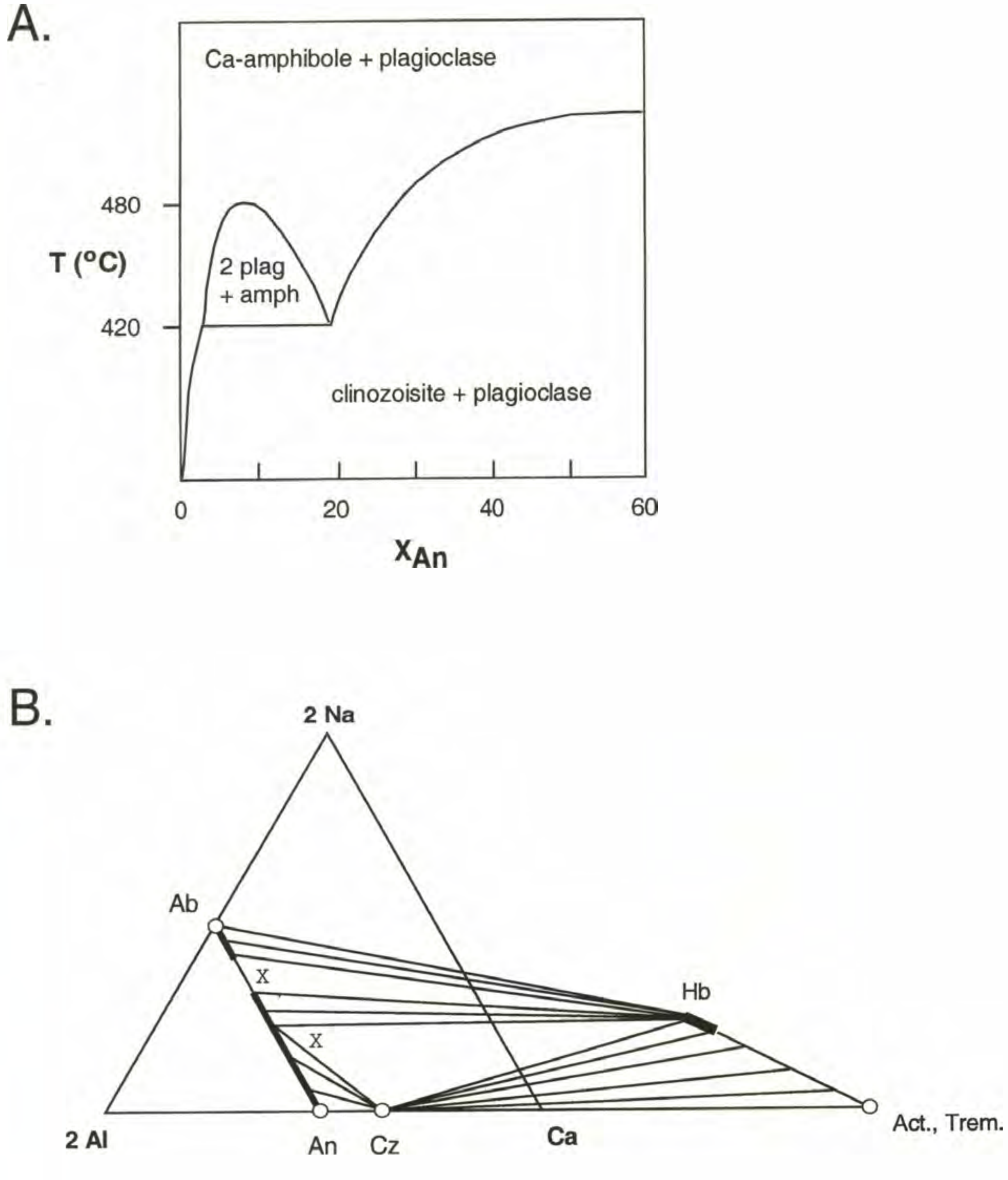

Figure 4.12 . **A.** T-X_{An} graph drawn along the albite-anorthite join of figure 4.12.B. **B.** Compositional phase diagram showing plagioclase stability with various phases. "X" marks the likely compositions of different flows within the meta-volcanic unit of the Slollicum schist. Ab=albite, Act=actinolite, An=anorthite, Cz=clinozoisite, Hb=hornblende, Trem=tremolite, (Modified from Maruyama et. al., 1982).

(1982) as a guide, assuming a similarly shaped solvus as those shown and correcting adding 20°C/kb for an assumed 5 kb pressure in the study area, a temperature of approximately 420°C-480°C can be estimated for the transition zone in the study area (fig. 4.12.A)

Isograd Summary

The regional isograds in this portion of the Harrison Lake area are composites of several different tectonic and plutonic events. Data suggest at least greenschist facies metamorphism and possibly uppermost greenschist facies was reached during terrane-stacking. This metamorphic event was overprinted by the Spuzzum pluton contact metamorphism in the south-east and also overprinted by the high-grade event best observed in the north-west portion of the study area. These three events together help create the composite regional thermal gradient that we see in the study area.

The presence of superimposed metamorphic isograds makes it difficult to evaluate the effects of a single pro-grade metamorphic event. For example, if upper greenschist or even amphibolite facies was reached during regional metamorphism, any evidence has been obliterated by a later post-tectonic amphibolite grade metamorphic event. Alternatively, the later amphibolite event may not have obliterated all evidence of the lower-grade event making it hard to determine which mineral assemblages relate to which event.

Thermobarometry

In order to determine pressures and temperatures at the time of metamorphism, a thermobarometric analysis was carried out on four samples in this study to augment pre-existing data from the surrounding area (See table 4.1). Two samples (181-171 and 181-173a) are near the contact of the Spuzzum pluton, one (181-136) is near the outermost aureole of the Spuzzum pluton and the last (181-60c) is located at the north-western end of the ultramafic unit (plate 1, and figures 4.11 and 4.13).

Dr. E.H. Brown carried out the microprobe analysis at the University of Washington using the JOEL electron microprobe. Rim sites on garnet and other minerals were assumed to be in equilibrium with the surrounding matrix material for the purpose of calculating pressures and temperatures based on mineral compositions.

Temperatures were obtained using the GABI thermometer involving the garnet-biotite Fe-Mg exchange, and the GAHB thermometer involving the garnet-hornblende Fe-Mg exchange. Pressures were obtained using the garnet-biotite-muscovite-plagioclase barometer (GAMI), and the garnet-hornblende-plagioclase barometer (GAHP).

Table 4.1. Thermobarometry results. Sample locations are shown on Plate 2. Site letters are keyed to figures 4.11 and 4.13. Sites O-X correspond to samples from this study.

site	Sample #	Equilibrium	Pressure (kbars)	Temp. (°C)	Plag. An %
A	JT-88-6c				33
B	NB-19	GAMI	8.80	597	
C	NB-66	GAHB, GAHP	7.60	607	
D	162-7				02
E	162-32		4.50		01
F	162-35	NaM4	3.00		03
G	162-46	NaM4			53
H	162-57				02
I	162-58				<5
J	162-78				27
K	162-121				23
L	162-192	GABI, GASP(Ky)	5.40	572	
M	162-196	GABI, GAMI	4.60	575	25
N	162-202	GAHB, GAHP	7.60	530	20
O	181-34				34
P	181-53				03, 19
Q	181-60c	GAHB, GAHP	8.80	490	18
R	181-65				04
S	181-98				25
T	181-122				01, 13
U	181-129				02, 15
V	181-136	GABI, GAMI	6.05	498	26
W	181-171	GAHB, GAHP	7.25	540	29
X	181-173a	GABI, GAMI	3.40	605	25

*GAHB garnet-hornblende Fe-Mg exchange (Graham and Powell, 1984)
GAHP garnet-hornblende-plagioclase (Kohn and Spear, 1984)
GAMI garnet-biotite-muscovite-plagioclase (Berman, 1991)
GASP garnet-aluminosilicate-plagioclase-quartz (Berman, 1991)
NaM4 Crossite component of actinolite (Brown, 1977)

Results of Thermobarometry

Samples 181-171 and 181-173a (sites W and X, this study, table 4.1) are within 1 km of each other in the Spuzzum aureole. Different thermobarometers were used to obtain pressure and temperature values at the different sites. The GABI,GAMI thermobarometer was used on the sample from site X and gave pressure and temperature values of 3.40kb and 605°C, while the GAHB,GAHP thermobarometer was used on the sample from site W and gave a pressure and temperature of 7.25kb and 540°C. A similar discrepancy using the above mentioned different thermobarometers was found by Bennett (1989) between sample sites M and N (table 4.1; figs. 4.11 and 4.13) also in the Spuzzum aureole.

Pressures at sample sites M and X were determined using the GABI,GAMI thermobarometer (table 4.1). With a 1 kb error, the values correspond to approximately 3-4 kb of pressure at time of emplacement of the Spuzzum pluton. This supports a model for a shallow level of intrusion for the Spuzzum pluton, as evidenced by andalusite found elsewhere in the Spuzzum aureole (Pigage 1973; Bartholemew, 1979; Brown and Walker, 1993).

Sample 181-136 (table 4.1) yields a pressure of 6.05 kb and a temperature of 498°C using the GABI,GAMI thermobarometer. This value falls within range of previously assigned P-T curves for the area by Brown and Walker (1993).

Divergently high pressure values from sample sites W and N (Spuzzum aureole), and Q and C (northwest portion of the study area; fig. 4.13) were obtained using the GAHB,GAHP equilibrium

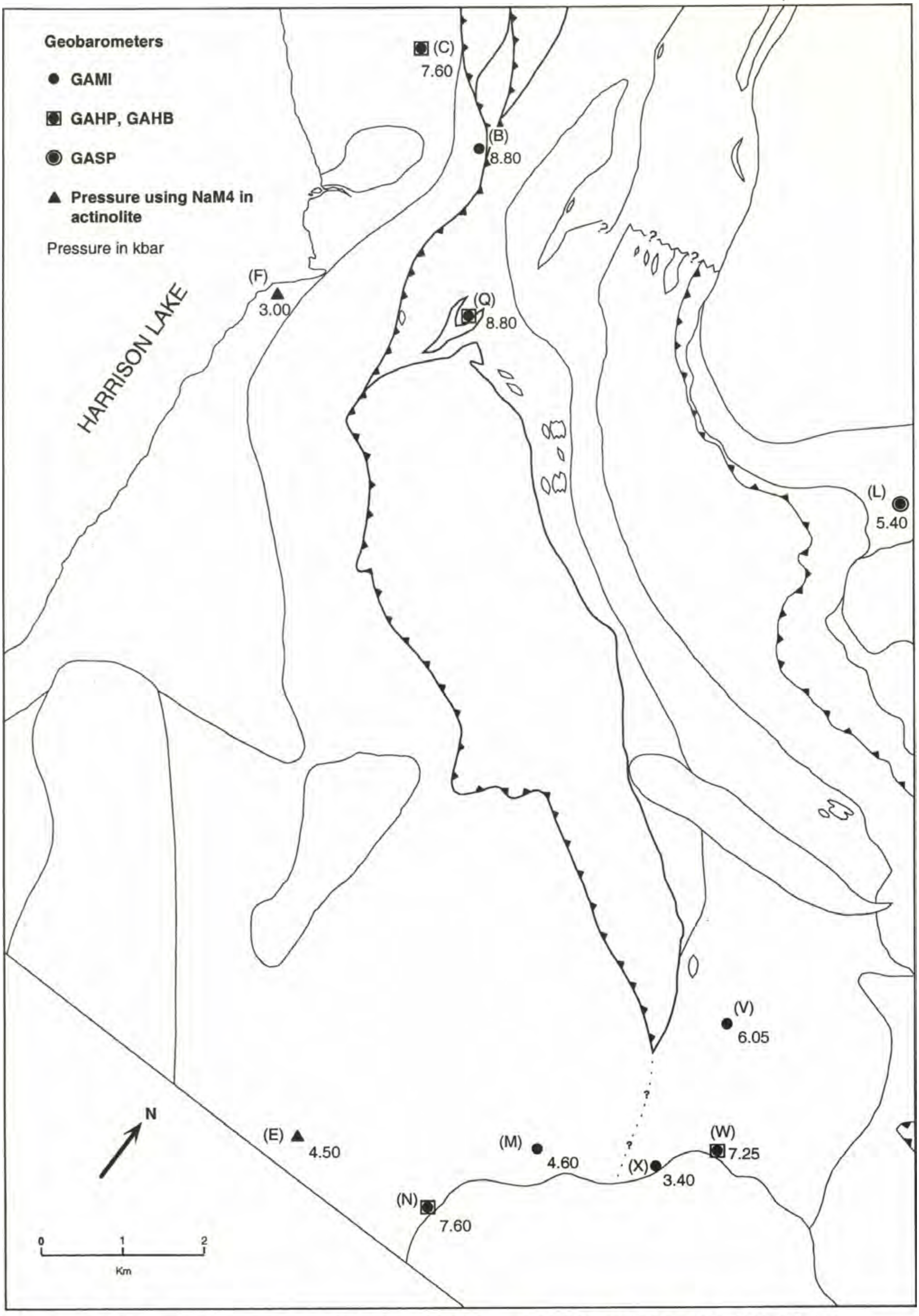

Figure 4.13. Pressures and barometers. Letter sites are keyed to table 4.1. Geobarometers are listed at the bottom of table 4.1. See figure 1.4 for rock units.

(table 4.1). All pressure values are higher than previously suggested by Brown and Walker (1993) for the area in which they occur. This could be a result of: 1) an essentially unproven GAHB barometer involving hornblende; 2) disequilibrium between porphyroblasts and matrix phases at specific sample localities; or 3) a combination of both.

Values at sample site B (table 4.1; fig. 4.12 and 4.13) are also higher than suggested by Brown and Walker (1993) for that area but were obtained using the GAMI thermobarometer. The GAMI is considered a reliable thermobarometer. The fact that sites C and Q are proximal to site B and have similar values as those from site B may lend credence to the GAHB barometer used in obtaining pressure and temperature values at sites C and Q. The implications of these higher pressure values is discussed in the Pressure Gradient section.

Temperature Gradient

In the northwest portion of the study area, along the strike of the orogen, temperatures of 490°C to 498°C (sites Q and V) were obtained using thermobarometry, both from samples which are considered affected by M_3 metamorphism. The breakdown of serpentine to forsterite + talc does not appear to have been reached, limiting the temperature of metamorphism in the ultramafic rocks to below 500°C based on phase relations and pressures and temperatures determined for those phases (Tracy and

Frost, 1991). Figure 4.14 shows probable pressure-temperature ranges of the three metamorphic events.

Temperatures jump significantly in a relatively short distance from site Q (490°C) northwest to sites B and C (597°C and 607°C respectively). The cause for this temperature increase is unknown.

Pressure Gradient

Pressures obtained from samples 181-60c and 181-171, are higher than other lines of evidence suggest and because they were obtained using the uncertain GAHB barometer are considered suspect. However the presence of three similar values at sites B, C and Q, all within close proximity, illustrates a need for testing of the GAHB barometer and the necessity for further research in the area encompassing those sample sites.

If the values at sites B, C, and Q are reliable, they imply deep burial and considerable exhumation of these particular rocks. Finding an explanation for these divergent high pressures is essential to the understanding of the structure and metamorphic history of the area.

Regional development of map-scale upright folding is described in Reamsbottom (1974) and Feltman (1997). Feltman (1997) describes the Breakenridge antiform with vertical uplift during doming to explain presence of high pressure rocks in the core of the antiform. A similar structure in the area encompassing sites C, Q, and B might explain the high pressure

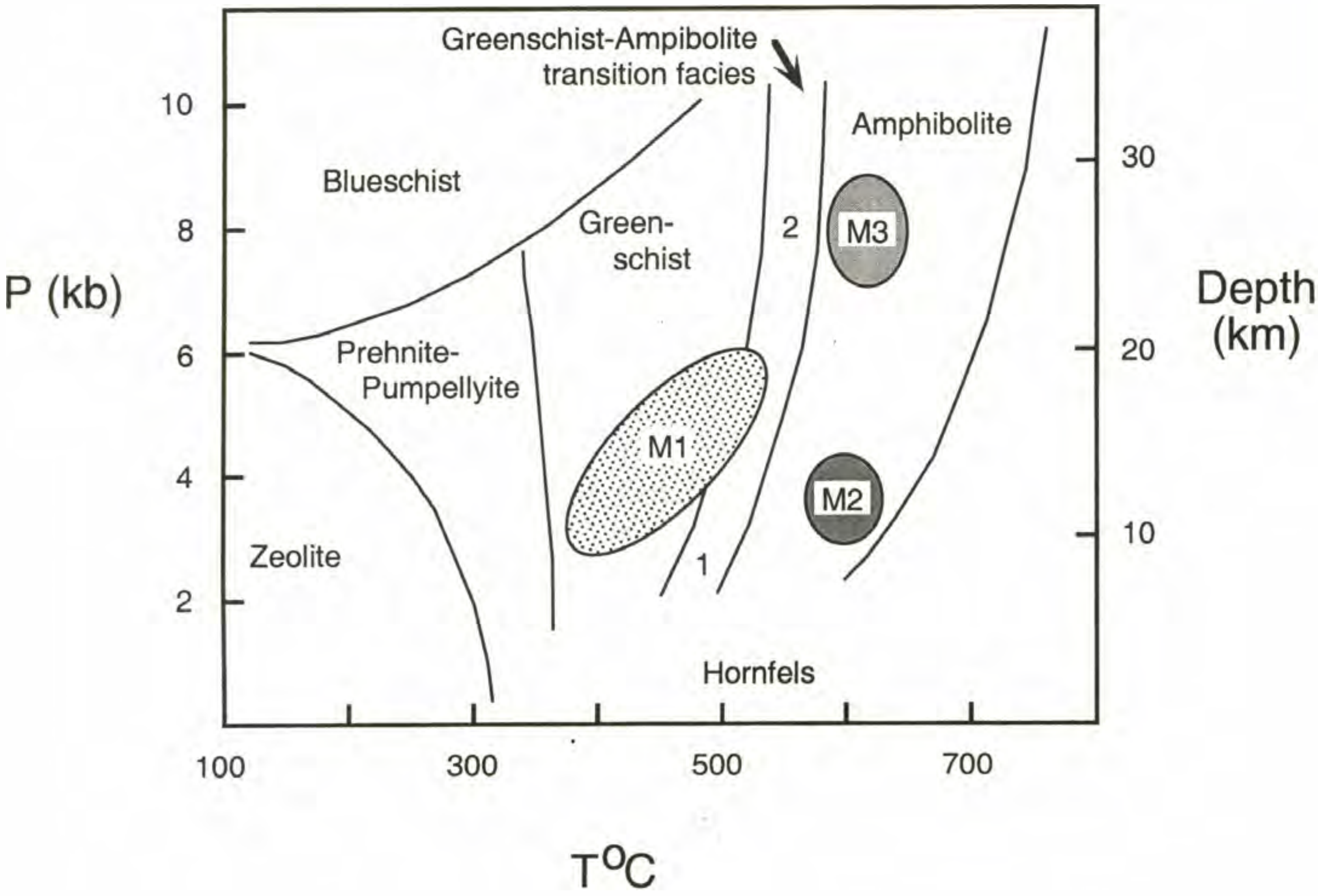

Figure 4.14. Pressure-Temperature diagram showing metamorphic facies and approximate **peak** pressures and temperatures of the different metamorphic events within the study area. M1 may have reached 5-6 kb based on hornblende if hornblende was produced during M1, or M1 may have only reached approximately 3 kb and 400-450°C. 1. Lower transition facies in which actinolite and oligoclase co-exist with clinozoisite. 2. Upper transition facies where hornblende exists with albite and cliozoisite. Maruyama et. al. (1983) suggest assemblages of the lower transition zone dominate around 2 kb while those in the upper transition zone dominate between 5-7 kb. Modified after Blatt and Tracy (1996).

values obtained for those rocks. The presence of a map scale fold in the vicinity was presented in the Structure chapter and cross-section but lack of outcrop prevents a conclusive interpretation within the scope of this study and much more information is needed to test this possibility.

Summary

The metamorphism throughout the study area is a result of a combination of at least three different events. However, the increase in grade across the study area has been attributed mainly to the latest M_3 event. The data on hornblende is inconclusive and may have formed in either the M_1 or M_3 events or both. If the first metamorphism produced hornblende then it may have also produced oligoclase and garnet. Further observation and thermobarometry analysis on suitable rocks might increase the understanding of metamorphism throughout the study area and surrounding region.

V. DISCUSSION OF TIMING OF OROGENIC AND METAMORPHIC EVENTS

Superterrane Amalgamation

In order to estimate the timing of thrust stacking of the Slollicum, Cogburn, and Settler packages, the timing of accretion of the outboard Insular to the inboard Intermontane is of value in determining the age of terrane stacking in the study area.

One view is that the Intermontane superterrane was considered the edge of the North American plate up to Mid-Cretaceous time. This is based on the collisional model outlined in the Introduction chapter which proposes the outboard Insular terrane did not accrete to the Intermontane terrane until Mid-Cretaceous time after closure of a wide oceanic basin.

But, a wealth of arguments have surfaced which support a pre-Early-Cretaceous superterrane amalgamation that would preclude the collisional model. For example Armstrong (1988) argues that an Early-Cretaceous arc is superimposed on both superterranes.

Perhaps the most substantial arguments are those involving overlap assemblages. Woodsworth and Tipper (1980) argued that the Early-Cretaceous Gambier Group rocks in central and southern B.C. constitute an overlap assemblage that represents an arc built across both superterranes. Monger (1991) inferred an extensional setting for the Gambier Group. Deposition of the Gambier Group would have been across an intra-arc basin in which extension was occurring. This would require amalgamation prior to the onset of Gambier deposition which began in the Early-Cretaceous.

Brew and Ford (1993) suggested the Gravina-Nutzotin assemblage in the northern Coast Belt represents a Late-Jurassic to Early-Cretaceous intra-terrane rift basin superimposed on previously amalgamated Alexander, Wrangellia and Stikinia terranes. van der Heyden (1992, p.85) lists evidence from other workers which supports this idea.

Mahoney and Journeay (1993) describe the Cayoosh assemblage as conformably overlying rocks of the Bridge River terrane and laterally equivalent to and gradationally overlain by rocks of the Brew Group. According to the authors, the Bridge River-Cayoosh-Brew Group succession records uninterrupted Jura-Cretaceous sedimentation in the eastern portion of the Coast belt. This succession is topped by plutonic clast bearing conglomerates that coarsen upward. The authors correlate these conglomerates to the basal conglomerates of the Penninsula Formation of the Gambier group. Mahoney and Journeay (1993) believe this succession marks the end of pelagic sedimentation in the Bridge River ocean, the initiation of Middle to Late Jurassic Arc volcanism associated with basin closure and the eventual uplift of this arc in Late Jurassic-Early Cretaceous which supports amalgamation prior to the Early Cretaceous.

These arguments and supporting evidence are substantial and the model for at the least a pre-Mid-Cretaceous (Mid-Jurassic to Early-Cretaceous) amalgamation of superterranes similar to that presented by van der Heyden (1992) is accepted here as a basis for the remaining interpretations of this study. The timing of this and the events mentioned below is illustrated in figure 5.1.

Stacking of Slollicum, Cogburn, and Settler units

Two possibilities for the age of terrane stacking of the Slollicum/Twin Island, Cogburn and Settler packages are: 1) terrane stacking occurred shortly after deposition of the Slollicum (146Ma) unit but before or during deposition of the Peninsula formation of the Gambier group in the late Berriasian; 2) terranes were in close proximity after superterrane amalgamation but final juxtaposition did not take place until Mid-Cretaceous after the majority of the Gambier group was deposited (102 Ma).

The lower age bracket for thrusting is constrained by the 146 Ma U/Pb zircon age of the Slollicum schist (Bennett, 1989). Final amalgamation had to occur prior to the 96 Ma age of the crosscutting Spuzzum pluton (Brown and Walker, 1993).

Several more recent correlations between Slollicum rocks and other units may help constrain the timing of thrust stacking of the Slollicum, Cogburn, and Settler terranes. The Slollicum/Twin Island schist has been grouped with the younger volcanics of the Harrison Lake terrane on the west side of Harrison Lake by Monger (1990). More specifically, protolith lithologies in the lower meta-sedimentary unit of the Slollicum/Twin Island schist are most likely correlative to the Mysterious Creek and Bill Hook Creek

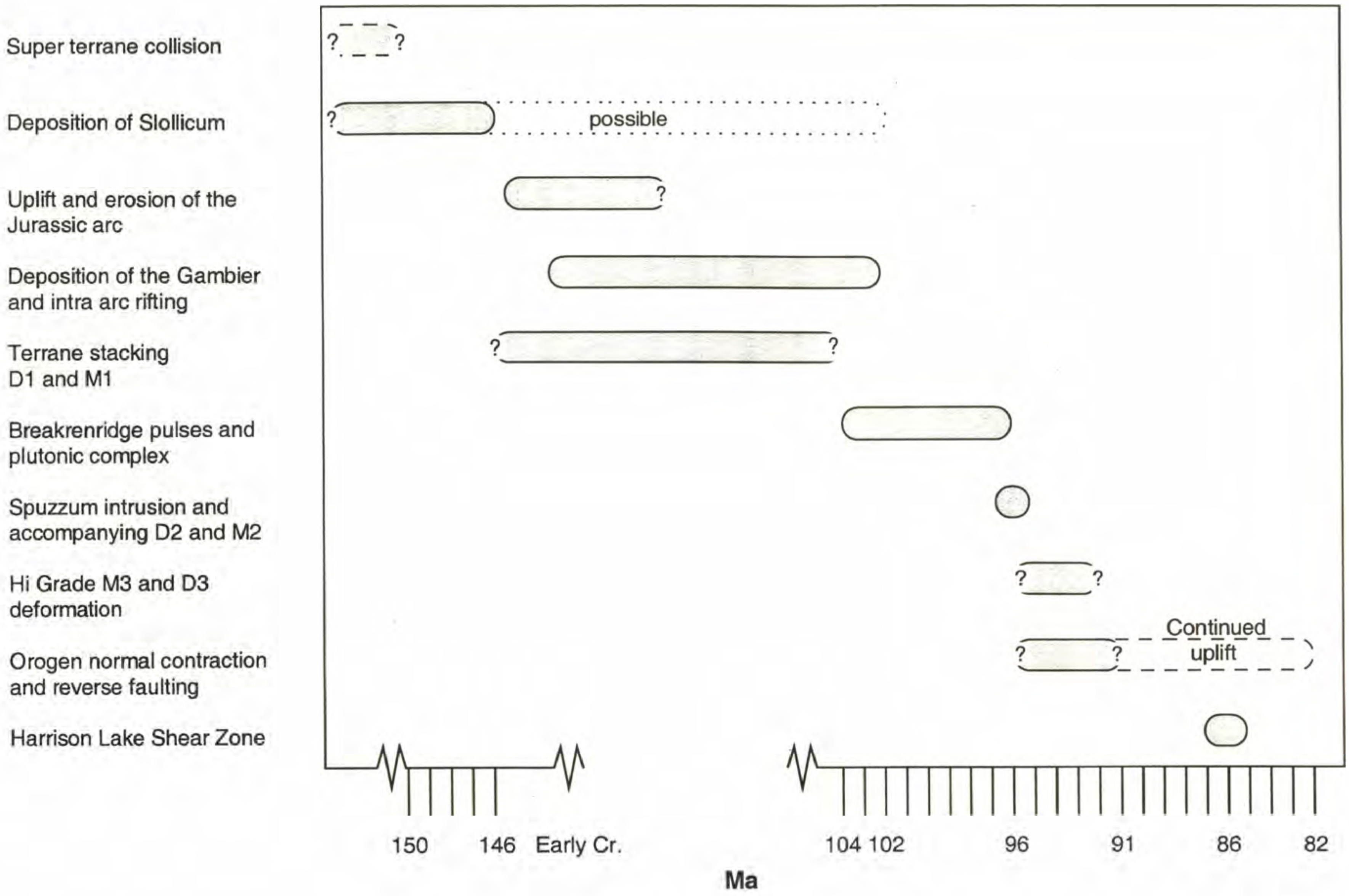

Figure 5.1 Diagram showing possible timing of major events that affected the Harrison Lake area from approximately 170 Ma to 82 Ma.

formations of the Harrison Lake terrane according to Journeay and Friedman (1993).

The Mysterious Ck. and Bill Hook Ck formations are part of a broken succession extending from the lower Mid-Jurassic Harrison Lake formation to the Early-Cretaceous Gambier group rocks. A major unconformity is present between the Bill Hook Ck. formation and overlying Gambier Group rocks (Arther, 1986) which Lynch (1992) interpreted to be of regional extent. This unconformity marks a time of major uplift and erosion of Jurassic plutons and associated volcanic rocks during the latest Jurassic and Early-Cretaceous (Arther, 1986).

Relative plate motions between the oceanic Farallon plate and the North American plate from approximately 145-135 Ma were relatively slow and subduction was oblique to the SE (Engebretson et. al. 1985). At approximately 135my BP, plate velocities increased and direction of convergence was almost directly east-west (Engebretson et. al., 1985). This may be responsible for the uplift and unconformity described in Arther (1986).

The idea that terrane-stacking took place during uplift at this time, after Slollicum/Twin Island deposition at 146 Ma but prior to the onset of Gambier deposition in Lower Berriasian, was suggested by Jeletzky (1965, 1984; in Lapen 1998) and adopted by Lapen (1998). This interpretation is supported by deformational fabrics present in the underlying Bill Hook Ck. formation that are absent in overlying Peninsula formation (Gambier group rocks) on the Cascade Peninsula (Arthur et. al., 1993). That the orogenic event responsible for deformation in the Bill Hook Ck formation took place prior to deposition of the Peninsula formation was proposed by Crickmay (1931; in Arthur et. al., 1993). However, Arthur et. al.(1993) agree that it is unclear whether the presence or absence of fabric is due to compositional differences between units or a deformational event in the lower unit. In either case Arthur (1986) and Arthur et. al. (1993) describe the orogenic event as minor suggesting that although major uplift took place, internal deformation was minor.

It would follow that terrane stacking could have taken place as the plate motions changed around 135 B.P. The timing would require: 1) final deposition of the Slollicum unit some time after 146Ma; and 2) burial of at least 10-15 km before mylonitic fabrics could dominate during faulting. All of this must have occurred before the onset of Gambier group deposition in the Late Berriasian during the major uplift suggested by Arthur (1986) starting in latest Jurassic. Thrusting could sufficiently bury the Slollicum rocks before terrane stacking but no late Jurassic thrust related fabrics are documented elsewhere in the region.

Journeay (1990) and Journeay and Friedman (1993) suggested possible correlations of Slollicum rocks and rocks of the Peninsula and Broken Back Hill formations of the Gambier group. Because the Gambier group has no noted unconformities, a relatively quiet tectonic regime must have existed during deposition which spans the Early and Mid-Cretaceous. If the Slollicum unit is part of the Gambier group, then terrane stacking occurred after deposition of the Gambier group which has an upper age bracket of 102 Ma (Parrish and Monger, 1992).

Another argument for timing of terrane stacking comes from Feltman (1997) who notes a 104-96Ma age of intrusion of the Breakenridge orthogneiss into the Twin Island/Slollicum schist. He found fabric relationships to suggest intrusion was subparallel to original layering and was followed by regional S_1 foliation development in the Breakenridge Orthogneiss associated with orogen parallel deformation that probably occurred after 96 Ma. This would require a timing for thrust stacking prior to 104 Ma age of intrusion as the Breakenridge Orthogneiss bears no orogen normal fabrics.

Fabrics in the Breakenridge Orthogneiss and its intrusion into the Slollicum/Twin Island schist is perhaps the best evidence for the upper age limit of the thrusting. The relationship requires thrusting before 104 Ma and orogen parallel fabric development after 104 Ma. However it still possible that thrusting occurred after the deposition of the Gambier Group rocks after 102 Ma. A plausible explanation would be that strain partitioning was occurring around this time in which orogen normal contraction is taken up in the upper crustal regions while orogen parallel movement is dominant in the lower crustal regions.

Engebretson et. al. (1985) describe a major change in relative plate velocities that accompanied a change in plate motions at approximately 100 Ma. Convergence became even more oblique, which probably resulted in or enabled continuation of a transpressional tectonic regime throughout the region. This could have caused thrusting and related fabric development in the upper crustal regions, such as in the Gambier, Slollicum and Cogburn rocks, while orogen-parallel deformation began in the lower crustal regions, such as in the Breakenridge Orthogneiss and the deeper Slollicum rocks it intruded into, resulting in strain partitioning of the crust.

D1 and D2 Deformation

Regional deformation and resulting fabrics, D_1, observed in the study area are attributed to thrust stacking of the Slollicum, Cogburn, and Settler terranes. Index minerals, including chlorite, biotite, and bladed actinolite to hornblende, define regional foliation requiring syn-tectonic greenschist metamorphism, M_1. Timing for D_1 and M_1 is constrained by the same restrictions set forth for terrane thrust stacking as D_1 and M_1 are attributed to thrusting (post 146 Ma and pre 96Ma).

Foliation defined mainly by biotite that formed as a result of intrusion of the Spuzzum pluton, D_2, is superimposed onto regional fabrics. No direct relation between D_2 and D_3 deformational fabrics was observed in this study.

High-Pressure Metamorphism

High-pressure metamorphism, M_3, post-dates D_1 and associated metamorphism. High-grade index minerals include garnet and hornblende. Garnets are euhedral and often cut or incorporate D_1 foliation. Post-kinematic hornblende is commonly radiating and incorporates D_1 foliation. These observations suggest high-incorporates D_1 foliation. These observations suggest high-pressure metamorphism took place in a static environment after D_1 around 96 Ma. Occurrences of aligned hornblende may suggest an overlap of D_1 and the high-pressure metamorphism. Alternatively, the high-pressure metamorphism is partly coeval with orogen-normal contraction described in Feltman (1997) and Lapen (1998) and assigned as their D_2 event which occurred sometime after 96 Ma but before 91 Ma (Lapen, 1998).

Map scale folding of the region, due to orogen-normal contraction after 96 Ma, is most likely the source of the late stage D_3 strain described in the Structure chapter in this study. Deformation of the high pressure minerals after peak metamorphism suggests D_3 took place near the end of high-pressure metamorphism. In some samples, deformation is post peak metamorphism, while in others, metamorphism outlasts deformation.

The timing of uplift of high-grade rocks to the north of the study area is partly related to uplift along the Breakenridge and Fire Creek faults (Lapen, 1998). These faults are pinned by the 91 Ma Lillooet pluton. Feltman (1997) established that uplift continued after 91 Ma using Ar/Ar dating of hornblende and mica in the southern Breakenridge area. His findings indicated that hornblende cooled below its 500°C closure temperature by 87 Ma and biotite and muscovite cooled below 300-350°C by 82 Ma. The data concludes that uplift of the Breakenridge Plutonic Complex and high-grade the minerals within began prior to 91 Ma and continued until at least 82 Ma.

VI DISCUSSION

The spatial relationship between the syn-tectonic regional and post-tectonic high-pressure metamorphism needs better understanding. Delineating the spatial boundaries of the high-grade metamorphism would greatly help in deciphering isograds from the different metamorphic events and might create boundaries for which to look for possible structures that may exist but have not been documented.

The occurrence of high-pressure metamorphism requires that loading took place sometime after D_1 or 96Ma. Journeay and Friedman (1993) present a two stage model for the spatial and temporal relationships seen in the study area and surrounding region. They suggest that the high-grade metamorphism in the Breakenridge Plutonic Complex north of the current study area was caused by loading from low-angle, orogen-normal thrusting occurring during their late stage of deformation. These thrust were later folded and cut by out-of-sequence thrusts and high-angle reverse faults, the latter being responsible for the emplacement of the high-grade rocks at shallow structural levels.

Feltman (1997) however, illustrated that fabrics in the Breakenridge orthogneiss are orogen-parallel, not orogen-normal; precluding thrusting within the Breakenridge Plutonic Complex as the cause for loading. However, if transpression was occurring, causing strain partitioning in the crust, thrusting in the upper crustal levels could have buried the Breakenridge Plutonic Complex significantly.

Lapen (1998) discovered that the high pressure metamorphism in the northern Breakenridge area was syn-chronous with orogen-parallel fabric development. He suggests the Terrarosa thrust may be part of a family of now obscured thrusts that could have been the cause for loading of the Breakenridge Plutonic Complex because the Terrarosa thrust displays orogen parallel movement.

Alternatively, the high-grade metamorphism may have been caused by magma loading as proposed by Brown and Walker (1993). This model involves vertical ballooning of plutons at shallow to intermediate depths and depressing or loading of the underlying country rock. The Mt. Urquhart pluton with a post 96 Ma intrusion could be responsible for this process in the study area. Another possibility is that the belt of 104-96 Ma plutons including the Spuzzum, Settler Creek, Hut Creek and Hornet Creek plutons was much more voluminous, and being at higher structural levels than the Breakenridge Plutonic Complex, these plutons could be the source of loading.

In either case a relatively long static period is required to allow for the growth of the large static porphyroblasts observed in this study area (figs. 1.2 and 2.7). This would mean deformation ceased in the study area by at least 96 Ma and lasted for some time even though orogen-parallel deformation was occurring north of the study area (Lapen, 1998).

Uplift of the high-pressure minerals is not well understood within the scope of this study. Feltman (1997) and Lapen (1998) offer an explanation that the Breakenridge and Fire Creek faults respectively, both north of the study area, aided in the uplift of the high-pressure minerals in the Breakenridge Plutonic Complex. Although no high angle reverse faults have been delineated in the study area, such a structure should not be totally ruled out without further study.

A fault and fold structure similar to that proposed by Feltman (1997) could possibly explain the several anomalous pressures and temperatures obtained in this study described in the Metamorphism chapter as well as outcrop patterns in the northwest portion of the study area. Continued research in critical areas could be extremely useful in deciphering unexplained structural and metamorphic data already obtained.

Questions that remain unanswered are: 1) can the spatial pattern of isograds and pressure gradient be explained by isostatic uplift as suggested in Brown and Walker (1993)?; 2) Is folding similar to that portrayed in the cross section sufficient to explain the presence of the high-pressure rocks in the study area?; 3) Is the presence of a high-angle fault necessary to raise the high-pressure rocks to shallower crustal levels? or 4) Is a positive flower structure, as suggested by Feltman (1997), present in the region which could be the cause of emplacement of the high-pressure rocks? or 5) Does the whole area represent higher pressures than previously thought? The lack of good thermobarometry data in the study area and structural data in the northwest portion of the study area makes any conclusions tentative.

The Central Coast Belt Detachment, part of the Coast Belt Thrust System of Journeay and Friedman (1993), is defined as a high angle out-of-sequence ductile reverse fault formed during their late stage of deformation. They extend the Coast Belt Thrust System south to Talc Creek (Journeay and Friedman, 1993; figs. 2 and 3) but they do not show it beyond that. However they do infer the Coast Belt Thrust System to be the boundary between the Slollicum-Twin Island schists and the Cogburn Creek group.

This deformation is bracketed by crosscutting relations of other out-of-sequence faults and dated plutons. The 96+6/-3 Ma Ascent Creek pluton constrains the lower age limit while the 91+/-3 Ma Castle Towers pluton constrains the upper age limit (Journeay and Friedman, 1993). The Slollicum-Cogburn fault and related D_1 fabrics in the study area are bracketed by the age of the Slollicum unit at 146 Ma (Bennett, 1989) and the 96 Ma age of the crosscutting Spuzzum pluton and related D_2 fabrics (Brown and Walker, 1993). The Slollicum-Cogburn fault in the study area is an east dipping mylonitic thrust fault but is pre-96 Ma where the CCBD is post 96 Ma. Therefore, the Slollicum-Cogburn fault cannot be a southerly continuation of the Coast Belt Thrust System.

Another question that remains unanswered within the scope of this study is, does the Coast Belt Thrust System possibly cut the Slollicum/Cogburn thrust fault and partially extend into the current study area? This could explain the emplacement of the high-pressure rocks into the study area and possibly the outcrop pattern of the ultramafic rock in the northwest portion of the study area.

VII. CONCLUSIONS

The conclusions of this study are as follows:

(1) Thrusting of the Slollicum and Cogburn terranes occurred after 146 Ma but prior to the 96 Ma age of intrusion of the Spuzzum pluton. An initial deformation, D_1, accompanied by M_1 upper greenschist facies metamorphism, produced a penetrative foliation and down dip lineations. These fabrics are attributed to thrust stacking. Greenschist facies metamorphism (3.0 kb) is associated with thrusting.

(2) Hornblende is observed as aligned and randomly oriented prisms on the foliation surfaces of Slollicum and Cogburn rocks. The relationship of the hornblende to M_1 or M_3 is still uncertain and the extent to which mimetic textures might dominate is unknown.

(3) A period of non-deformation occurred in the current study area at 96 Ma as indicated by the presence of the non-deformed Spuzzum pluton. The intrusion of the Spuzzum pluton pinned the Slollicum-Cogburn fault and developed a foliation parallel to the pluton contact that cuts across D_1 fabrics. The index minerals biotite, garnet, and hornblende grew as a result of intrusion.

(4) A third metamorphic event occurred after 96 Ma consisting of a post-tectonic static overprint of amphibolite facies minerals. Large garnet and radiating hornblende porphyroblasts commonly are helecitic with respect to the D_1 foliation. This static environment lasted long enough to allow

for the growth of large grains of the high grade minerals that overprint earlier structures in the study area before orogen-normal shortening began again.

(5) A third deformational event occurred in the northwest part of the study area after the peak of high grade metamorphism (8.8 kb). This deformation may have folded the Slollicum-Cogburn thrust contact. Reactivation of foliation, which caused rotation and distention of post-tectonic high grade minerals, is attributed to the large scale folding which in turn is attributed to orogen-normal shortening.

These events likely took place in a transpressional tectonic regime influenced by oblique subduction of the outboard oceanic plate with strain partitioning occurring in the crust. Plate motions and velocities dictated periods of deformation and non-deformation throughout the mid-Cretaceous orogeny.

REFERENCES CITED

Armstrong, R.L., 1988, Mesozoic and early Cenozoic evolution of the Canadian cordillera: Geol. Soc. Am. Special Paper 218, p. 55-91.

Arthur, A.J., 1986, Stratigraphy along the west side of Harrison Lake, southwestern British Columbia: *in* Current Research, Part B, Geological Survey of Canada. Paper 86-1B, p. 715.

Arthur, A.J., et. al, 1993, Mesozoic stratigraphy and Jurassic paleontology west of Harrison Lake, southwestern British Columbia: Geological Survey of Canada Bulletin 441, 62 pp.

Bartholomew, P.R., 1979, Geology and metamorphism of the Yale Creek area: Unpublished M.S. Thesis, University of British Columbia, 105 pp.

Bennett, J.D., 1989, Timing and conditions of deformation and metamorphism of the structural packages east of Harrison Lake, B.C.: Unpublished M.S. Thesis, Western Washington University, Bellingham, 87 pp.

Blatt, H., and Tracy, R.J., 1996, Petrology: Igneous, Sedimentary, and Metamorphic; Second Ed.:W.H. Freeman and Co., New York.

Brandon, M.T., and Cowan, D.S., 1985, The Late Cretaceous San Juan Islands-Northwestern Cascades Thrust System [abs.]: Geol. Soc. Am., Abstracts with Programs, v. 17, p. 343.

Brandon, M.T., Cowan, D.S., and Vance, J.A., 1988, The Late Cretaceous San Jaun Thrust System, San Jaun Islands, Washington: Geol. Soc. Am. Special Paper 221, 81p. and 1 Plate.

Brandon, M.T., Cowan, D.S., and Freehan, J.G., 1994, Fault-zone structures and solution-mass-transfer cleavage in Late Cretaceous nappes, San Jaun Islands, Washington in *Geologic field trips in the Pacific Northwest*, Swanson, D. A., and Haugerud, R. A., eds., Geol. Soc. Am. Ann. Mtg., ch. 2L.

Brown, E.H. 1987, Structural geology and accretionary history of the Northwest Cascades system, Washington and British Columbia: Geol.Soc. Am. Bull., v. 99, p. 201-214.

Brown, E.H., and Talbot, J. L., 1989, Orogen-parallel extension in the North Cascades Crystalline Core, Washington: Tectonics, v. 8, p. 1105-1114.

Brown, E.H., and Walker, N.S. 1993, A magma-loading model for Barrovian metamorphism in the southeast Coast Plutonic Complex, British Columbia and Washington: Geol. Soc. of Am. Bull., v. 105, p. 479-500.

Brew, D.A., and Ford, A. B., 1983, Comment and reply on "Tectonic accretion and the origin of the two metamorphic and plutonic welts in the Canadian Cordillera", Geology, 11, p. 427-429.

Coney, P.J., 1989, Structural aspects of suspect terranes and accretionary tectonics in western North America: Journal of Structural Geology, v. 11, n. 1-2, p. 107.

Cowan, D.S., and Brandon, M.T., 1994, A symmetry-based method for kinematic analysis of large-slip brittle fault zones: American Journal of Science, v. 294, p. 257-306.

Crawford, M.L., Hollister, L.S., and Woodsworth, G.J., 1987, Crustal Deformation and Regional Metamorphism Across a Terrane Boundary, Coast Plutonic Complex, British Columbia: Tectonics, v. 6, no. 3, p. 343-361.

Duggan, K.M., and Brown, E.H., 1994, Correlation of the Tonga Formation and the Chiwaukum Schist, North Cascades, Washington: Implications for Late Cretaceous orogenic mechanisms: Tectonics, v. 13, n. 6, p. 1411-1424.

Engebretson, D.C., Cox, A., and Gordon, R.G., 1985, Relative Motions Between Oceanic and Continental Plates in the Pacific Basin. Special Paper 206. 54 pp.

Evans, B.W., and Berti, J.W., 1986, Revised metamorphic history for the Chiwaukum Schist, North Cascades, Washington: Geology, 14, p. 695-698.

Feltman, J.A., 1997, Structure, Metamorphism, and Geochronolgy Along the Southern Margin of the Breakenridge Orthogneiss, Coast Range, Southern British Columbia. Unpublished M.S. thesis, Western Wa. Univ., Bellingham, 128 pp.

Gabites, J.E., 1985, Geology and Geochronometry of the Cogburn Creek-Settler Creek area, Northeast of Harrison Lake, B.C.: Unpublished M.S. thesis, University of British Columbia, Vancouver, 153 pp.

Ghosh, S.K., and Ramberg, H., 1976, Reorientation of inclusions by combination of pure shear and simple shear: Tectonophysics, v. 34, p. 1-70.

Hettinga, M.A., 1989, Metamorphic Petrology, Geothermobarometry and Structural Analysis of a Portion of the area East of Harrison Lake, British Columbia: Unpublished M.S. Thesis, Western Washington University, Bellingham, 106 pp.

Journeay, J.M., and Csontos, L., 1989, A preliminary report on the structural setting along the southeast flank of the Coast Belt, British Columbia: Geol. Surv. Can. Paper 89-1E, p. 177-187.

Journeay, J.M. and Friedman, R. M., 1993, The Coast Belt Thrust System: Evidence of Late Cretaceous shortening in Southwest British Columbia: Tectonics, v. 12, no. 3, p. 756-775.

Journeay, J.M., 1990, A progress report on the structural and tectonic framework of the Southern Coast Belt, British Columbia, in Current Research, Part E, Geol. Surv. of Can., Paper 90-1E, p. 183-195.

Lapen, Thomas, A. Structure and Metamorphism of the Southern Lillooet River-Northern Breakenridge area, Southern Coast Mountains, British Columbia. Unpublished M.S. thesis, Western Wa. Univ., Bellingham, 135 pp.

Leake, B.E., 1978, The Earth through time: Saunders College Publishing, Philadelphia, 513 pp.

Lowes, B.E., 1972, Metamorphic Petrology and Structural Geology of the Area East of Harrison Like, British Columbia: Unpublished Ph.D. Thesis, University of Washington, Seattle, 162 pp.

Maekawa, H., and Brown, E.H., 1991, Kinematic analysis of the San Juan thrust system, Washington: Geol. Soc. Am. Bull., v. 105, p. 1007-1016.

Mahoney, J.B. and Journeay, J.M., 1993, The Cayoosh Assemblage, southwestern British Columbia: last vestige of the Bridge River Ocean: in Current Research, Part A; Geol. Surv. of Can. Paper 93-1A, p. 235-244.

Maruyama, S., Suzuki, K., and Liou, J.G., 1983, Greenschist-amphibolite transition equilibria at low pressures: Journal of Petrology, v. 24, n. 4, p. 538.

McGroder, M.F., 1991, Reconciliation of two-sided thrusting, burial metamorphism, and diachronous uplift in the Cascades of Washington and British Columbia: Geol. Soc. of Am. Bull., v. 103, p. 189-209.

Misch, P., 1966, Tectonic Evolution of the Northern Cascades of Washington State- a west-Cordilleran case history: Canadian Institute of Mining and Metallurgy, Special Volume 8, p. 101-148.

Monger, J.W.H., 1986, Geology Between Harrison Lake and Fraser River, Hope Map Area, Southwestern British Columbia: in Current Research, Part B, Geol. Surv. of Can., Paper 86-1b, p 699-706.

Monger, J.W.H., 1990, Correlation of Settler Schist with Darrington Phyllite and Shuksan Greenschist and its tectonic implications, Coast and Cascade mountains, British Columbia and Washington: Can. J. Earth Sci., v. 28, p447-458.

Monger, J.W.H., 1991, Georgia Basin Project: structural evolution of parts of southern Insular and southwestern Coast belts, British Columbia; in Current Research, Part A, Geological Survey of Canada Paper 91-1A, p. 219-228.

Monger, J.W.H., Price, R.A., and Templeman-Kluit, D.J., 1982, Tectonic Accretion and the Origin of the two major metamorphic and plutonic welts in the Canadian Cordillera: Geology, v. 10, p. 70-75.

Nelson,J.A., 1979, The western margin of the Coast Plutonic Complex on Hardwicke and West Thurlow Islands, British Columbia: Can. J. Earth Sci., v. 16, p. 1166-1175.

Parish, R.R., and Monger, J. W. H., 1992, New U-Pb dates from southwestern British Columbia, Geol. Surv. of Can. Special Paper, 91-2, p. 87-108.

Pigage, L.C., 1973, Metamorphism Southwest of Yale, British Columbia, M.S. Thesis: Vancouver, British Columbia, University of British Columbia, 95 pp.

Richards, T.A., and McTaggart, K.C., 1976, Granitic rocks of the southern Coast Plutonic Complex and northern Cascades of British Columbia: Geol. Soc. of Am. Bull., vol. 87, p. 935-953.

Rubin, C.M., Saleeby, J.B., Cowan, D.S., Brandon, M.T., and McGroder, M.T., 1990, Regionally extensive mid-Cretaceous west-vergent thrust system in the northwestern Cordillera: Implications for continent-margin tectonism: Geology, v. 18, p. 276-280.

Smith, M.T., 1986, Structure and Petrology of the Grandy Ridge-Lake Shannon Area, North Cascades, Washington: Unpublished M.S. Thesis, Western Washington University, Bellingham, 156 pp.

Thorkelson, D.J., and Smith, A.D., 1989, Arc and intraplate volcanism in the Spences Bridge Group: Implications for Cretaceous tectonics in the Canadian Cordillera: Geology, v. 17, p. 1093.

Tracy, R.J., and Frost, B.R., 1991, Phase eqilibria and thermobarometry of calcareous, ultramafic, and mafic rocks, and iron formations. Rev. Mineral., v. 26, p.207.

Turner, F.J., 1981, Metamorphic Petrology: Mineralogical, Field, and Tectonic Aspects. Second Ed. Hemisphere Pub. Corp., NY.

van der Heyden, P., 1992, A Middle Jurassic to early Tertiary Andean-Sierran arc model for the Coast Belt of British Columbia: Tectonics, v. 11, p. 82-97.

Walker, N.W., and Brown. E.H., 1991, Is the Coast Plutonic Complex the consequence of accretion of the Insular Super terrane?: Evidence from U-Pb zircon geochronometry in the northern Washington Cascades: Geology, v. 19, p. 714-717.

Wells, P.R.A., 1980, Thermal models for the magmatic accretion and subsequent metamorphism of continental crust: Earth and Planetary Science Letters, v. 46, p. 253-265.

Woodsworth,G.J., and Tipper, H.W., 1980, Stratigraphic framework of the Coast Plutonic Complex, western British Columbia, in Volcanogenic Deposits and Their Regional Setting in the Canadian Cordillera: Cordilleran Section, Geol. Assoc. Can. Program Abstr., 32-34.

Zen, E., 1988, Tectonic significance of high-pressure plutonic rocks in the western Cordillera of North America, <u>in</u> *Metamorphism and Crustal Evolution of the Western United States*, edited by W. G. Ernst, pp. 41-67, Prentice-Hall, Englewood Cliffs, N.J.

APPENDIX A. MINERAL ASSEMBLAGES IN THIN SECTION

Basic Assemblages

Sample #	Qtz	Plag	Biot	Musc	Chl	Epi/Cz	Hb/Act	Gt	Op	Sph	Tour	Gr	Calc	Other
181-1	X	X			X	X	X			X				
181-2	X	X			X	X	X			X				
181-3	X	X		X		X			X					
181-4b	X		X		X				X			X		
181-5	X	X			X	X	X							
181-6a	X	X			X	X	X			X	X			
181-6b	X	X			X	X	X			X				
181-7	X	X			X	X	X		X					
181-12b	X	X	X	X		X								
181-16	X	X	X		X	X	X	X	X				X	
181-17	X	X				X	X							
181-18b	X	X			X	X	X		X					
181-19	X	X	X		X	X			X	X				
181-20	X		X											apatite
181-21	X	X			X	X	X		X					
181-25	X	X		X										
181-26	X	X	X				X		X				X	
181-28	X	X	X		X	X	X		X	X				
181-32	X	X	X		X	X	X		X	X				apatite
181-33	X	X			X	X	X		X	X			X	
181-34	X	X			X	X	X							apatite
181-36a	X	X			X	X	X		X					
181-37	X	X	X		X	X	X		X				X	
181-38	X	X	X		X		X	X	X					apatite
181-40	X	X	X		X				X			X		
181-42a	X	X			X	X	X			X				
181-42c	X	X	X		X		X	X	X			X		
181-43	X	X			X		X							stilp
181-44	X	X	X		X	X	X		X					
181-45b	X	X			X	X	X				X			
181-46	X	X	X		X		X		X				X	
181-47	X	X	X		X	X	X							

Sample #	Qtz	Plag	Biot	Musc	Chl	Epi/Cz	Hb/Act	Gt	Op	Sph	Tour	Gr	Calc	Other
181-49	X	X		X					X		X	X	X	
181-50c	X	X			X	X	X			X				
181-51b	X	X	X	X					X			X		
181-53	X	X				X	X		X	X			X	
181-54a	X	X			X	X	X		X					
181-54b	X	X			X	X	X		X					
181-55	X	X			X	X	X			X				
181-57	X	X				X	X		X					
181-58	X	X			X	X	X			X				
181-60c	X	X	X				X	X	X		X		X	
181-60d	X	X			X	X	X		X	X				
181-65	X	X					X							
181-66	X	X			X	X				X				
181068	X	X	X		X	X	X							
181-71a	X	X	X	X					X					
181-72	X	X		X	X	X			X			X		
181-74	X	X			X	X	X		X	X			X	
181-76	X	X	X			X	X		X	X				
181-78	X	X	X		X	X	X		X					
181-78d1	X	X	X		X	X	X		X					apatite
181-79	X	X			X	X	X						X	
181-88a	X		X		X									
181-88b	X	X	X		X	X	X		X				X	
181-89	X	X			X	X	X		X	X				
181-91b	X	X			X	X	X		X	X				
181-92	X	X	X		X	X	X			X	X		X	
181-93	X	X	X	X	X			X	X		X	X		stilp
181-94a	X	X	X	X	X				X			X	X	
181-94b	X	X	X		X		X						X	
181-94c	X	X	X		X	X		X	X			X		
181-98	X	X	X		X	X	X		X					
181-99a	X	X	X		X	X	X		X					
181-104	X				X		X							
181-114	X	X	X		X	X	X		X				X	
181-115b					X	X	X							
181-117	X	X				X	X			X				
181-119b	X	X			X	X				X				
181-121	X	X			X	X	X		X	X				

Sample #	Qtz	Plag	Biot	Musc	Chl	Epi/Cz	Hb/Act	Gt	Op	Sph	Tour	Gr	Calc	Other
181-122	X	X				X	X							
181-125	X	X	X	X	X	X		X						
181-126	X	X				X	X			X				
181-127	X	X			X	X	X		X		X			
181-128	X	X			X	X	X		X					apatite
181-129	X	X			X	X							X	zoisite
181-132	X	?			X	X	X		X	X				
181-135	X	X	X		X	X	X		X					
181-136	X	X	X	X	X			X	X			X		zoisite
181-137	X	X	X	X	X			X	X			X		
181-141	X	X	X	X	X			X	X			X	X	
181-142	X	X	X	X										
181-144	X	X			X	X	X		X					
181-146	X	X			X	X	X			X				
181-148	X	X			X	X	X		X	X				
181-149	X	X			X	X	X			X				
181-150	X	X	X		X			X						
181-151b	X	X	X		X					X				
181-151c	X	X	X		X	X				X				
181-152a	X	X	X		X	X			X					
181-152b	X	X			X			X	X					
181-153	X	X		X	X									
151-154	X	X	X		X			X	X					
181-155a	X	X		X	X	X		X						
181-155b	X	X		X	X	X	X	X			X			
181-156	X	X			X	X	X							
181-157	X	X	X			X	X		X					apatite
181-157b	X	X			X	X	X	X	X					apatite
181-158	X	X				X	X		X					
181-159	X	X				X	X		X					apatite
181-160	X	X	X		X	X	X		X					apatite
181-62	X	X				X	X			X				
181-164	X	X			X	X	X			X			X	
181-165	X	X	X			X	X	X	X	X				
181-166	X	X	X				X		X			X		
181-168	X	X	X	X	X						X			
181-169	X	X	X	X		X			X					
181-170a	X	X	X	X	X	X	X		X					sericite

Sample #	Qtz	Plag	Biot	Musc	Chl	Epi/Cz	Hb/Act	Gt	Op	Sph	Tour	Gr	Calc	Other
181-170b	X	X		X	X	X	X							
181-171	X	x	X				X	X						
181-173a	X	X	X	X	X			X						
181-173b	X	X	X	X	X	X	X		X					apatite
181-175	X	X	X	X		X			X	X			X	
181-176	X	X	X		X	X		X	X			X		
181-178	X	X	X	X	X	X	X		X	X				
181-180	X	X	X			X	X		X					
181-183	X	X			X	X	X		X					
181-182	X	X	X		X	X	X		X					
181-185	X		X		X	X	X		X				X	
181-186	X	X	X			X	X		X	X			X	
181-187	X	X			X		X		X					
181-188	X	X	X		X	X	X		X					
181-189	X	X			X	X	X		X	X				
181-191	X	X	X		X	X	X		X					
181-192	X	X	X	X					X			X	X	
181-193	X	X				X	X		X				X	
181-194b	X	X		X	X	X			X	X			X	
181-195	X	X			X	X								
181-196	X	X		X	X	X	X		X	X				apatite
181-200	X	X	X		X	X	X		X					
181-201a	X	X			X	X	X		X					
181-202	X	X			X	X	X		X					
181-203	X	X			X	X	X		X					
181-204a	X	X			X	X	X			X				
181-204c	X	X	X		X	X	X			X				
181-206	X	X	X		X	X	X		X					
181-210	X	X			X	X	X							zoisite
181-211	X	X	X		X		X		X	X				
181-212	X	X	X		X		X		X			X		
181-213	X	X	X		X	X	X		X					

Qtz = quatrz; Plag = plagioclase; Boit = biotite; Musc = muscovite; Chl = chlorite; Epi = epidote; Cz = clinozoisite; Hb = hornblende/Act = actinolite; Gt = garnet; Op = opaques; Sph = sphene; stilp=stilpnomelene; Tour = tourmaline; Gr = graphite; Calc = calcium carbonate

Ultramafic Assemblages

Sample #	For	Serp	Trem	Op	Chl	Calc	Talc
181-8a		X	X	X			
181-14a		X		X		X	
181-29	X		X			X	X
181-39		X	X			X	X
181-59		X	X				
181-62	X	X		X	X		
181-81	X	X		X			
181-86	X	X		X			
181-101		X	X	X			X
181-106	X	X		X			
181-109	X	X				X	
181-112	X	X			X		
181-133		X		X		X	
181-143	X	X		X		X	
181-147	X	X		X			
181-163b	X	X				X	
181-167	X	X		X			X

For=forsterite; Serp=serpentine, mainly the antigorite variety; Trem=tremolite; Op=opaque minerals, most likely magnetite; Chl=al-rich chlorite; Calc=calcium carbonate, most likely magnesite; Talc=talc

APPENDIX B. MINERAL COMPOSITIONS USED IN THERMOBAROMETRY (in formula proportions)*

Sample 181-60c

	Garnet	Hblde	Plag
Si	3.018	6.331	2.795
Al4	-------	1.669	-------
Al6	1.985	1.091	1.208
Ti	0.006	0.027	-------
Fe	1.501	2.357	0.006
Mg	0.090	1.705	-------
Mn	0.617	0.043	-------
Ca	0.767	1.743	0.184
Na	-------	0.527	0.806
K	-------	0.069	0.011

Sample 181-136

	Garnet	Biotite	Musc	Plag
Si	3.022	5.542	6.320	2.732
Al4	-------	2.458	1.680	-------
Al6	1.987	0.844	3.618	1.266
Ti	0.001	0.178	0.025	-------
Fe	1.779	2.615	0.193	0.004
Mg	0.152	2.224	.0242	-------
Mn	0.427	0.010	-------	-------
Ca	0.616	-------	-------	0.258
Na	-------	0.002	0.170	0.750
K	-------	1.402	1.690	0.005

Sample 181-171

	Garnet	Hblde	Plag
Si	3.014	6.404	2.695
Al4	-------	1.596	-------
Al6	1.986	1.184	1.305
Ti	0.002	0.037	-------
Fe	2.040	2.265	0.004
Mg	0.243	1.661	-------
Mn	0.186	0.008	-------
Ca	0.522	1.757	0.301
Na	-------	0.423	0.693
K	-------	0.087	0.002

Sample 181-173a

	Garnet	Biotite	Musc	Plag
Si	2.993	5.511	6.206	2.714
Al4	-------	2.489	1.794	-------
Al6	2.013	0.678	3.643	1.262
Ti	-------	0.216	0.040	-------
Fe	2.243	2.401	0.185	0.003
Mg	0.450	2.465	0.228	-------
Mn	0.226	0.004	-------	-------
Ca	0.076	-------	-------	0.248
Na	-------	0.044	0.280	0.741
K	-------	1.813	1.603	0.007

*Analyses by E.H. Brown